Transmission design and optimization at the national level

by

Yifan Li

A thesis submitted to the graduate faculty
in partial fulfillment of the requirements for the degree of
DOCTOR OF PHILOSOPHY

Major: Electrical Engineering

Program of Study Committee:
James D. McCalley, Major Professor
Ian Dobson
Venkataramana Ajjarapu
Sarah Ryan
Zhijun Wu

Iowa State University
Ames, Iowa
2014

TABLE OF CONTENTS

LIST OF FIGURES

LIST OF TABLES

ACKNOWLEDGEMENTS

Thanks God for leading me to Iowa State University, where I was so lucky to meet Dr. James D. McCalley and got the opportunity to work in his research group on this very interesting and challenging topic. Dr. McCalley's thoughtful suggestions and valuable comments made it possible for me to finish this work during my PhD program. His advises on selecting courses and research directions are always longsighted. Besides, he always cares much about students' feelings. Without his tremendous support, both academic and financial, I would not be able to get the work done by any means.

Besides my advisor, I want to express my gratitude to Dr. Ian Dobson, Dr. Venkataramana Ajjarapu, Dr. Sarah Ryan and Dr. Zhijun Wu for taking time from their very busy schedule to read, listen, and provide inspiring comments about my research work. I appreciate it very much.

I owe my parents such a debt that I will never be able to fully pay back. I came to the U.S. to pursue graduate studies thus would not be able to go back to see them frequently, even during Chinese Spring Festival, when families are supposed to reunion as a tradition. Not only they support me financially during the first two years, but more importantly, they are always supportive for me to pursue my PhD, and help me overcome any possible difficulties heart and soul. No single word in any language on the earth can express my appreciation to them.

ABSTRACT

Nowadays, interconnection wide electric transmission system has been envisioned to facilitate the growth of renewable energy, enhance reliability, improve system operating efficiency and reduce greenhouse gas emissions. In this thesis, we articulate an explicit planning framework for high-capacity, inter-regional transmission system design. The study framework begins with generation scenario design, followed by an innovative transmission candidate selection algorithm derived from graph theory applications. Then, a new modeling approach has been introduced to efficiently model the transmission network expansion optimization problem at the interconnection wide level. Global uncertainties have been addressed as well to design a transmission overlay which is robust to different future scenarios. Last, steady state operating benefits, in terms of total cost, CO_2 emissions, energy price change and employment opportunity creation, are evaluated by a series of comparison studies between systems with and without designed overlays. The complete study process has been applied to an aggregated U.S. power system study case to design, optimize and evaluate transmission overlays for multiple future generation scenarios. Associated simulation results suggest that a national transmission overlay provides economic and environmental benefits.

CHAPTER 1. INTRODUCTION

1.1 Research Background and Motivation

The U.S. electric transmission system expansion has been lagging behind generation and load increase for decades. According to the U.S. Department of Energy's study results [1], congestion has inhibited inter-regional power exchange in some major areas of the country. Moreover, since electric transmission is the only way to carry renewable energy, and high quality renewable resources are generally remote from load centers, the growth of renewable generation is also inhibited by insufficient transmission. A recent study [2] concludes that a national transmission overlay, defined as a high capacity, multi-regional grid that spans all three interconnections, provides overall economic, environmental, and system performance benefits for the U.S.

There has been previous interest in considering transmission planning beyond the regional level. References [3]–[4] perform interconnection wide transmission studies, focusing on renewable generation deliverability; Figure 1.1 illustrates associated transmission needs. References [5]–[9] are overlay designs at the national level, from various industry and research institutes; Figure 1.2 illustrates a conceptual design from [5], and Figure 1.3 illustrates transmission needs from [7]. Besides the U.S., Europe also conducts significant efforts in designing continental level super transmission grid [10]. However, except for [4] and [7], most of these designs have not resulted from rigorous

engineering analysis. Even for [4] and [7], engineering judgment plays an important role in transmission decision-making, without a strict mathematic optimization approach which can select and justify the design. Moreover, [5]–[9] are dramatically different from each other in terms of their chosen network topology and transmission technology.

New academic and engineering challenges exist when planning on the national level, requiring new planning methodology. These new challenges include, but are not limited to: interdependencies between energy and transportation system [11], treatment of global uncertainties in future generation, different interconnection synchronization, greenhouse gas emissions, system robustness [12], transmission candidate selection for integrated system design [13], and modeling of multiple parallel circuit additions [14].

In this thesis, we propose an innovative design framework for pure engineering studies and apply it to the aggregated U.S. system model. It begins with generation forecast under different future scenarios. Next, an innovative graph theory application, referred to as the Iterative Reweighting Minimum Spanning Tree (IRMST) algorithm, has been developed and implemented to select good transmission candidate in terms of right of way (ROW) availability, geographical conditions and economic value. Based on the location-specified loadability and cost data of selected candidates, we formulate the multi-stage/circuit/technology transmission network expansion planning optimization (TNEP) problem as a mixed integer linear programming (MILP) model. We have also extended the traditional modeling approach to allow multiple parallel circuit additions, aiming to satisfy the needs of large scale transmission planning [14]. We develop a particular design for each scenario; we also develop a single flexible design for all scenarios, and then we evaluate their steady state operating benefits.

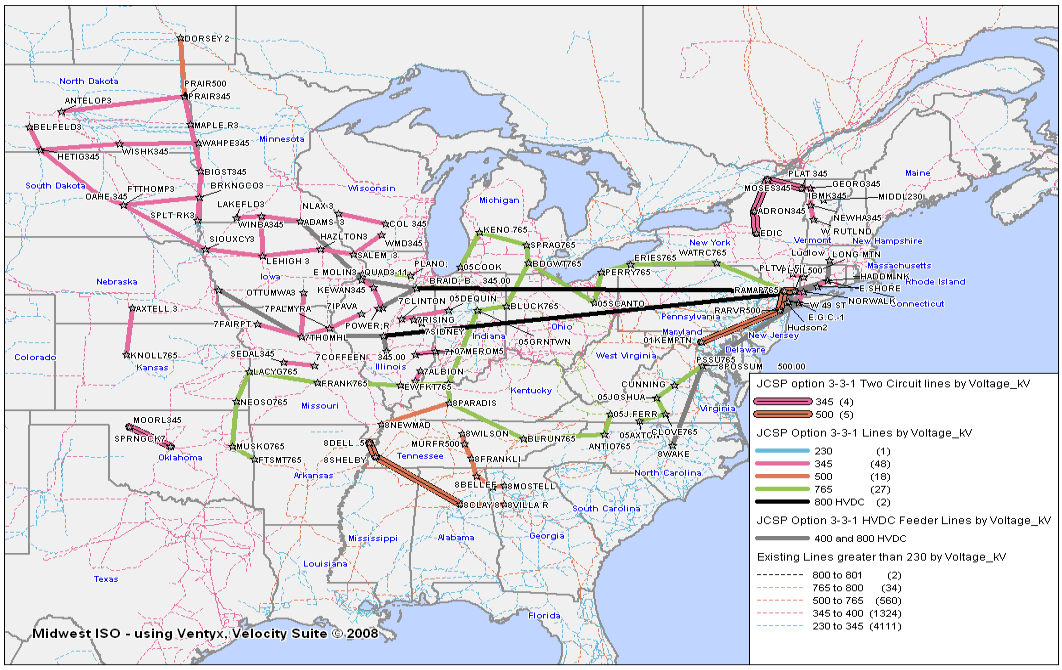

Fig. 1.1: Eastern Wind Integration Study Transmission Overlay Design (Source: [4])

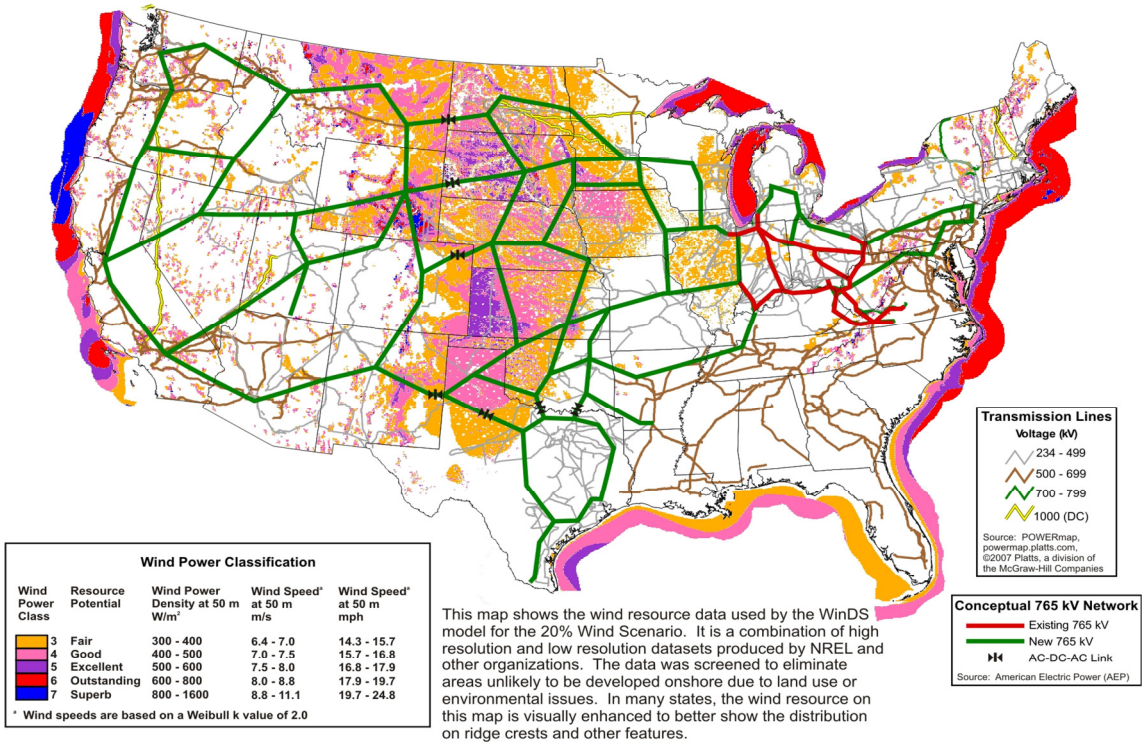

Fig. 1.2: National 765kV EHVAC Transmission Overlay Concept (Source: [5])

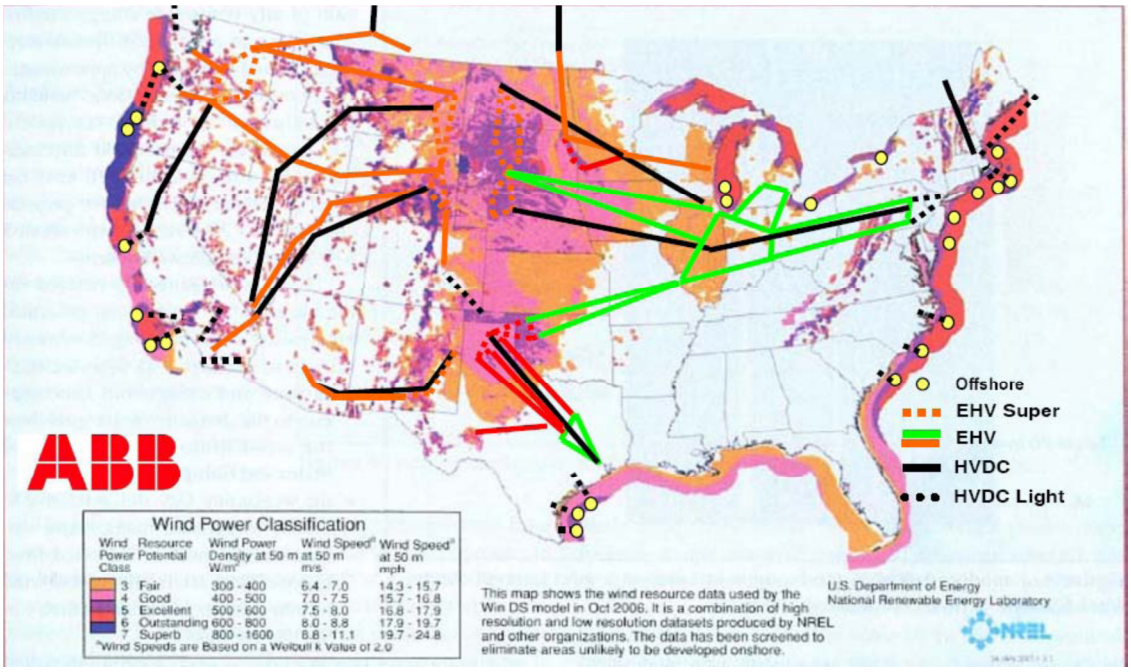

Fig. 1.3: National 765kV EHVAC Transmission Overlay Design (Source: [7])

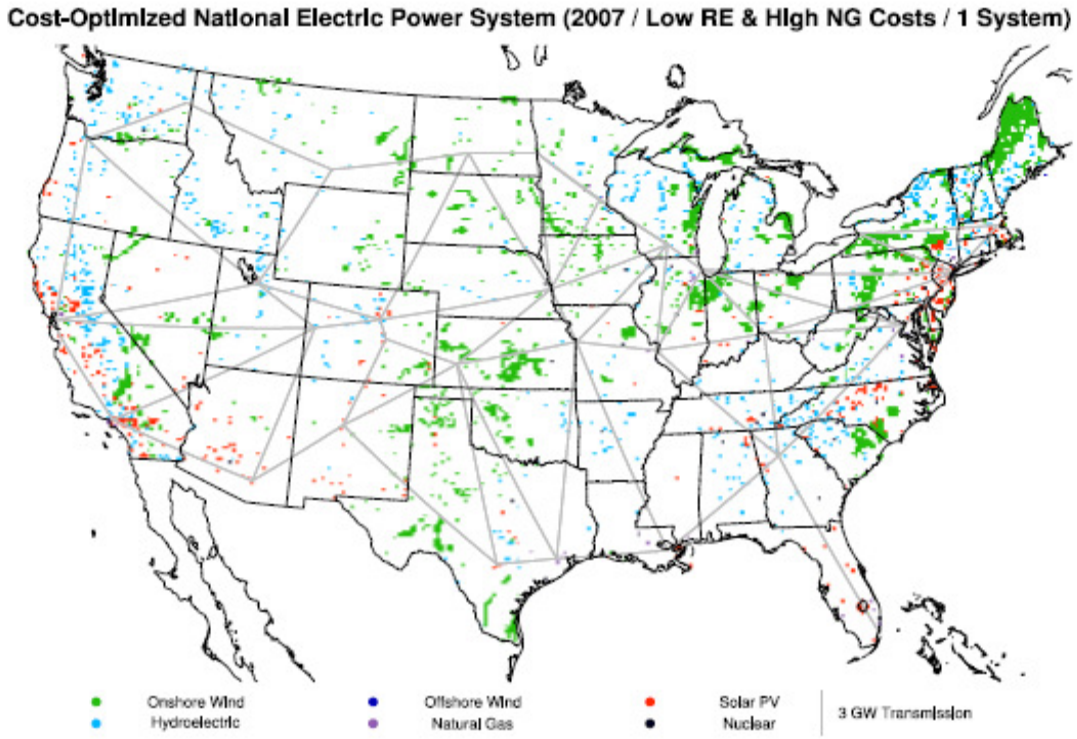

Fig. 1.4: National 765kV EHVAC Transmission Overlay Design (Source: [8])

1.2 Major Contributions

Traditionally, transmission planning has been done in such a way that transmission circuits are studied and invested one by one, i.e., our current system is actually a piecemeal or incremental solution. For this national transmission overlay design problem, we propose a study method to develop a single integrated high capacity transmission network within a single design effort. We believe that doing so will provide a superior solution than piecemeal solutions. The work presented in this thesis may provide insight for future investment in high capacity inter-regional transmission. Although national transmission overlay design differs from conventional transmission planning, some methods described here may be applicable to conventional planning as well. Major contributions of this research include:

a) Study framework: A well-articulated study framework for national level transmission design will be described. This is a contribution because transmission at this scale has never been designed before. Although some features of the study framework also apply to existing planning studies in the literature [1]–[4], the scale of the design has resulted in features that are unique to this particular design problem.

b) Transmission candidate selection method: Reference [15] from the California Independent System Operator provides a method to estimate transmission line costs. References [16] and [17] introduce the minimum spanning tree (MST) problem and associated solution algorithms. In this study, we identify and prove a new characteristic of MST, which can be summarized as: The MST *T* of graph G remains the MST of another graph G' which has the same topology with G, as

long as each of the edges in G'\T has a length greater than or equal to the same edge in G. We then take advantage of this characteristic and also apply the reweighting method in [15] to develop a systematic approach to select and evaluate transmission candidates on large geographical horizon with consideration of major influencing factors.

c) Decimal-binary disjunctive modeling approach for TNEP: References [18] and [19] have summarized the current planning models and test systems. The traditional disjunctive model in [20] and [21] eliminates the nonlinearities due to the product between investment decision variables and bus angle, by using disjunctive formatted mixed integer constraints. However, its decision variable on each candidate is binary, i.e., multiple parallel circuit additions cannot be conveniently addressed. Our new approach extends the traditional disjunctive model to efficiently represent multiple parallel circuit additions on a single transmission corridor. This is important because multiple parallel circuit additions are common in bulk transmission system planning and tend to create computational burden for large real system. We also developed approaches to determine the ideal number of parallel candidates needed, handle multiple candidate circuit type problems, and implement Benders decomposition, so as to further enhance the ability to efficiently model large-sized problems.

d) Hybrid AC/DC transmission expansion planning (TEP) model: This thesis develops a TEP formulation which enables multiple AC transmission levels and multiple DC transmission levels for circuit selection, with appropriate representation of AC capacity dependence on length and corresponding cost of

substations, and with appropriate representation of terminal costs for DC circuits.

e) Transmission overlay designs for the contiguous U.S.: Literature [5]–[9] provides national transmission designs, but it is not from a systematic optimization and evaluation approach. Our study is the first attempt to systematically design and optimize a national hybrid AC/DC transmission overlay over a long time period (40 years) to facilitate the growth of different types of renewable generation. Key findings and conclusions have also been made from these results.

f) Transmission overlay benefit quantification: This contribution confirms the conclusion made in [2] that a national transmission overlay provides economic and environmental benefits, but it does so using a more granular national electric system model.

g) Design transmission overlay with consideration of flexibility to different scenarios: This thesis extends the "flexibility design" idea from [22] to transmission expansion, and applies it to design a single transmission overlay balancing both optimality and flexibility.

1.3 Thesis Organization

The remainder of this thesis is organized as follows: Chapter 2 introduces the study frame work and necessary study assumptions. Chapter 3 presents the generation forecast model assumptions and methods. Chapter 4 introduces and implements the IRMST algorithm. Chapter 5 deduces the innovative TNEP modeling approach which is suitable for the national transmission design problem. Chapter 6 introduces the flexibility

design approach. Chapter 7 discusses the study results. Chapter 8 evaluates the steady state operational benefits of designed overlays. Chapter 9 concludes and proposes possible future work on this topic.

CHAPTER 2. METHODOLOGY AND ASSUMPTIONS

2.1 Interdependencies between Transmission and Generation

Transmission expansion planning is usually driven by demand increase and generation interconnection needs, in compliance with reliability and other planning requirements, aiming to improve system operating performance and efficiency. Thus, inherent interdependencies exist between generation and transmission expansion planning activities. Generation expansion may lead to future transmission investments and vice versa, building a new circuit may also provide transmission access for future generation units and could thus influence generation expansion decisions. Transmission investments may also reduce the need for generation expansion and overall operation costs, as will be discussed in Chapter 5.

Transmission and generation expansion planning studies are usually conducted separately in both vertically-integrated utilities and deregulated markets [23] because, for large power systems, the resulting model will generally be complex and thus very challenging to solve. In most classic transmission planning models [18], [19], and [24], generation outputs of each unit are determined *a-priori*, so the only objective is to minimize transmission investment costs. The "value-based" planning approach [25]–[27] is a step forward from this approach; it evaluates the benefit of transmission investments in terms of generation production cost reduction. Its objective function contains both transmission investment costs and generation production costs. Some existing studies do

examine coordination between generation and transmission expansion [28]–[30]. Reference [31] implements Benders decomposition and Lagrangian relaxation to coordinate between generation and transmission. Reference [32] introduces a co-optimization model based on micro-grids, and reference [33] studies the coordination between generation-unit commitment and transmission switching. Reference [34] performs co-optimization using a superconducting fault current limiter (SFCL), while reference [35] investigates coordination between generation and transmission maintenance outage scheduling.

Generally speaking, there are three major approaches to performing joint transmission and generation planning in engineering studies and addressing interdependencies between them. The most widely used current method in both industry and academia is the so-called “copper sheet” analysis [4]. This method first releases all transmission capacity constraints and then optimizes a generation investment and production plan to forecast a Locational Marginal Price (LMP). The LMP is often used as an indicator of future transmission needs.

A second commonly-used method is to alternatively perform generation and transmission expansion optimization using a carefully-designed iterative procedure. Reference [31] implements Benders decomposition and Lagrangian relaxation to implement an iterative process for simulating interactions among GENCOs, TRANSCOs, and Independent System Operators (ISOs). Still another common method is to first simply perform “copper sheet” analysis to obtain a generation portfolio under ideal conditions, and then perform transmission optimization using this generation portfolio. The optimized transmission investment plan is then fed back to the original generation

investment optimization problem and re-optimized for a new generation portfolio. This updated generation portfolio is used to again perform transmission expansion optimization. This process is iteratively repeated until the mismatch between two consecutive solutions is reduced to a value within an acceptable tolerance. This method is illustrated in Fig. 2.1. As in most situations of this type, generation investment cost turns out to be more significant than transmission investment cost and generation production cost, so it is possible, but not guaranteed, that such an iterative process will rapidly converge.

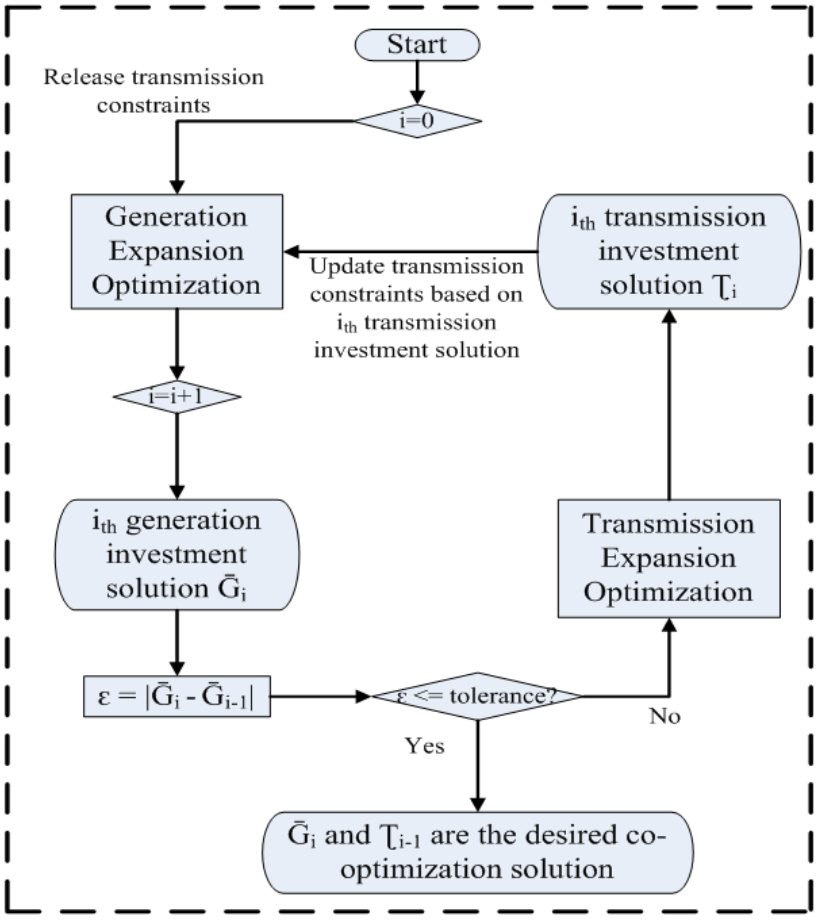

Fig. 2.1: An iterative approach for joint transmission-generation expansion optimization.

A third method is to perform a single, integrated co-optimization with both transmission and generation considered together. This is obviously the most direct way to coordinate between generation and transmission, but this method tends to introduce excessive computational load for large systems, especially when reliability requirements like N-1 security constraints must be included.

2.2 Study Framework

This thesis reflects a large geographical scope and long planning horizon. It is based on the "copper sheet analysis" approach mentioned in the previous section, and is extended from the planning methodology described in the Midcontinent Independent System Operator (MISO)'s MTEP 2010 report [36]. It proposes a well-articulated study framework consisting of four major steps (Fig. 2.2). The study framework is limited to pure engineering analysis without considering any concerns regarding legislation, political issues, or stakeholder interaction.

In this thesis, all studies have been performed to reflect a 40-year planning horizon. The length of the planning horizon is chosen to be longer than what is typically used in industry. To the extent that a circuit is economically justified in that it allows investment in better performing (higher capacity factor) generation, short planning horizons are generally fine, to the extent that generation capacity investment occurs within the planning horizon. But if a circuit is partially justified by the operational benefits (e.g., lower production costs and/or lower regulation costs) it enables, then a long-term planning horizon may be critical.

The first step of the process developed in this thesis is generation forecast using NETPLAN[1] software. This step determines the amount, timing, location, and type of future generation; transmission capacity is assumed here to be infinite. The second step is transmission candidate selection to reduce the solution space by identifying promising nationwide transmission candidates and develop their location-specified information. The third step is network expansion optimization, the most crucial part of the study framework. It models the TNEP as a MILP model based on step 1 and step 2 results. Steady-state contingency analysis is also be performed after solving the original model to obtain an updated model with appended security constraints is then solved to obtain a transmission plan reflecting certain security requirements. For each scenario, we obtain a transmission investment plan, followed by a design methodology implemented to balance optimality and flexibility among different scenarios and produce a single overlay adaptable to various possible futures. The final step is to perform benefit analysis to quantify these designs' overall economic and environmental benefits in terms of total cost and CO_2 emissions. In the next three chapters, we describe each step of the study method.

[1] NETPLAN software tool is developed by Eduardo Ibanez at Iowa State University. It can be used to perform resource adequacy studies and generation planning. More details will be introduced in the next chapter.

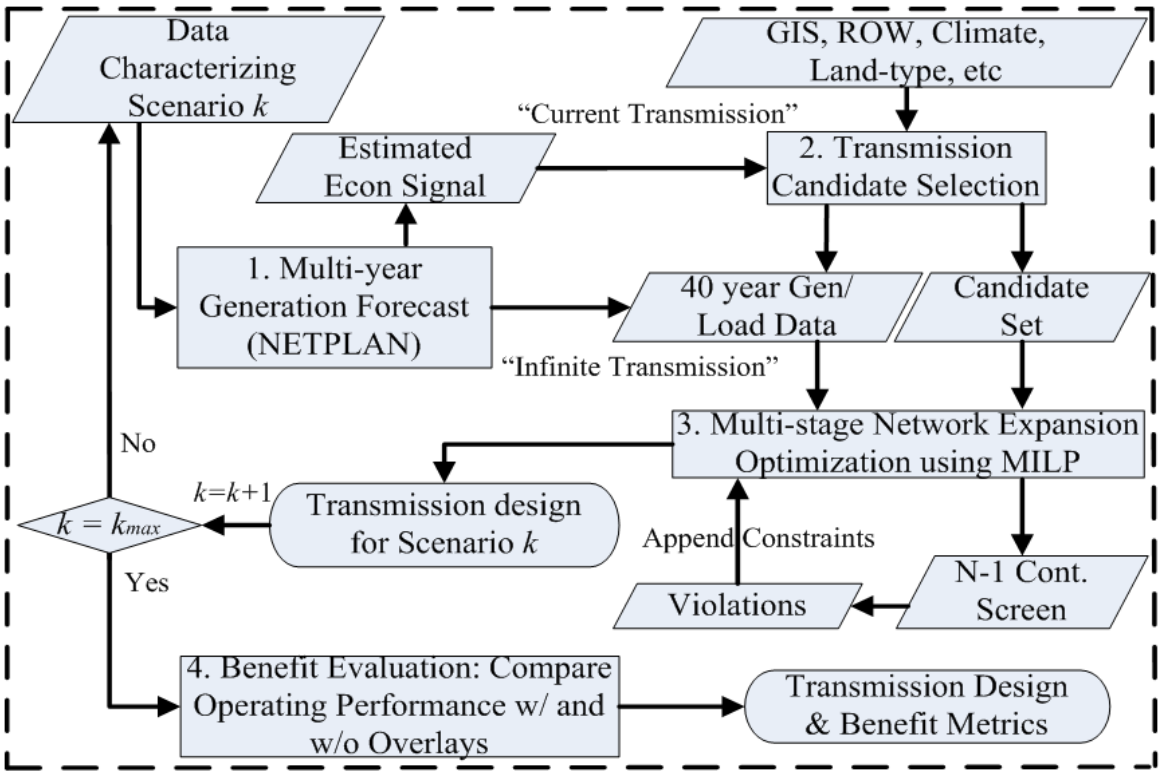

Fig. 2.2: Study framework of this thesis.

CHAPTER 3. GENERATION FORECAST

3.1 Introduction to NETPLAN Multi-Objective Planning Tool

The National Energy and Transportation Planning Tool (NETPLAN) is the implementation of a long-term investment and operation model for the energy and transportation systems [37]. The software is developed by Eduardo Ibanez, who obtained his PhD degree at Iowa State University in 2011. NETPLAN models energy systems[2], transportation systems[3], and interdependencies between the two sectors. It has a two-layer optimization architecture, built on CPLEX solver, shown in Fig. 3.1. The lower layer is a linear programming model, which minimizes the overall investment and production costs. The upper layer is a multi-objective solver to balance between cost, emission and resiliency [12]. In this thesis, we only utilize its lower layer as the scenario design tool. Its functionality is similar to industry level applications like Electric Generation Expansion Analysis System (EGEAS) [38] and PLEXOS [39]. One thing that needs to be pointed out is that NETPLAN does not support transmission expansion planning with DC power flow constraints. Thus, we use it to optimize generation investments under certain assumptions to minimize total cost, including generation investment cost, operation and maintenance cost, fuel cost and other related costs.

[2] Including conventional and renewable generation, transmission, and other energy demands.
[3] Including railways, highways, natural gas pipelines, trucks, electric vehicles, ships, airlines and other transportation freights and infrastructures.

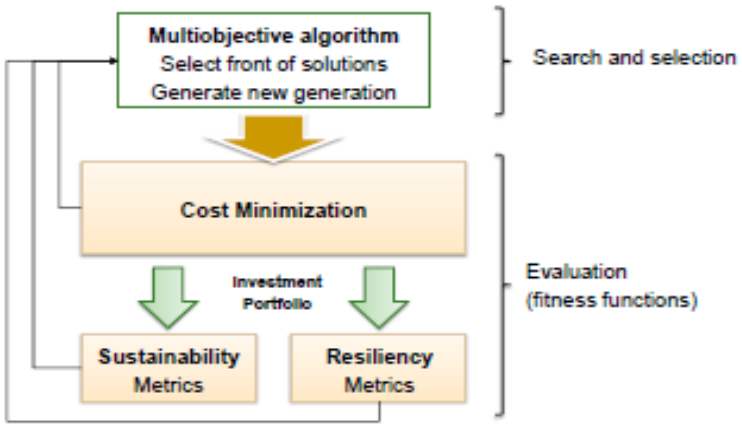

Fig. 3.1: NETPLAN optimization architecture (source: [37]).

3.2 62-Node National Electric System Model

The model shown in Fig. 3.2 is an aggregated electric system model reduced from a national production cost dataset. In this thesis, we will use this model as our base study case. The model has 62 nodes, one of each representing a certain area or sub-area in U.S. contiguous power system (excluding Alaska, Hawaii and other Pacific islands) [40]. Generally speaking, the area boundaries are divided according to North American Electric Reliability Corporation (NERC)'s region and sub-region map [41]. Table 3.1 is a summary of node name abbreviations and each region's name list. Another map using clearer geographical locations and systematic node naming system in accordance with NERC's region names is displayed in Fig 3.3. In the remainder part of this thesis, all transmission investment maps will be in the format of Fig. 3.3.

On each node, we define 15 equivalent generation units, with each one representing a certain generation technology. The 15 generation technologies include: nuclear, pulverized coal, natural gas combined cycle, combustion turbine, hydro, inland wind, off -shore wind, oil generation, IGCC, solar PV, solar thermal, geothermal, IPCC,

tidal power and OTEC. There are 142 existing transmission paths, representing major existing paths (in the West) and flowgates (in the East and Texas) all around the contiguous U.S.

Table 3.1: Explanation of node name abbreviations.

Abbreviation	Zone Name	Abbreviation	Zone Name
AZ	Arizona - PV	FE	FirstEnergy ATSI
AE	Associated Electric	P6	PJM MidAtlantic - East PA
CS	CAISO - SCE	P7	PJM MidAtlantic - SW
CD	CAISO - SDGE	P8	PJM MidAtlantic – W. PA
CZ	CAISO - ZP26	SE	Southeastern
CB	CAISO Bay Area	S1	SPP - Central
CN	CAISO North	S2	SPP - KSMO
CA	Carolinas	TV	TVA
CV	Central Valley	UT	Utah
CI	Cincinnati	WY	Wyoming
CE	Colorado East	FL	Florida
LP	LADWP	DK	Dakotas
CW	Colorado West	II	Imperial Irrigation District
M1	MISO - Gateway	S3	SPP - Louisiana
M2	MISO - Indiana	S4	SPP - Nebraska
M3	MISO - Iowa	P1	PJM - AEP
M5	MISO - Michigan	ID	Idaho
M6	MISO - Minnesota	NS	NE - SWCT
M7	MISO - North Dakota	NW	Northwest - MID-C
M8	MISO - WI-UPMI	N1	NY-AB (West)
NN	N Nevada	N2	NY-CDE (Cent North)
NE	NE - East	N3	NY-F (Capital)
NI	NE - Maine	N4	NY-GHI (Southeast)
P5	PJM MidAtlantic - E	N5	NY-J (NY City)
ET	Entergy	N6	NY-K (Long Island)
EH	ERCOT - Houston	SN	S Nevada - MEAD
EN	ERCOT - North	P2	PJM - APS
ES	ERCOT - South	P3	PJM - COMED
EW	ERCOT - West	P4	PJM - South
KY	Kentucky	NT	NE - West
NM	New Mexico	MT	Montana

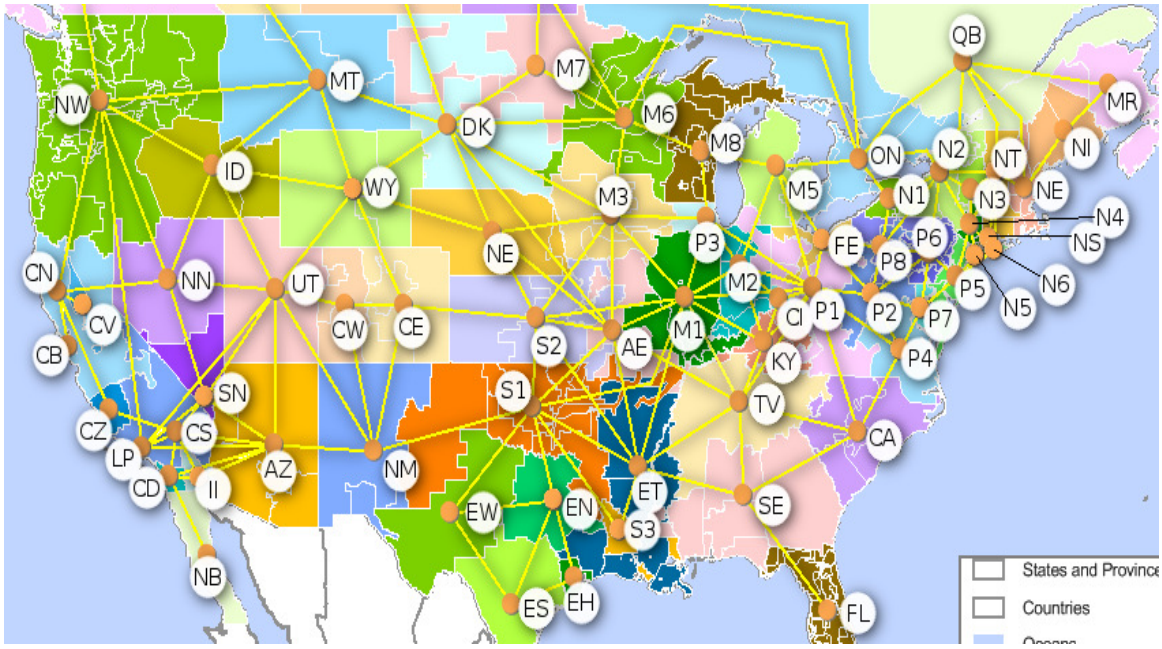

Fig. 3.2: Map of the 62-node model for U.S. contiguous power system.

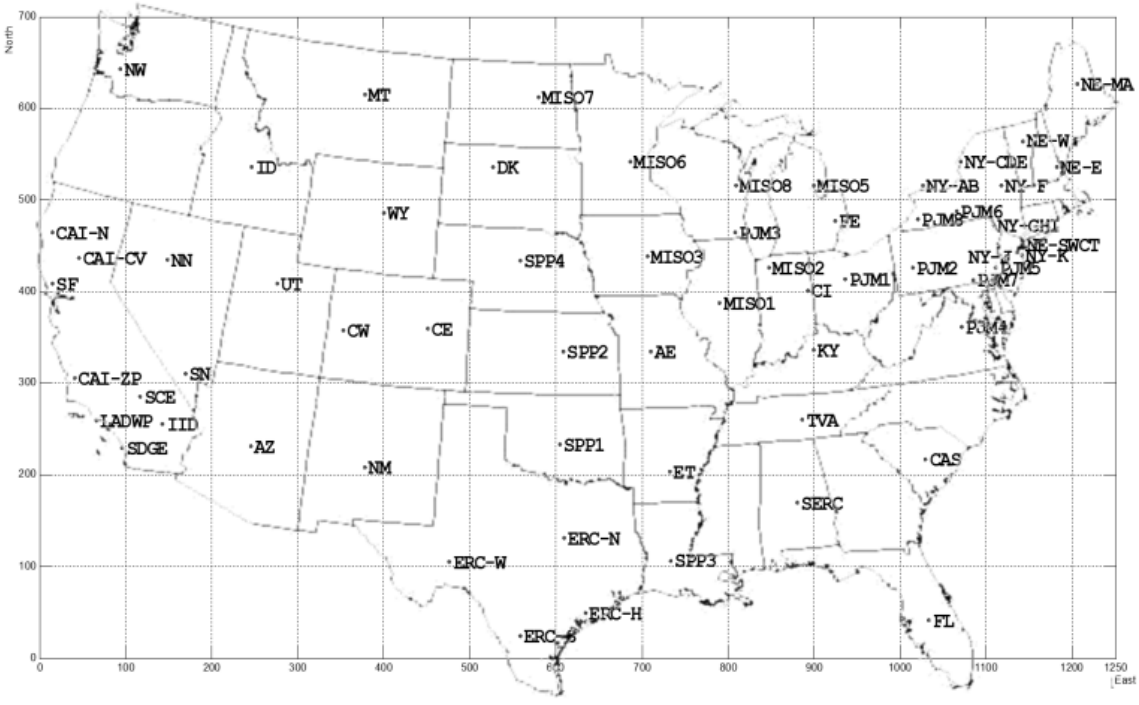

Fig. 3.3: Map of the 62-node model with NERC's region naming routine.

The model also identifies location-specified generation investment costs, renewable generation capacity factors and CO_2 emission rates. It covers not only the electric sector, but also the transportation sector. It has been prepared in NETPLAN input format thus ready for use in NETPLAN simulations. The model is originally prepared by Joseph Slegers, a M.S. student at Iowa State University. However, in order to perform accurate simulations focusing on power system sector, his original model needs refinement in renewable capacity factors, generation investment cost and some other dataset, which will be introduced in the next few sections.

3.3 Scenario Design Assumptions

Based on the original 62-node model and a few credible data sources, we made several reasonable data adjustments and assumptions to enhance it for national transmission study purposes.

3.3.1 The "Annual Energy Outlook"

The Energy Information Administration's Annual Energy Outlook [42] is a comprehensive summary of energy system data and forecast across the U.S. It provides a good reference of credible data acquisition for this study. Particularly, it includes projections of U.S. energy supply, demand and prices. In this thesis, we assume major types of conventional generation, including nuclear, hydro, and combustion turbine, maintain the investment trends consistent with projections up to year 2035 from [42].

3.3.2 Load growth and regional reserve requirement

Another major reference we used in editing study cases is [41], the Long Term Reliability Assessment 2010 from NERC. It contains credible predictions of regional

electricity demand growth rate, and precise regional reserve requirements, which we keep consistent within this study. These data are summarized in Table 3.2 and Table 3.3.

Table 3.2: Regional active load growth rate.

Node	Demand Growth Rate	Node	Demand Growth Rate	Node	Demand Growth Rate
AE	0.63%	ET	1.55%	NY-J	0.64%
AZ	2.00%	ERC_W	1.72%	NY-K	0.64%
CAS	1.72%	FE	1.40%	NY-CHI	0.64%
SF	1.10%	FL	1.30%	NY-F	0.64%
SDGE	1.20%	ID	2.20%	NY-CDE	0.64%
CE	1.80%	IID	1.20%	NY-AB	0.64%
CI	1.40%	KY	1.40%	NE-MA	1.40%
CAI_N	1.10%	LADWP	1.20%	NE-W	1.40%
SCE	1.20%	MISO1	0.63%	NM	2.00%
CAI_CV	1.10%	MISO2	1.40%	NN	2.20%
CW	1.80%	MISO3	1.24%	NE-E	1.40%
CAI_ZP	1.20%	MISO5	1.40%	NESWCT	1.40%
DK	1.24%	MISO6	1.24%	NW	1.20%
ERC_H	1.72%	MISO7	1.24%	PJM1	1.40%
ERC_N	1.72%	MISO8	1.24%	PJM2	1.40%
ERC_S	1.72%	MT	2.20%	PJM3	1.40%
PJM4	1.40%	SPP1	1.30%	SN	2.00%
PJM5	1.40%	SPP2	1.30%	TVA	1.82%
PJM6	1.40%	SPP3	1.30%	UT	2.20%
PJM7	1.40%	SPP4	1.24%	WY	2.20%
PJM8	1.40%	SERC	1.96%		

Table 3.3: Regional reserve requirements.

Sub-region	NERC Reference Reserve Margin Level (%)
FRCC	15.00%
MRO	15.00%
NPCC	15.00%
New	15.00%
New	18.00%
RFC	15.00%
SERC	15.00%
Central	15.00%
Delta	15.00%
Gateway	11.90%

Table 3.3. (Continued).

Sub-region	NERC Reference Reserve Margin Level (%)
Southeastern	15.00%
VACAR	15.00%
SPP	13.60%
TRE	12.50%
WECC	14.70%
Basin	12.00%
Cal-N	14.60%
Cal-S	14.80%
Desert	13.60%
Northwest	18.60%
Rockies	12.30%

3.3.3 "Copper Sheet Analysis"

The "copper sheet analysis" is to release all transmission thermal, voltage and stability constraints to perform generation investment and/or production cost simulations, so as to roughly identify the ideal generation investment and operation patterns and in consequence, the transmission needs. By comparing the power flow simulations with and without transmission limits, one can easily tell where the transmission needs are. The areas where the Locational Marginal Price is low will be treated as "sources," while areas where the Locational Marginal Price is high will be treated as "sinks." Promising transmission candidates are usually the connections between a source and a nearby sink. Although controversy exists that post-investment LMP may drop and reduce the economic benefit prediction justified based on pre-investment transmission network, the "copper sheet analysis" could still provide good estimations for selecting transmission candidates, indicating possible bottlenecks of current system. In general, its results tends to over-estimate, but not under-estimate the economic benefit of a candidate route, thus will be adequate for selecting transmission candidates for further refinement and

optimization.

In this study, we implement this approach by setting all transmission capacity limits to be infinite in the base case, and perform generation investment optimization in NETPLAN.

3.3.4 Geothermal investment cost estimation

Location specified geothermal investment costs are estimated mainly based on references [43] and [44]. We apply the method introduced in [43] to approximate the relationship between drilling depth and investment cost (illustrated in Fig 3.4), and estimate the drilling depth of geothermal resources on each of the 62 nodes based on the information in [43] and [44]. Figure 3.5 gives the geothermal resource map of the U.S.

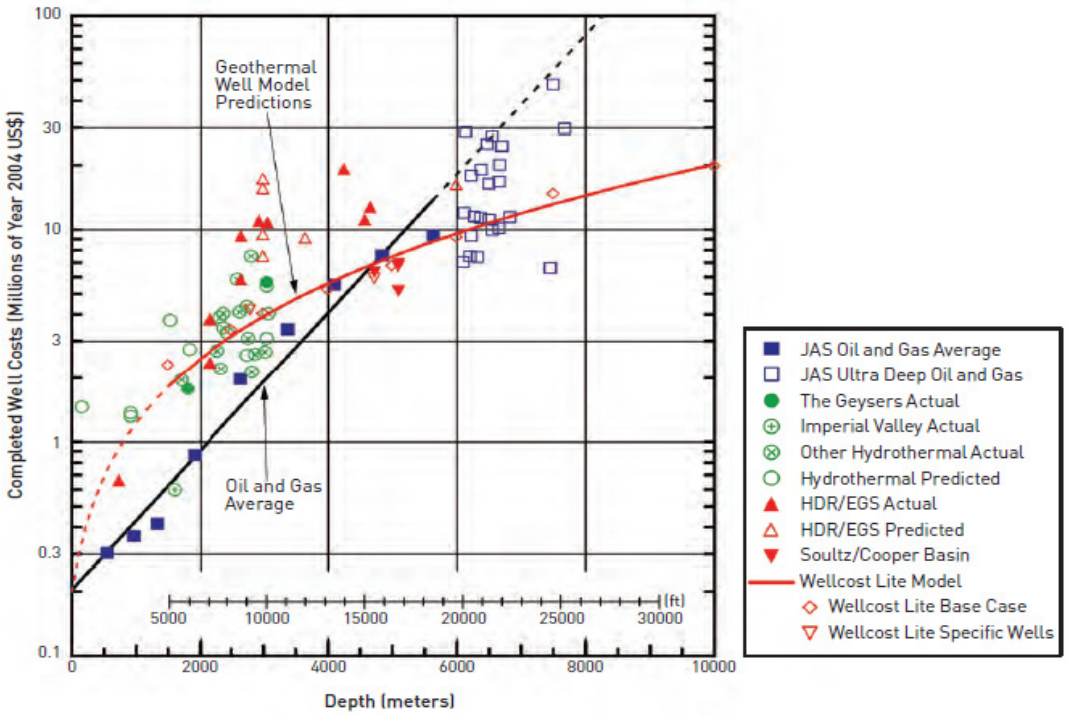

Fig. 3.4: Well costs as a function of depth[4] (source: [43]).

[4] 1. JAS = Joint Association Survey on Drilling Costs.

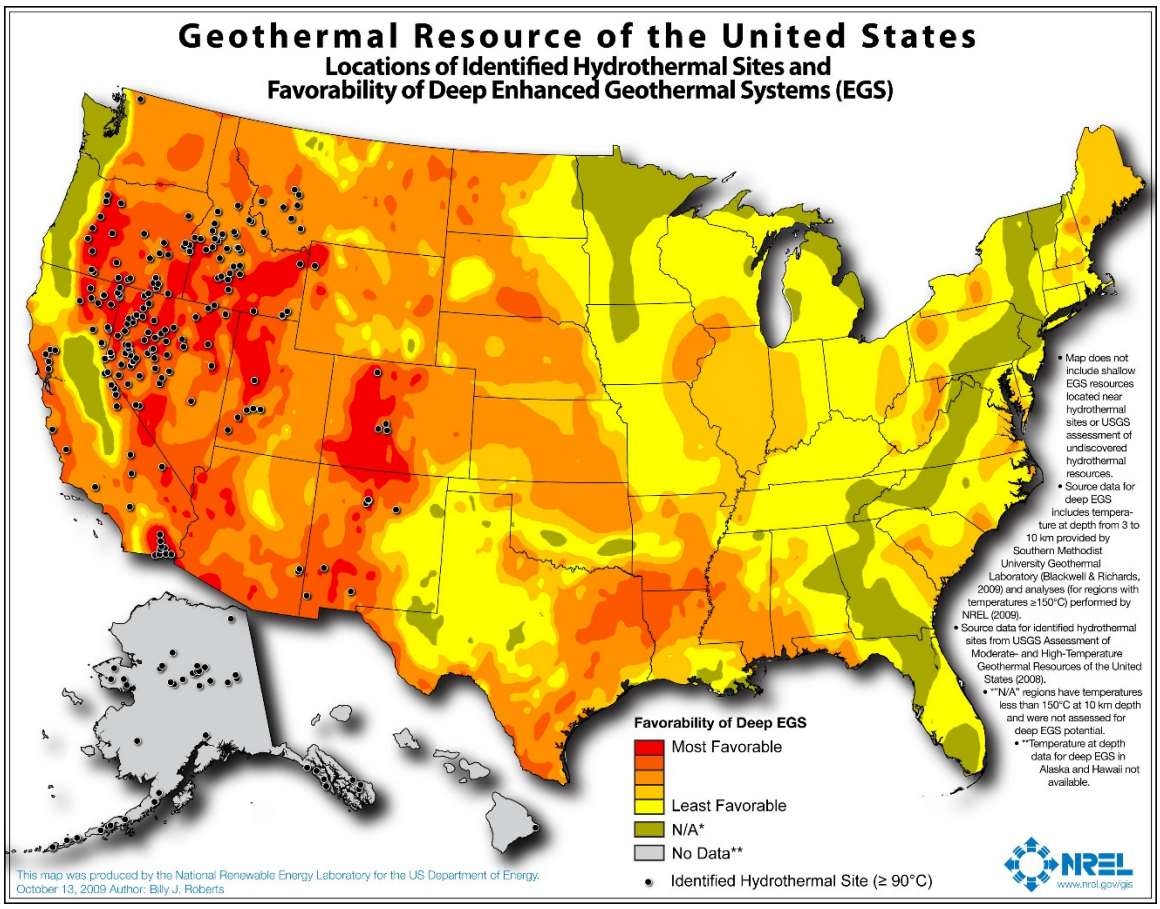

Fig. 3.5: Geothermal distribution map of the U.S. (source: [44]).

The resulting geothermal investment cost estimation on each node is summarized in Table 3.4. All costs have been discounted to 2010 dollars.

2. Well costs updated to US$ (yr. 2004) using index made from 3-year moving average for each depth interval listed in JAS (1976-2004) for onshore, completed US oil and gas wells. A 17% inflation rate was assumed for pre-1976 years.

3. Ultra deep well data points for depths greater than 6 km are either individual wells or averages from a small number of wells listed in JAS (1994-2000).

4. "Other Hydrothermal Actual" data include some non-US wells (Source: Mansure 2004).

Table 3.4: Geothermal generation investment cost.

Node	Investment Cost (M$/GW)	Node	Investment Cost (M$/GW)
AE	3190.797	E1MT	2628.672
AZ	2628.672	E1N1	3752.921
CA	3752.921	E1N2	3752.921
CB	2628.672	E1N3	3752.921
CD	2628.672	E1N4	6563.543
CE	3190.797	E1N5	6563.543
CI	4315.045	E1N6	6563.543
CN	3752.921	E1NE	3752.921
CS	2628.672	E1NI	3752.921
CV	1504.424	E1NM	1504.424
CW	1504.424	E1NN	1504.424
CZ	2628.672	E1NS	4315.045
DK	1504.424	E1NT	6563.543
EH	2628.672	E1NW	1504.424
EN	2628.672	E1P1	4315.045
ES	2628.672	E1P2	4315.045
ET	3190.797	E1P3	4315.045
EW	6563.543	E1P4	4315.045
FE	4315.045	E1P5	4315.045
FL	6563.543	E1P6	6563.543
ID	1504.424	E1P7	3190.797
II	1113.626	E1P8	3752.921
KY	6563.543	E1S1	2628.672
LP	2628.672	E1S2	2628.672
M1	3752.921	E1S3	3190.797
M2	4315.045	E1S4	2628.672
M3	3752.921	E1SE	6563.543
M5	6563.543	E1SN	1504.424
M6	6563.543	E1TV	4315.045
M7	6563.543	E1UT	1504.424
M8	6563.543	E1WY	1113.626

3.3.5 Offshore wind investment cost estimation

Offshore wind investment cost is related to the location's bathymetry, particularly the depth and distance to shore. The deeper the location is, the higher the turbine and cable construction cost is. The farther from shore, the higher the transmission cable cost will be. Based on data from the National Renewable Energy Lab's [45], we estimated the

offshore wind investment costs for the nodes where offshore wind resources exist, as listed in Table 3.5. All costs have been discounted to 2010 dollars. Figure 3.6 gives the offshore wind resource map of continental U.S.

Table 3.5: Offshore wind generation investment cost.

Node	Investment Cost (M$/GW)	Node	Investment Cost (M$/GW)
CA	2332	NI	2854
EH	2227	NW	2854
ES	2227	P4	2680
S3	2367	P5	2680
N5	2576	P7	2680
N6	2576	CN	2738
NE	2854	CB	2738

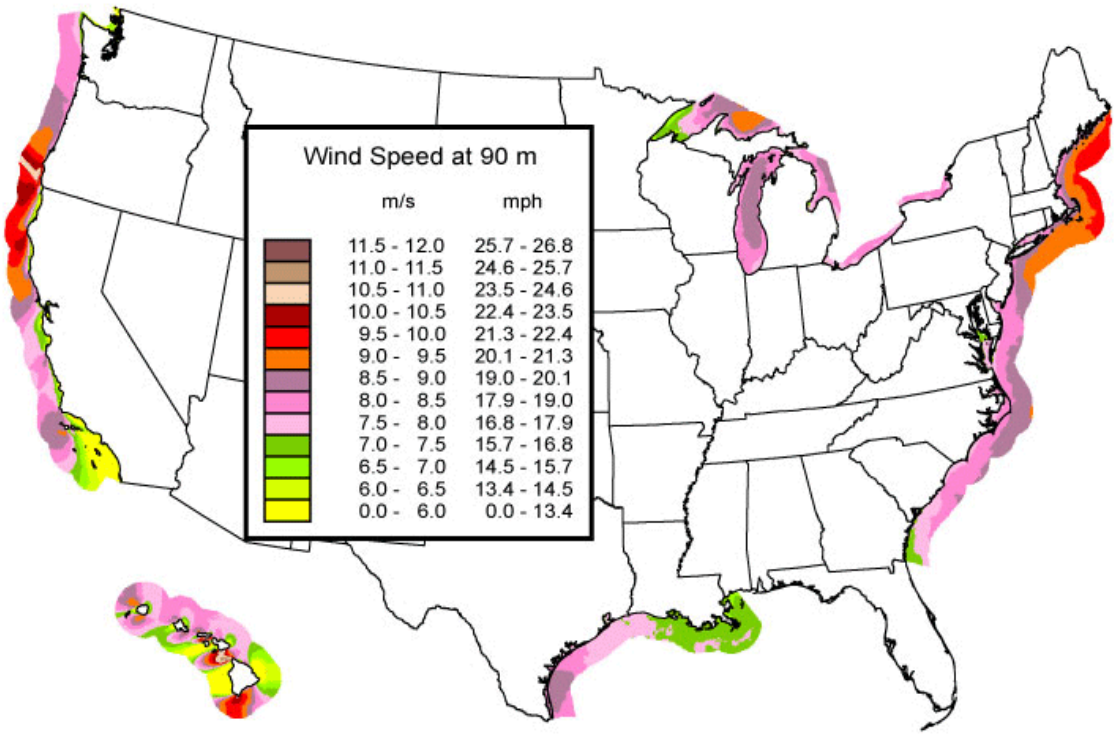

Fig. 3.6: Offshore wind distribution map of the U.S. (source: [45]).

3.3.6 Other data adjustments and assumptions

Other renewable and conventional generation investment and production cost data were well developed in the original base case. Location specified renewable capacity factors have also been calibrated according to reference [3]–[4] and [43]–[45]. In addition, we assume that there are no future investments in coal-fired plants.

3.4 Multi-case Study Based on Global Uncertainties

Transmission investment solutions will be significantly influenced by the types of renewable generation selected as major elements of future generation portfolios. As we can roughly observe from Figs. 3.5 through 3.8, in the contiguous U.S. each type of renewable resource (inland wind, offshore wind, solar, or geothermal) has its own unique distribution pattern, so transmission access needs can vary dramatically among different types of renewable generation.

Generally speaking, most high-quality inland wind capacity in the contiguous U.S. exists in certain states in Midwest areas and near Great Basin, including Montana, Wyoming, the Dakotas, Minnesota, Iowa, Colorado, Nebraska, Kansas, Oklahoma, and Texas. Unfortunately, these areas are far away from major load centers. Offshore wind resources, on the other hand, relatively concentrated in the San Francisco bay area and the Atlantic coast near New England and New York, obviously need less transmission access because they are close to a number of major load centers. The best solar resources are in Arizona, New Mexico, Colorado, California, and Florida, located relatively distant from load centers. Final, geothermal resources are scattered across the whole Western Electricity Coordinating Council (WECC) area, are distant from load centers, and

consequently require numerous transmission additions for interconnection. Transmission needs, distribution patterns, and distances to load centers for the four types of renewable resources are summarized in Table 3.6.

Table 3.6: Renewable resource distribution and transmission needs.

Type of Resource	Distribution	Distance to Major Loads	Transmission Needs
Inland Wind	Scattered	Remote	Medium
Offshore Wind	Concentrated	Close	Low
Solar	Concentrated	Remote	Medium
Geothermal	Highly Scattered	Remote	High

This thesis is motivated by the potential of large renewable penetrations. Thus, we designed four future scenarios as study cases: a reference case, a large offshore wind case, a large solar case, and a high geothermal case. These four cases are representative of future renewable generation patterns that may require significantly different transmission designs. We will introduce these four case studies in Chapter 7.

Currently, among all available renewable generation technologies, inland and offshore wind, solar thermal and solar PV, and geothermal energy are the most economically promising ones. Particularly, inland wind has the highest maturity level and has already been implemented in a relatively large scale. Thus, we select the future with in-land wind as the major renewable resource as the reference study case, and we select three other futures as derivative from this reference future. The major renewable generations considered are offshore wind, solar and geothermal, respectively. The four scenarios, though not exhaustive by any means, provide a representative sample of possible futures.

For the reference case, we follow all assumptions introduced in the previous sections to prepare data. For each of the other three high renewable cases, we assume the investment cost of a certain type of renewable generation (offshore wind, solar, or geothermal) becomes relatively lower, respectively, representing a situation where the technology matures more quickly, becoming more economically attractive. We assume the generation investment costs of offshore wind, solar, or geothermal have been reduced to 50%, 22.5% and 60% of original values, respectively, in each of the three cases. This enables NETPLAN, which is based on economic optimization, to increase the technology's penetration level to the desired level. However, in assessing benefits in Chapter 8, we maintain the original cost estimates of each technology.

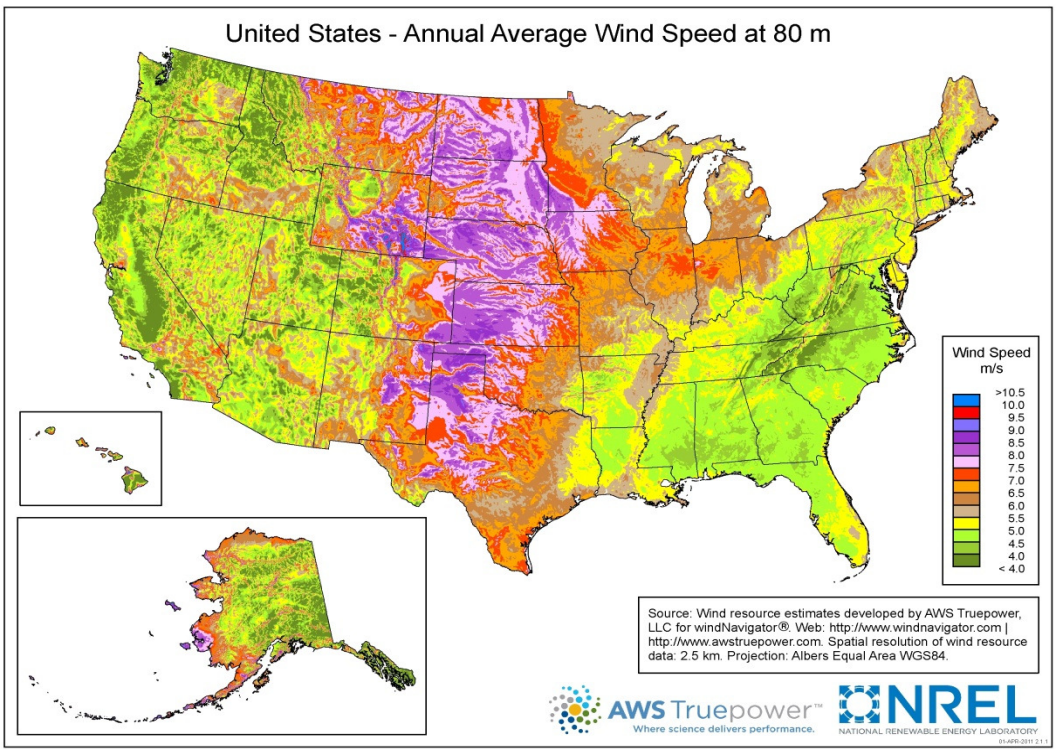

Fig. 3.7: Inland wind distribution map of the U.S. (source: [46]).

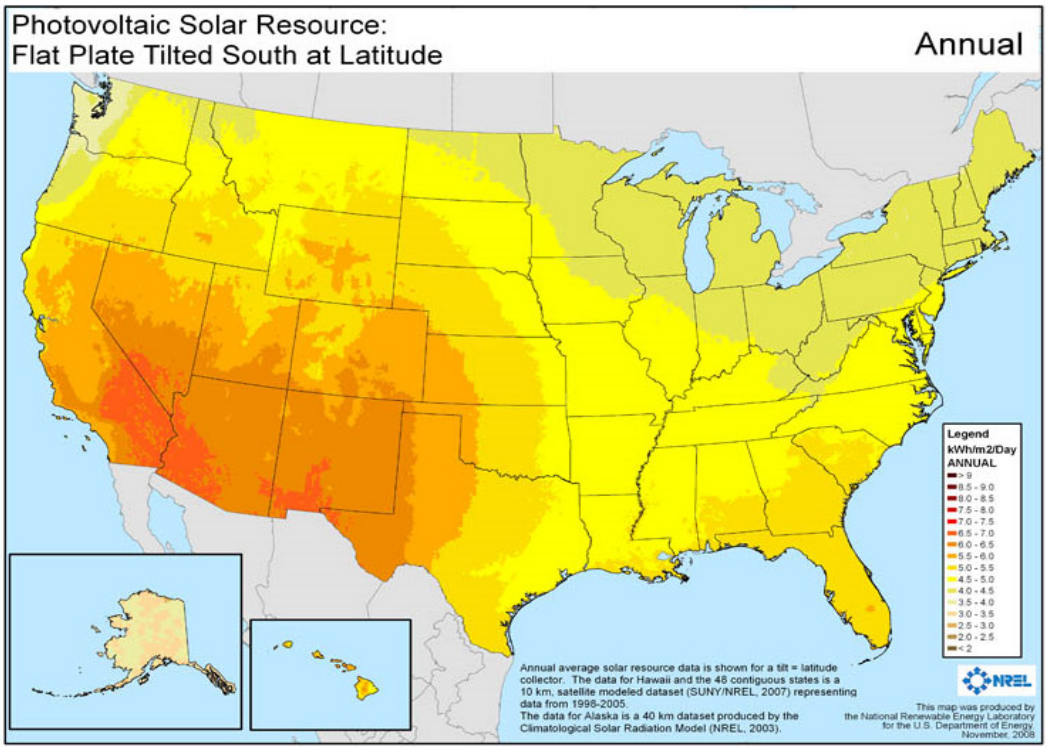

Fig. 3.8: Annual PV solar radiation at 10km (source: [47]).

CHAPTER 4. TRANSMISSION CANDIDATE SELECTION

4.1 Transmission Routing

In this chapter, we describe and illustrate the method developed to select promising nationwide transmission candidates. Selecting many transmission candidate routes for a single integrated system design is rare in traditional planning processes because, in traditional transmission studies, transmission circuit investments are usually studied one at a time or at most in limited numbers. Thus, selecting a good candidate route set for a large network is a new challenge requiring a systematic approach.

Transmission candidate routing is among one of the most complex engineering problems. A very wide variety of issues, including socio-economic features, health and safety features, engineering features, environment and geographical features, should be addressed in the selection process [48]. To simplify this problem without losing too much accuracy, and since our study is from pure engineering point of view and is focusing on cost minimization, we carefully select a few representative i factors which could significantly influence transmission investment decisions. These factors include: right-of-way (ROW) availability, restricted lands including Native American reserves, national and state parks and extreme natural conditions such as high lightning density regions, terrain condition, population density along the route, forest areas, wind and ice-loading, and economic values. A “good” transmission circuit candidate set should consider all of the above factors and meet the following criteria:

a) It should contain all good arcs which might be invested in the TNEP optimization;

b) It should contain a limited number of arcs to avoid causing excessive TNEP optimization model size;

c) It should form an N-1 connected network to ensure feasibility for TNEP optimization with reliability constraints (although it is not necessary that it be a complete network[5]);

d) The major selecting objective should be consistent with TNEP optimization, which is to minimize total cost. An acceptable approximation is allowed as it is unnecessary to ensure optimality in this step.

We developed an innovative method which takes consideration of all major influencing factors and is able to pick up promising candidates from a network point of view based on these criteria above. The method is introduced in the following sections below.

4.2 Introduction to Minimum Spanning Tree Problem

4.2.1 Problem formulation

The Minimum Spanning Tree (MST) problem is one of the most frequently cited problems in graph theory. Before we proceed to discuss it, there are several key definitions that we need to repeat [17]:

a) ***Graph:*** An ordered pair G = (E, V) comprising a set V of vertices or nodes together with a set E of edges or lines, which are 2-element subsets of V;

[5] A complete network is defined as a graph in which each node is connecting to each other [17].

b) ***Connected graph:*** A graph with all of its vertices being connected by edges;

c) ***Connectivity:*** The minimum number of elements (nodes or edges) which need to be removed to disconnect the remaining nodes from each other;

d) ***Edge-connectivity:*** A graph is k-edge-connected if it remains connected whenever fewer than k edges are removed;

e) ***Vertex-connectivity:*** A graph G is said to be k-vertex-connected (or k-connected) if it has more than k vertices, and the result of deleting any (perhaps empty) set of fewer than k vertices is a connected graph;

f) ***Directed graph:*** A directed graph (or digraph) is a graph, or set of nodes connected by edges, where the edges have a direction associated with them;

g) ***Undirected graph:*** An undirected graph is one in which edges have no orientation;

h) ***Tree*****:** In graph theory, a tree is an undirected graph in which any two vertices are connected by exactly one simple path;

i) ***Forest*****:** A forest is a disjoint union of trees;

j) ***Spanning Tree:*** Given a connected, undirected graph, a spanning tree of that graph is a sub-graph that is a tree and connects all the vertices together;

k) ***Cycle:*** In this thesis, we only refer to simple cycle, which is a closed walk consists of a sequence of vertices starting and ending at the same vertex, with each two consecutive vertices in the sequence adjacent to each other in the graph, and no repetitions of vertices or edges allowed, other than the repetition of the starting and ending vertex.

Based on these definitions, the MST of a certain graph has been defined as a spanning tree with weight less than or equal to the weight of every other spanning tree. The MST problem is simply to find the MST of a given graph. Obviously, if a graph has *n* vertices, then its MST will have *n*-1 edges. For any connected undirected graph, there must be at least one MST of it. There may be several MSTs of the same weight having a minimum number of edges; in particular, if all the edge weights of a given graph are the same, then every spanning tree of that graph is minimum.

The MST problem has a wide application in many different areas, like network design for computer engineering, telecommunication, water supply, transportation system, and electric power systems. Actually, power system engineering is one of the earliest applications of MST [49].

4.2.2 "Greedy Algorithms"

The first algorithm for finding a MST was developed by Otakar Borůvka in 1926 [50]. Its purpose was an efficient electrical coverage of Moravia. Currently, two algorithms are commonly used, Prim's algorithm and Kruskal's algorithm [16]. All of these algorithms are greedy algorithms that run in polynomial time. To avoid redundancy, we only briefly introduce Kruskal's algorithm in this thesis. More detailed information can be found in reference [16]. The algorithm is very explicit and straightforward, which has been summarized below:

1. Existing graph G = (E, V) and solution T= ∅;
2. Select the minimum weight edge *e* in E\T. If there is more than one edge with the same minimum weight, arbitrarily pick any one of them. If the selected edge *e* will form a cycle with other edges in current T, discard *e* and go back to (b). Else,

T=T∪ *e*;

3. If size of T is smaller than |V|-1, go back to (b) and continue. Else, stop. Current solution set T is the desired MST.

Reference [16] provides the proof of correctness of this algorithm. It is summarized here.

Proof of Kruskal's Algorithm:

The proof consists of two parts. First, it is proved that the algorithm produces a spanning tree. Second, it is proved that the constructed spanning tree is of minimal weight.

Spanning tree:

Let G be a connected, weighted graph and let T be the sub-graph of G produced by the algorithm. T cannot have a cycle, been within one sub-tree and not between two different trees. T cannot be disconnected, since the first encountered edge that joins two components of T would have been added by the algorithm. Thus, T is a spanning tree.

Minimal:

We show that the following proposition P is true by induction: If F is the set of edges chosen at any stage of the algorithm, then there is some MST that contains F.

Clearly P is true at the beginning, when F is empty: any MST will do, and there exists one because a weighted connected graph always has a MST.

Now assume P is true for some non-final edge set F and let T be a MST that contains F. If the next chosen edge *e* is also in T, then P is true for F + *e*. Otherwise, T + *e* has a cycle C and there is another edge *f* that is in C but not F. (If there were no such edge *f*, then *e* could not have been added to F, since doing so would have created the cycle C.)

Then T $-f+e$ is a tree, and it has the same weight as T, since T has minimum weight and the weight of f cannot be less than the weight of e, otherwise the algorithm would have chosen f instead of e. So T $-f+e$ is a MST containing F + e and again P holds.

Therefore, by the principle of induction, P holds when F has become a spanning tree, which is only possible if F is a MST itself.

4.3 Iterative Reweighting MST Algorithm

In section 4.1, we have listed the influencing factors that need to be addressed in selecting transmission candidate set. Here, we divide these factors into three categories, introduced as follows.

4.3.1 Right-of-Way and restricted lands

The first factor is the ROW availability and restricted lands. ROW availability will facilitate transmission investment, while restricted lands generally inhibited any transmission investments.

Despite that exceptions may exist in certain regions, ROW is generally easier to access along Interstate Highway systems (Fig. 4.2), railway routes or existing transmission lines (Fig. 4.1). Although in some situations a straight line can be used as the transmission route, in most cases, transmission lines will follow a certain route based on a variety of locational-specified concerns. In this study, to simplify the problem, without losing too much accuracy, we follow these existing ROWs to select the shortest path between nodes and then obtain the actual route distance l_{at} for each arc. We also make the minimum modification necessary to get around restricted lands, including

American Indian Reserves (Fig. 4.4), national parks and severe natural condition areas like high lightning density region (Fig. 4.3), where transmission investments are generally prohibited.

4.3.2 Investment cost equivalent

The second category of factors contains elevation (mountainous, hilly or flat land, Fig. 4.5); population density (urban, suburban or rural, Fig. 4.6); forest areas (Fig. 4.6); wind and ice-loading. They are all geographical and climate factors which usually do not prohibit transmission investment but will dramatically influence transmission investment cost. The basic idea is to estimate the investment cost increase rate incurred by those conditions. This method, called per unit cost guide, has been widely used by utilities and ISOs to estimate transmission line building cost in their generation interconnection process [15]. Assume m_t is the overall cost increase rate. It can be calculated by (4.1) below:

$$m_t = k_{tr} + k_p + k_f + k_{wi} - 3 \tag{4.1}$$

Values of k_{tr}, k_p, k_f, k_{wi} represent cost increase rates due to land forms, population, forest and wind/ice-loading, respectively. When a route passes two or more different types of land setting, weighted summation with regard to distance is used as the average reweighting factor. Their standard values are also calibrated from **[15]** and summarized in Table 4.1. From now on, we refer m_t as investment equivalent reweighting coefficient.

Table 4.1: Reweighting parameters.

Terrain k_{tr}	Population k_p	Forest k_f	Wind & Ice k_{wi}
Hilly 1.2	Urban 1.5	1.5	1/2" ice, or 20# wind 1.35
Mountainous1.3	Suburban 1.2		1" ice, 6# wind 1.45 > 2" ice, 6# wind 1.6

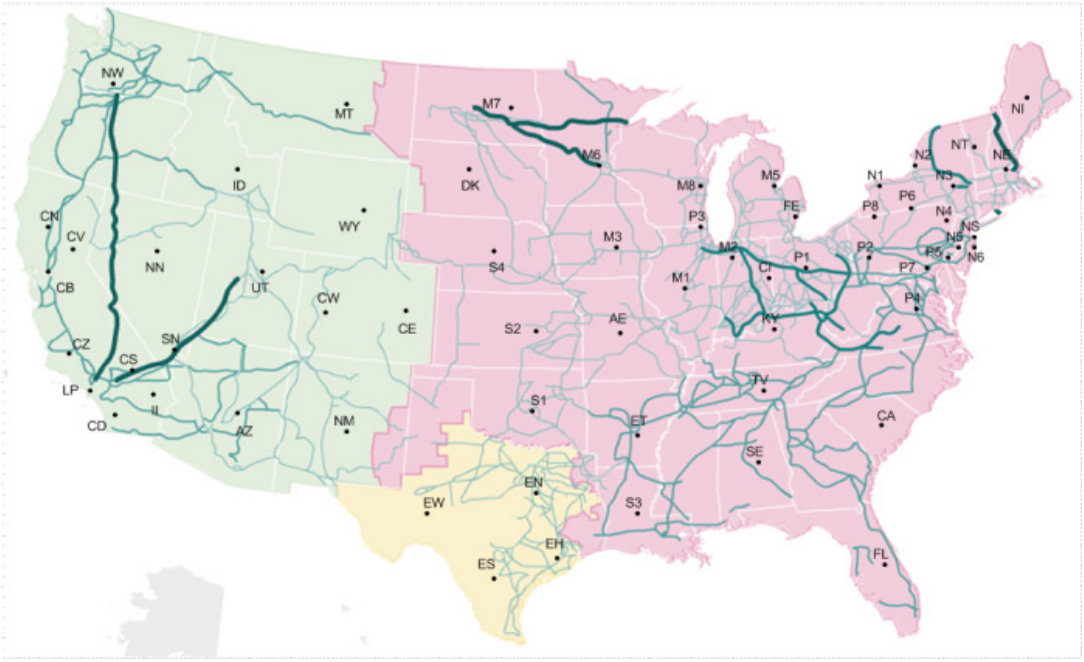

Fig. 4.1: Existing electric transmission map for the U.S. (source: [51]).

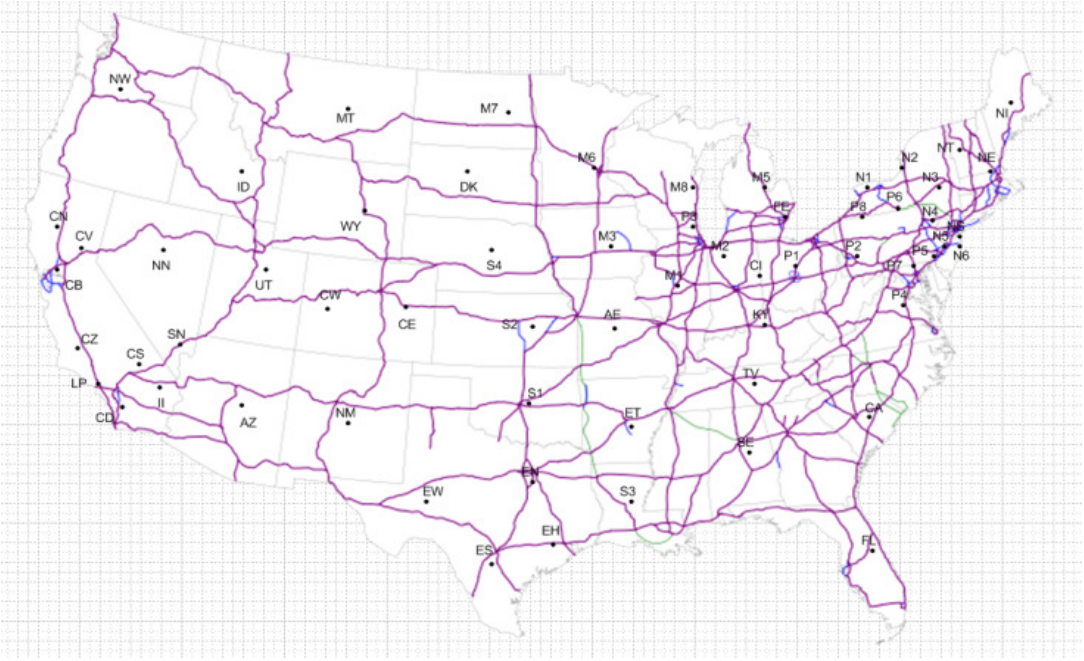

Fig. 4.2: Interstate highway system. (source: [52]).

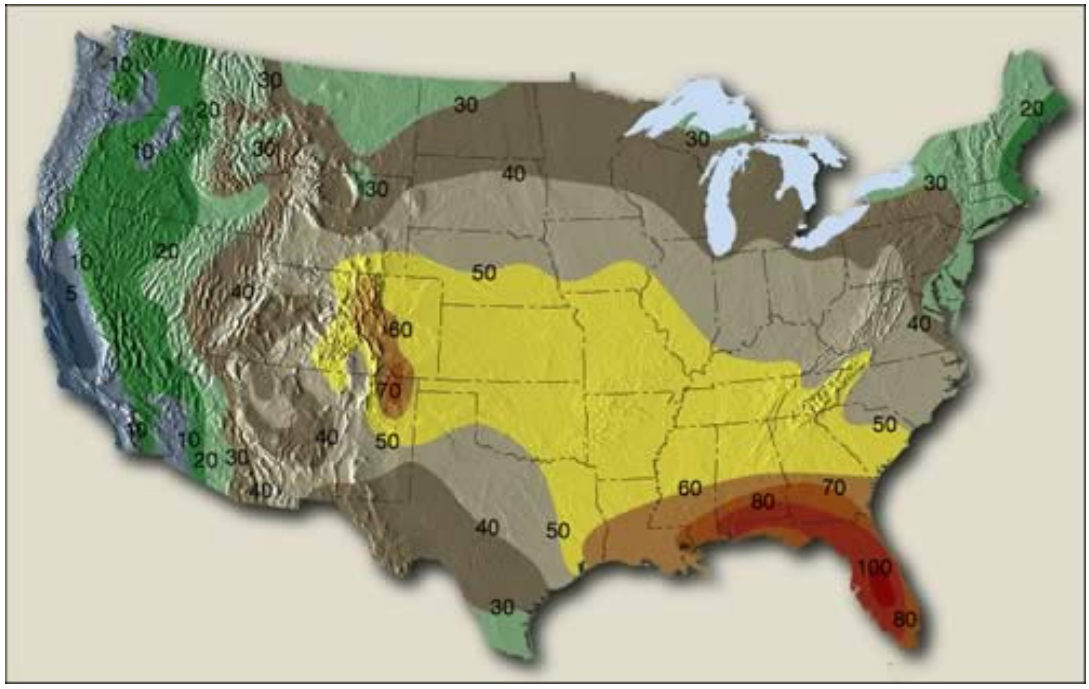

Fig. 4.3: Isoceraunic map for the U.S. (source: [53]).

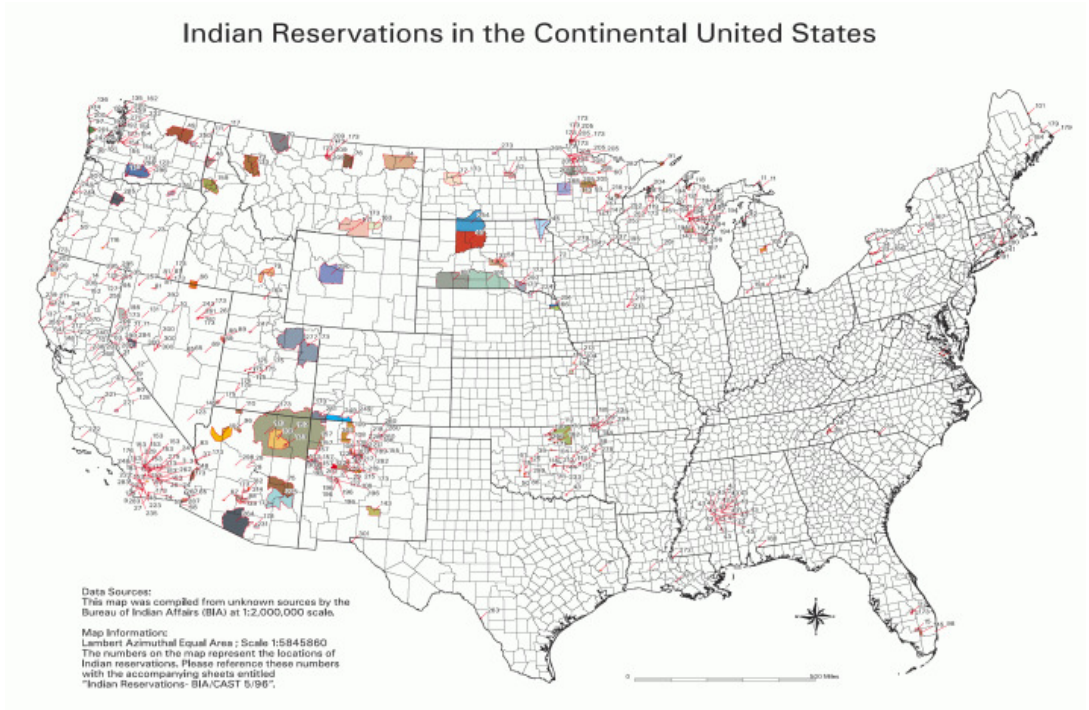

Fig. 4.4: Indian reservations in the continental U.S. (source: [54]).

Fig. 4.5: Elevation map for the U.S. (source: [55]).

Fig. 4.6: Population and forest map for the U.S. (source: [56]).

4.3.3 Production cost equivalent

The third type of factor is actually the economic value of transmission candidate. As we know, a transmission investment may reduce congestion and thus reduce system overall production cost. The economic value of a transmission investment can be evaluated by the system production cost reduction brought in by this investment. Economic value of a transmission investment is difficult to precisely predict before any Transmission Network Expansion Planning (TNEP) optimization are performed, particularly for long term planning. However, it can be roughly estimated using nodal prices of production cost simulation. The method of using nodal prices to predict transmission needs have been implemented in [4]. In this study, we perform a 40-year simplified production cost study using NETPLAN for the U.S. system with fixed current transmission capacities to get the nodal prices forecast, and then derive another type of reweighting factor which represents the economic values of candidates, referred to as n_t, as illustrated below:

To remain consistent with the objective function of TNEP, which is to minimize total investment and production cost, and also to remain consistent with the criterion (d) mentioned in section 4.1, we set the objective function of candidate selection to be maximizing profit, expressed in (4.2):

$$Max \quad \sum_{t \in E_p} \int_0^{Ct} S_{pt} dC_t - Ci_t \approx \sum_{t \in E_p} \int_0^{Ct} S_{pt} dC_t - k_t l_{at} m_t C_t \tag{4.2}$$

where S_{pt} is the sensitivity of production cost reduction on arc t, C_t is the capacity increase on arc t in candidate set E_p, Ci_t is the investment cost on arc t. Ci_t can be approximately expressed as the product of technology cost ratio k_t in M$/GW/mile, arc

actual route distance l_{at}, reweighting coefficient m_t and C_t.

To simplify the problem while maintaining acceptable accuracy for candidate selection, here we make three further assumptions:

a) S_{pt} remains constant as C_t increases;

b) Ignore technology selection at this time. Thus k_t will become a constant value;

c) In order to concentrate on potential economic value estimation, we assume all arc t have the same length l_{a0} and capacity C_t.

The objective function becomes

$$Max \quad \sum_{t \in E_p} \frac{S_{pt}}{k_t} - l_{at} m_t \tag{4.3}$$

or

$$Min \quad \sum_{t \in E_p} l_{at} m_t \left(1 - \frac{S_{pt}}{k_t l_{at} m_t}\right) \tag{4.4}$$

By introducing $S_{p0} = \max\{S_{pt}, t \in E_p\}$, (4.4) could be rewritten as

$$Min \quad \sum_{t \in E_p} l_{at} m_t n_t \tag{4.5}$$

where

$$n_t = \left(1 - \frac{S_{pt} - S_{p0}}{k_t l_{a0} m_t}\right) \tag{4.6}$$

n_t is referred to as the revenue equivalent coefficient in the remainder of this thesis. S_{pt} can be estimated by calculating the nodal prices difference between the two ends of a candidate. The nodal prices data are available in NETPLAN's solution folder of the production cost simulation with fixed existing transmission infrastructure.

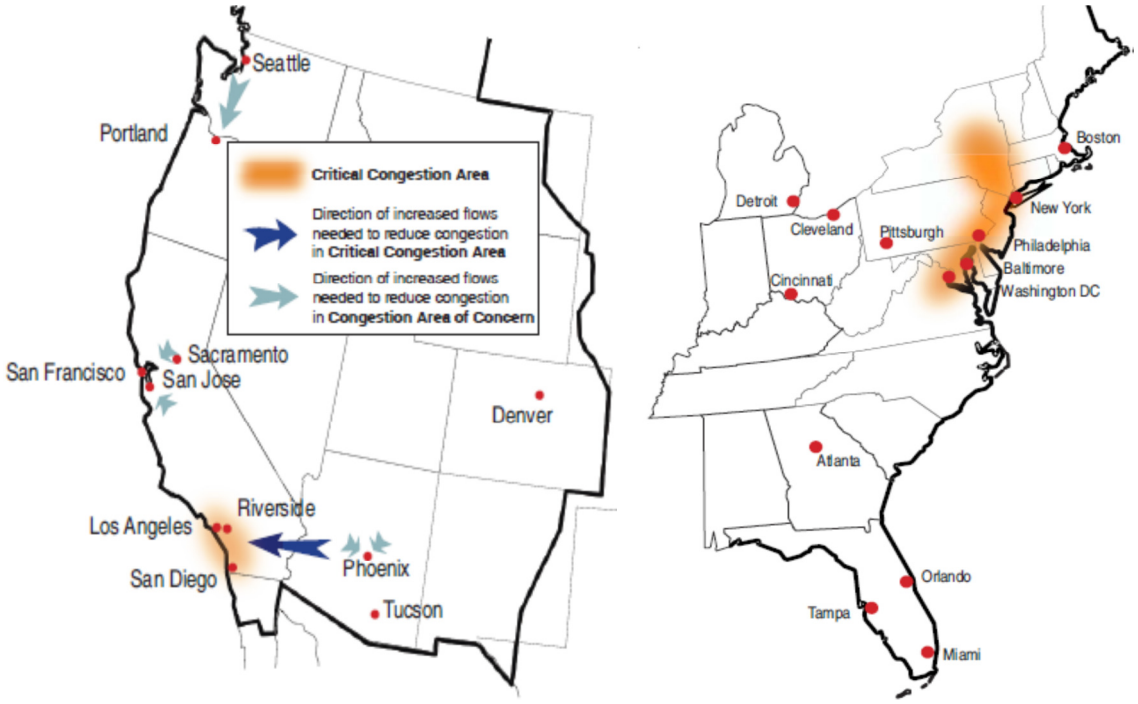

Fig. 4.7: National congested areas in the U.S. (source: [1]).

4.3.4 Summary of procedure

According to section 4.1 criteria (c), we need not only to find the MST, but we need to find a redundant sub-network which is N-1 connected. Significant difficulties may exist when trying to find a minimum N-1 connected candidate set for a general planning problem. First, it will be a very tedious work to estimate l_{at}, m_t and n_t for all arcs in a complete network. For the 62 nodes model, there will be 62×(62-1)/2=1891 possible connections. Secondly, the minimum edge and vertices bi-connectivity problem has been proved to be NP-hard [57]. Therefore we have developed and implemented an approximation algorithm, called the IRMST algorithm. It can efficiently find a redundant network while giving preference to "short" arcs. The procedure is introduced below and in Fig. 4.8.

a) Initialization. j=1; Solution pool $S_0 = \emptyset$;

b) Obtain the longitude and latitude values for each node. Convert them into Cartesian coordinates;

c) Calculate the direct line distance joining each node pair from their coordinates;

d) Apply greedy algorithm [16] to obtain the MST T_1 of the original graph G_1. $S_1 = S_0 \bigcup T_1$;

e) Use the method introduced in part A and B of this section to calculate l_{at}, m_t and n_t. Reweight all edges in S_j - S_{j-1} to get updated graph G_{j+1};

f) Obtain the MST T_{j+1} of the reweighted graph G_{j+1};

g) $S_{j+1} = S_j \bigcup T_{j+1}$;

h) If $S_{j+1} \neq S_j$, j=j+1, go to step e; else, end;

i) The final tree T_{j+1} is the MST of G_{j+1}. It is also the MST of the complete graph with all of its edges reweighted (See Appendix A for proof). The desired candidate set is $T_1 \bigcup T_2 \bigcup ..... \bigcup T_{j+1}$. Its N-1 connectivity can be checked using a Laplacian matrix [17].

Convergence of this algorithm is guaranteed because the total number of arcs of the complete graph is finite. Convergence speed is related to the characteristics of original graph, and the value of reweighting factors. The greater the reweighting factors are, the greater the number of reweighted arcs and iterations will be, i.e., convergence speed will be slower. In addition, generally it is the case that the higher the standard deviation of all arc lengths in the original graph, the faster the convergence rate will be. The relationship is roughly illustrated in Table 4.2.

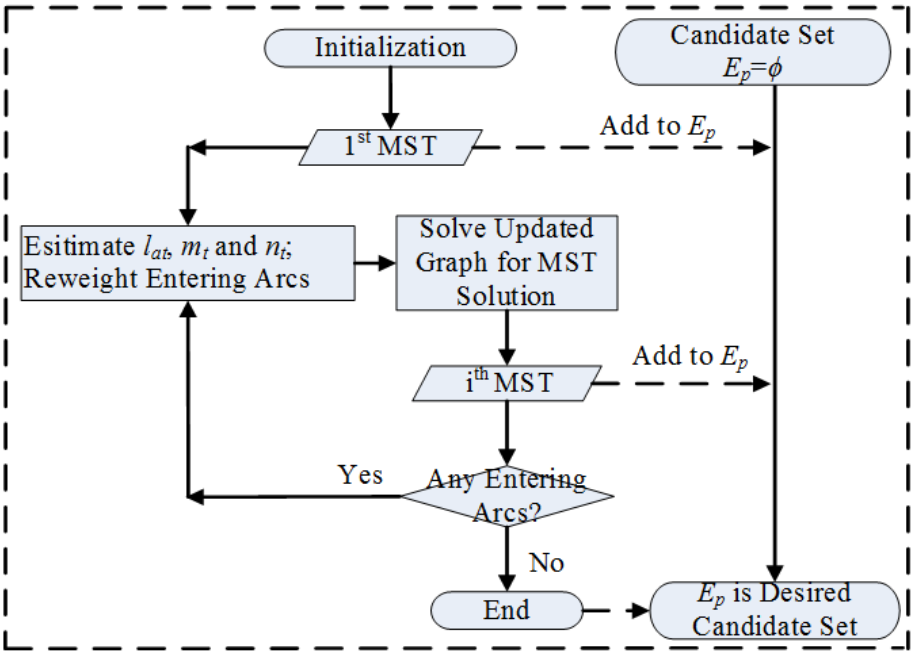

Fig. 4.8: Flow chart of iterative minimum spanning tree algorithm.

Table 4.2: Convergence Speed Illustration.

	Mean Value of Reweighting Factors	Number of Reweighted Arcs	Number of Iteration
Study #1	1.426836506	118	6
Study #2	1.905225644	155	8
Study #3	2.493877227	371	24

4.4 Nationwide Transmission Candidate Set

Performing the IRMST algorithm on the U.S. 62-node model, we obtain a 383-arc N-1 connected candidate set after 24 iterations, plotted in Fig. 4.9. Only 19.6% of all connections have been selected, greatly reducing the TNEP model size and computational

load. The l_{at}, m_t and n_t data have been collected for the use in the next chapter. This candidate set will be utilized for all TNEP studies in the remainder of this thesis.

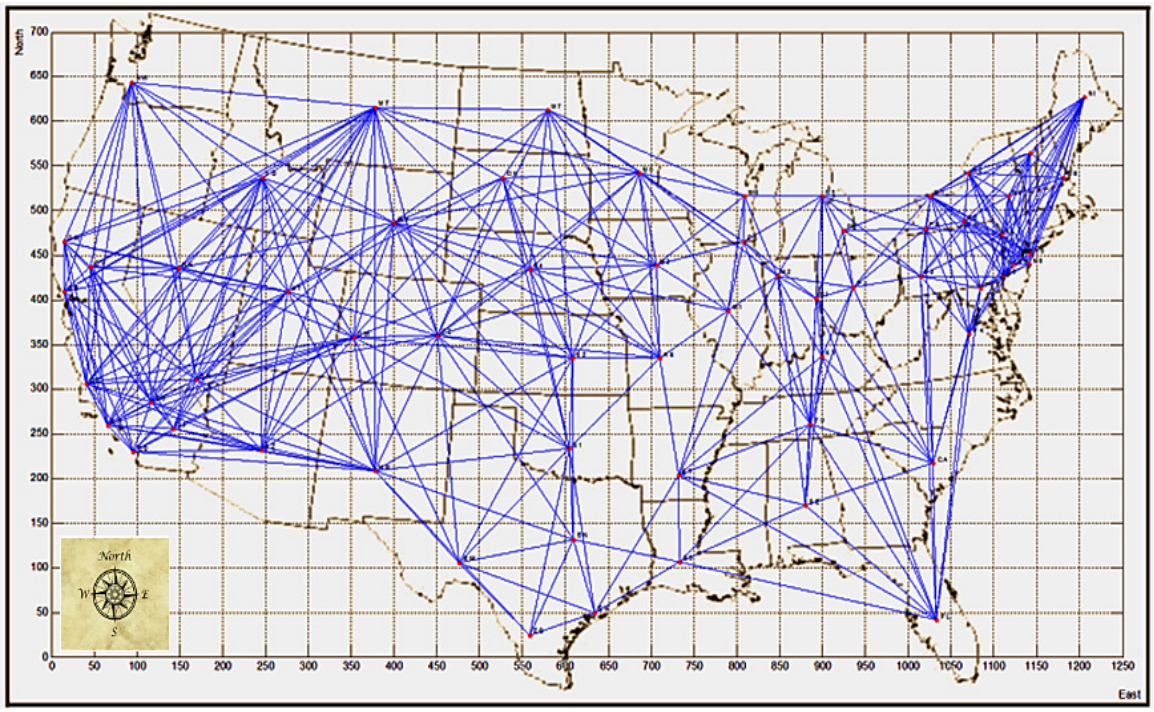

Fig. 4.9: Transmission candidate set of the U.S. 62 nodes model.

CHAPTER 5. NETWORK EXPANSION OPTIMIZATION

5.1 Classic Transmission Expansion Optimization Models

The primary objective of traditional electric transmission network expansion planning (TNEP) optimization is to determine transmission circuit additions with minimum investment cost to satisfy reliability criteria under future load and generation scenarios. Previous research has developed and well summarized the mathematical programming approaches. Generally speaking, except for the full AC power flow model which is considered only when the "sketch" of the network topologies has already been determined, there are four major types of existing transmission planning models [18]–[19].

5.1.1 DC model

This model uses DC power flow equations with binary transmission circuit investment decision variables. The problem statement for a single stage TNEP planning using this model can be expressed as follows:

Minimize

$$v = \sum_{(i,j)} c_{ij} n_{ij} \tag{5.1}$$

Subject to

$$S f + g = d \tag{5.2}$$

$$f_{ij} - \gamma_{ij}(n_{ij}^{0} + n_{ij})(\theta_i - \theta_j) = 0 \tag{5.3}$$

$$| f_{ij} | \leq (n_{ij}^{0} + n_{ij})\overline{f_{ij}} \tag{5.4}$$

$$0 \leq g \leq \overline{g} \tag{5.5}$$

$$0 \leq n_{ij} \leq \overline{n_{ij}} \tag{5.6}$$

n_{ij} integer, f_{ij} and θ_{ij} unbounded,

$$(i, j) \in \Omega \tag{5.7}$$

where c_{ij} is the investment cost of candidate route *i–j*. γ_{ij} is its susceptance, n_{ij} is the number of circuit additions. n_{ij}^{0} is the number of circuit in existing network on route *i–j*. f_{ij} is the power flow on *i–j*. $\overline{f_{ij}}$ is the transmission capacity on *i–j*. S is the branch-node incidence matrix. f is the vector of f_{ij}, g is the generation output vector, and $\overline{g}$ is the generation capacity vector. $\overline{n_{ij}}$ is the maximum number of circuit additions allowed on *i–j*. Ω is the set of all candidates.

Constraint (5.2) represents nodal power balance, i.e., the Kirchhoff's Current Law (KCL). Constraint (5.3) is the DC power flow equation, which is equivalent to Kirchhoff's Voltage Law (KVL). Constraints (5.4) and (5.5) are transmission and generation capacity limits, respectively. Equation (5.6) is the transmission investment maximum limit. Expression (5.7) defines integer investment decision variables. In equation (5.3), bus voltage angles and investment decision variables are multiplied together, creating a non-linear term. Thus, this model is an integer nonlinear program (INLP). It is a difficult combinatorial problem which can lead to combinatorial explosion

in the number of alternatives that have to he searched.

5.1.2 Transportation model and hybrid model

Simply relaxing (5.3) we will obtain the transportation model. Thus, this model does not consider KVL and is a mixed integer linear program (MILP). The solution of this model, however, is not necessarily the true optimal investment plan and may not satisfy DC flow equations. This model is useful when performing zonal level studies for large systems. A few industry software tools also implement this model as a feature to obtain approximate solutions within short computing time.

The hybrid model combines characteristics of the DC model and the transportation model. There are various ways of formulating hybrid models. The most commonly used method is to release KVL constraints for added circuits. In other words, it is assumed that the constraint in (5.2), KCL, is satisfied for all nodes of the network, whereas the constraint in (5.3), which represents KVL, is satisfied only by the existing circuits (and not necessarily by the added circuits). This model does not guarantee the feasibility of solution either.

5.1.3 Disjunctive model

This is model has been widely used in TNEP optimizations. The advantage of this model is that nonlinearities arising from use of the DC flow model, where bus voltage angles are multiplied by circuit investment decision variables, can be eliminated by applying the disjunctive mixed integer formulation [20], [21], [24], and [58], while it can be proved that under certain conditions the optimal solution of this model is the same with the DC model. Feasibility of its solutions can be guaranteed by properly selecting disjunctive penalty parameters. Before we introduce the model, we need to list a few

nomenclatures in ahead. We will use this nomenclature in the rest of this chapter.

5.1.3.1 Nomenclature

t:	Time step
n:	Number of nodes
m :	Number of candidate circuits
H:	Planning time horizon (set of time steps)
H_{inv}:	Set of Investment time steps within H
Ω_i^0:	Set of existing circuits connected to bus *i*, *i*=1, *n*
Ω_i^+:	Set of candidate circuits connected to bus *i*, *i*=1, *n*
Ω_i:	The union of Ω_i^0 and Ω_i^+
$f(t)$:	Vector of flows on step *t* (existing and candidates)
$f_0^{\max}(t)$:	Vector of circuit capacities on step *t* (existing)
$f^{\max}$:	Vector of circuit capacities (candidates)
$g(t)$:	Vector of bus generations on step *t*
$g^{\max}(t)$:	Vector of bus generation capacities on step *t*
$d(t)$:	Vector of bus active loads
$\theta(t)$:	Vector of bus voltage angles in radians on step *t*
$x(t)$:	Investment decision binary vector on step *t*
$S(t)$:	Cumulative investment decision vector on step *t*
c_I :	Vector of unit investment cost of candidates
c_o :	Vector of unit generation production cost
$\gamma 0$:	Vector of circuit susceptance (existing)
γ:	Vector of circuit susceptance (candidates)

M: Vector of penalty factors of candidate circuits

$\beta(t)$: Discount factor for step *t*

$\Delta(t)$: Time duration for step *t*

5.1.3.2 Model description

Using the nomenclature, the classic disjunctive model can be expressed as follows:

$$Min_{\{x,\, f,\, g,\, \theta\}} \sum_{t \in \mathrm{H}inv} \beta(t) cI x(t) \tag{5.8}$$

Subject to

$$\sum_{k=(i,j)\, j \in \Omega i} f_k(t) - g_i(t) = d_i(t), \qquad i = 1, n \quad \forall t \in \mathrm{H} \tag{5.9}$$

$$f_k(t) - \gamma 0_k(\theta_i(t) - \theta_j(t)) = 0,$$

$$k = (i, j),\ j \in \Omega_i^0,\ i = 1, n \quad \forall t \in \mathrm{H} \tag{5.10}$$

$$-M_k(1 - S_k(t)) \le f_k(t) - \gamma_k(\theta_i(t) - \theta_j(t)) \le M_k(1 - S_k(t)),$$

$$k = (i, j),\ j \in \Omega_i^+,\ i = 1, n \quad \forall t \in \mathrm{H} \tag{5.11}$$

$$S(t) = \sum_{i \in \mathrm{H}inv,\, i \le t} x(i) \tag{5.12}$$

$$-f0_k^{\max}(t) \le f_k(t) \le f0_k^{\max}(t),$$

$$k = (i, j),\ j \in \Omega_i^0,\ i = 1, n \quad \forall t \in \mathrm{H} \tag{5.13}$$

$$-f_k^{\max} S_k(t) \le f_k(t) \le f_k^{\max} S_k(t),$$

$$k = (i, j),\ j \in \Omega_i^+,\ i = 1, n \quad \forall t \in \mathrm{H} \tag{5.14}$$

$$0 \le g_i(t) \le g_i^{\max}(t), \qquad i = 1, n \quad \forall t \in \mathrm{H} \tag{5.15}$$

$$\theta_{ref}(t) = 0 \tag{5.16}$$

$$x(t), S(t) \in \{0,1\}^m \tag{5.17}$$

Equation (5.9) represents nodal power balance; (5.10) and (5.11) represent KVL for existing and candidate circuits, respectively; (5.12) relates transmission investment on each investment time step *t* and cumulative investment until time step *t* for multi-stage planning problem; (5.13) and (5.14) are transmission capacity constraints for existing and candidate circuits, respectively; (5.15) is the generation output limits; (5.16) sets the reference bus voltage angle to be 0; (5.17) defines investment variables to be binary. All circuit resistances are neglected.

In (5.11), when there is investment on a candidate circuit, then:

$$S_k(t) = 1 \tag{5.18}$$

and the constraint becomes:

$$0 \le f_k(t) - \gamma_k(\theta_i(t) - \theta_j(t)) \le 0,$$

$$k = (i, j),\ j \in \Omega_i^+,\ i = 1, n \quad \forall t \in \mathrm{H} \tag{5.19}$$

which enforces KVL across that circuit.

When there is no investment on a candidate circuit, then:

$$S_k(t) = 0 \tag{5.20}$$

and the constraint becomes:

$$-M_k \le f_k(t) - \gamma_k(\theta_i(t) - \theta_j(t)) \le M_k,$$

$$k = (i, j),\ j \in \Omega_i^+,\ i = 1, n \quad \forall t \in \mathrm{H} \tag{5.21}$$

If M_k is large enough, (5.21) is equivalent to releasing the KVL constraints. The minimum (optimal) value of M_k can be determined by the following approach [61].

5.1.3.3 Determination of optimal value of M_k

a) If there is an existing circuit on the same route of candidate k, the minimum value of M_k is the product of existing circuit flow capacity and the ratio of candidate susceptance and existing circuit susceptance. The reason is that in equation (5.21), as $S_k(t)$=0, according to equation (5.14), $f_k(t)$ will also be zero. Then we have:

$$-M_k \le -\gamma_k(\theta_i(t)-\theta_j(t)) \le M_k,$$

$$k=(i,j),\ j\in\Omega_i^+,\ i=1,n\quad \forall t\in \mathrm{H} \tag{5.22}$$

and independent of whether $\theta_i(t) \le \theta_j(t)$ or $\theta_i(t) \ge \theta_j(t)$, (5.22) is equivalent to:

$$\gamma_k\left|\theta_i(t)-\theta_j(t)\right| \le M_k,$$

$$k=(i,j),\ j\in\Omega_i^+,\ i=1,n\quad \forall t\in \mathrm{H} \tag{5.23}$$

Equation (5.23) means that in order to find the minimum value of M_k, we need to find out the maximum angle difference between bus i and j. Since there is an existing circuit between bus i and j, the maximum possible angle difference happens when the flow on the circuit reaches its maximum capacity, i.e.:

$$\left|\theta_i(t)-\theta_j(t)\right|_{\max} = f0_k^{\max} / \gamma 0_k,$$

$$k=(i,j),\ j\in\Omega_i^0,\ i=1,n\quad \forall t\in \mathrm{H} \tag{5.24}$$

Then, from (5.23) and (5.24), we get the minimum value of M_k, expressed in (5.25) below, which guarantee constraint (5.21) will not be binding.

$$M_k = f0_k^{\max}\gamma_k / \gamma 0_k$$

$$k=(i,j),\ j\in\Omega_i^0\bigcap\Omega_i^+,\ i=1,n\quad\forall t\in \mathrm{H} \tag{5.25}$$

b) If candidate k is in a new right-of-way, M_k is given by the product of the circuit's susceptance and the shortest distance between the circuit's terminal nodes which goes along existing circuits of other parts of the network. The distance, referred to as D_R below, is defined by [61] as the ratio of the circuit's flow capacity and its susceptance (in radians). D_R is an important indicator which forms a crucial pre-assumption in the new model (to be introduced in the next section). In this case, similar to a), we need to find the maximum possible angle difference between bus i and j. We may pick up the shortest path between the two buses, and the total distance of it will actually be the upper limit of angle difference, since for each sector on the path, its D_R is also the largest angle difference, and since electric power will always flow based on KVL. Then, M_k is given by (5.26) below:

$$\begin{aligned} &M_k=\gamma_k\min\{D_{Rk'}\}\\ &k=(i,j),\ j\in\Omega_i^+,\ i=1,n\\ &\forall t\in \mathrm{H},\ k' \text{ is a possible path between } i \text{ and } j \text{ in existing configuation.}\end{aligned} \tag{5.26}$$

One thing we need to point out is that, in (5.17), both S and x have been defined to be binary variables. Thus, during the entire planning horizon, there can be at most one circuit addition on a given candidate route.

5.2 Decimal-Binary Disjunctive Model

5.2.1 Multiple parallel circuit issue

The existing disjunctive model [20], [21], [24], and [58] requires all circuit

investment decision variables to be binary variables, i.e., it only allows one circuit to be built on a single candidate route during the planning horizon. Not only for national transmission design, but also bulk transmission grid expansion within a large geographical area may require building multiple parallel circuits on a certain candidate route ([2], [19], [20], [21], [24], [58], and [59]), for reliability and economic purposes [60], particularly in the multi-stage investment optimization problem. An obvious solution is to prepare enough parallel candidates (one for each possible circuit addition). However, doing this greatly increases the size of the mixed integer optimization model, especially when there is a possibility to invest a large number of parallel circuits on one route, or when the upper limit on number of parallel circuits is difficult to estimate in advance. We encountered an extreme case of this situation when designing a high capacity interregional transmission overlay for the U.S. under high renewable futures [13], which motivated the development reported in this thesis.

The most direct way to allow multiple parallel circuit additions is to simply duplicate the candidate as needed to make it a parallel candidate set. Consequently, constraints (5.11), (5.12) and (5.14) need to be duplicated as well, which is what is done in [19]. This method increases the number of KVL constraints by n-1 times when allowing up to n parallel circuits on a single candidate path. This creates computational burden when considering many candidate paths.

Here in this thesis, we present a more efficient approach. The essence of the approach is that by taking advantage of the information that some circuit additions will be of the same type, we will be able to limit combinations of identical and parallel transmission candidates to “bundles” of 1, 2, 4, 8, 16,…, and in consequence, to reduce

the number of corresponding decision variables, and corresponding constraints, to 1 each per bundle, instead of 1 each per circuit. Let the capacity and susceptance of a candidate to be f^{max} and γ. Assume for this certain route, all possible circuit additions are of the same type of transmission, i.e., D_R remains constant for all possible parallel circuits to be built. Then we make a few changes to the existing model (5.8)–(5.17), as introduced below.

5.2.2 Modeling of single-stage planning problem

Suppose there are a series of transmission bundles numbered in sequence ii=1, …, b. The f^{max}, γ and D_R values for the ii^{th} bundle, are:

$$f_{ii}^{\max} = 2^{ii-1} f_1^{\max} \tag{5.27}$$

$$\gamma_{ii} = 2^{ii-1}\gamma_1 \tag{5.28}$$

$$D_{Rii} = f_{ii}^{\max} / \gamma_{ii} = (2^{ii-1} f_1^{\max})/(2^{ii-1}\gamma_1) = f_1^{\max} / \gamma_1 \tag{5.29}$$

Parameters f_1^{max} and γ_1 are the capacity and susceptance of a single candidate circuit for this route. We rewrite the KVL and transmission capacity constraints as below:

$$-M_{kii}(1 - x_{kii}) \le f_{kii} - \gamma_{kii}(\theta_i - \theta_j) \le M_{kii}(1 - x_{kii}),$$

$$k=(i,j),\ j \in \Omega_t^+,\ i = 1,n \tag{5.30}$$

$$-f_{kii}^{\max} x_{kii} \le f_{kii} \le f_{kii}^{\max} x_{kii},$$

$$k=(i,j),\ j \in \Omega_t^+,\ i = 1,n \quad \forall t \in \mathrm{H} \tag{5.31}$$

where

$$f_{kii}^{\max} = 2^{ii-1} f_k^{\max} \tag{5.32}$$

$$\gamma_{kii} = 2^{ii-1}\gamma_k \tag{5.33}$$

In the objective function, the unit investment cost becomes:

$$c_{Iii} = 2^{ii-1} c_I \tag{5.34}$$

The value of b is determined by (5.35) below, where m_k is the maximum number of possible additions of identical parallel circuits on route k.

$$b_k = [\log_2 m_k] + 1, \tag{5.35}$$

Here, $[u]$ is the floor function (which maps u to the largest integer not greater than u), b_k is the number of parallel candidate bundles needed for m_k possible circuit additions on connection k in the network. It is easy to show that b_k is smaller than m_k. m_k/b_k is the ratio of the number of KVL constraints needed in existing disjunctive model to the number needed in the new model. The larger m_k is, the greater m_k/b_k will be. The relationship is illustrated in Fig. 5.1.

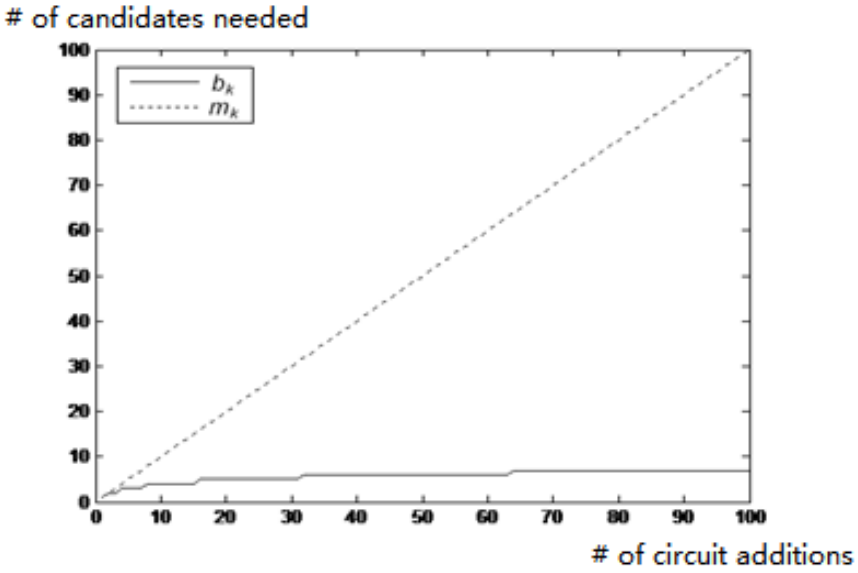

Fig. 5.1: Relationship between m_k and b_k.

For each connection k, we will have a binary investment decision vector [x_{k1}, x_{k2}, … , x_{kii}, … , x_{kb}]. Introduce a binary number x_{kB} which has x_{kii} as its digits, i.e., x_{kB} =

$x_{k1}x_{k2}\ldots\ x_{kii}\ldots\ x_{kb}$. Then, the total number of parallel circuit additions x_{kD} in decimal counting system is expressed as (5.36) below:

$$x_{kD} = \sum_{ii=1}^{b} 2^{ii-1} x_{kii} \tag{5.36}$$

or

$$x_{kD} = \mathbf{B}^{-1}(x_{kB}) \tag{5.37}$$

where **B** is the mapping from decimal numbers to binary numbers. $\mathbf{B}^{-1}$ is its inverse mapping. $\mathbf{B}^{-1}$ is a pure linear transformation, as expressed in (5.36).

5.2.3 Modeling of multi-stage planning problem

For the multi-stage planning problem, since a transmission investment on a previous stage cannot be removed in the subsequent stages, the previous method will not be able to perform automatic digit carry in the binary numbering system. As **B** (or $\mathbf{B}^{-1}$) is a linear one-to-one mapping, here we first transform the binary investment decision vector to a decimal number using $\mathbf{B}^{-1}$, then calculate the cumulative circuit additions, and finally transform back to binaries in KVL constraints. Let $S_{ii}(t)$ be the binary cumulative investment decision vector for the ii^{th} parallel bundle on time step t, $x_{ii}(t)$ be the binary investment decision vector for the ii^{th} parallel bundle on time step t, $S_D(t)$ and $S_B(t)$ be the vectors of total number of cumulative parallel circuit additions in time step t in decimal and binary format, respectively, and $x_D(t)$ and $x_B(t)$ be the vectors of number of parallel circuit additions in time step t in decimal and binary format, respectively. We deduce new constraints in (5.38)–(5.40):

$$x_D(t) = \mathbf{B}^{-1}(x_B(t)) = \sum_{ii=1}^{b} 2^{ii-1} x_{ii}(t) \tag{5.38}$$

$$S_D(t) = \sum_{j \in \mathrm{H}inv,\, j \le t} x_D(j) = \sum_{j \in \mathrm{H}inv,\, j \le t} \mathbf{B}^{-1}(x_B(j)) = \sum_{j \in \mathrm{H}inv,\, j \le t} \sum_{ii=1}^{b} 2^{ii-1} x_{ii}(j) \tag{5.39}$$

$$S_D(t) = \mathbf{B}^{-1}(S_B(t)) = \sum_{ii=1}^{b} 2^{ii-1} S_{ii}(t) \tag{5.40}$$

Combining (5.39) and (5.40), we get

$$\sum_{ii=1}^{b} 2^{ii-1} S_{ii}(t) = \sum_{j \in \mathrm{H}inv,\, j \le t} \sum_{ii=1}^{b} 2^{ii-1} x_{ii}(j) \tag{5.41}$$

Inserting (25) into the classical disjunctive model (5.8)–(5.17) together with necessary adjustments on expressions, we get the complete problem statement of the decimal-binary disjunctive model for multi-stage TNEP optimization:

$$Min_{\{x,\, f,\, g,\, \theta\}} \sum_{t \in \mathrm{H}inv} \sum_{k=1}^{k\max} \sum_{ii=1}^{bk} \beta(t) 2^{ii-1} c_I(k) x_{kii}(t) \tag{5.42}$$

Subject to

$$\sum_{k=(i,j)\, j \in \Omega_t^0} f_k(t) + \sum_{k=(i,j)\, j \in \Omega_t^+} \sum_{ii=1}^{bk} f_{kii}(t) - g_i(t) = d_i(t),\ i = 1, n\ \forall t \in \mathrm{H} \tag{5.43}$$

$$f_k(t) - \gamma 0_k(\theta_i(t) - \theta_j(t)) = 0,$$

$$k = (i, j),\ j \in \Omega_t^0,\ i = 1, n \quad \forall t \in \mathrm{H} \tag{5.44}$$

$$-M_{kii}(1 - S_{kii}(t)) \le f_{kii}(t) - \gamma_k 2^{ii-1}(\theta_i(t) - \theta_j(t)) \le M_{kii}(1 - S_{kii}(t)),$$

$$ii = 1, b,\quad k = (i, j),\ j \in \Omega_t^+,\ i = 1, n \quad \forall t \in \mathrm{H} \tag{5.45}$$

$$\sum_{ii=1}^{b} 2^{ii-1} S_{ii}(t) = \sum_{j \in \mathrm{H}inv,\, j \le t} \sum_{ii=1}^{b} 2^{ii-1} x_{ii}(j) \tag{5.46}$$

$$-f0_k^{\max}(t) \le f_k(t) \le f0_k^{\max}(t),$$

$$k = (i, j),\ j \in \Omega_i^0,\ i = 1, n \quad \forall t \in \mathrm{H} \tag{5.47}$$

$$-2^{ii-1} f_k^{\max} S_{kii}(t) \le f_{kii}(t) \le 2^{ii-1} f_k^{\max} S_{kii}(t),$$

$$ii = 1,b\,, \quad k = (i,j),\ j \in \Omega_i^+,\ i = 1,n \quad \forall t \in \mathrm{H} \tag{5.48}$$

$$0 \le g_i(t) \le g_i^{\max}(t), \qquad i = 1,n \quad \forall t \in \mathrm{H} \tag{5.49}$$

$$\theta_{ref}(t) = 0 \tag{5.50}$$

$$x_{ii}(t), S_{ii}(t) \in \{0,1\}^m \tag{5.51}$$

Optimal values of M_{kii} can be determined using the method of reference [61], introduced previously in section 5.1. Equation (5.46) is the added linear equality constraint. Let $t \in H_{inv}$, t_W be the maximum t value in H_{inv}, the investment decision solution x_{kB} will now become a matrix with binary entries:

$$\begin{pmatrix} x_{k1}(1) & \dots & x_{kii}(1) & \cdots & x_{kb}(1) \\ \vdots & \ddots & \vdots & \ddots & \vdots \\ x_{k1}(t) & \cdots & x_{kii}(t) & \cdots & x_{kb}(t) \\ \vdots & \ddots & \vdots & \ddots & \vdots \\ x_{k1}(tw) & \cdots & x_{kii}(tw) & \cdots & x_{kb}(tw) \end{pmatrix}$$

The key assumption for applying this new model is that all possible parallel circuit additions on a single arc in the network should have the same D_R value. This is equivalent to the requirement that all possible parallel circuit additions on a single arc in the network should be of the same type of transmission line. Refer to part 5.2.5 below for the modeling approach if there are multiple types of transmission circuits in the TNEP model.

Compared to the existing disjunctive model, the new approach can reduce the number of candidates by the amount of $m_k - b_k$, as illustrated in Fig. 5.1. In consequence, the number of KVL constraints and investment decision variables has been reduced by

that amount as well, at the cost of adding a limited number of decimal-binary transformation relationship equalities per (5.46). Hence, the new method may have significantly better computational efficiency than the existing disjunctive model, particularly for problems which have routes with potentially high values of m_k.

5.2.4 Optimal parallel candidate number determination

In most TNEP optimization problems, the number of parallel bundles b is unknown before solutions are obtained. One can always allow a large number of bundles to ensure there are enough, but this might cause a computational issue for large-scale problems. A more efficient approach has been introduced to address this issue, expressed as follows:

a) Get the linear root relaxation solution[6];

b) Estimate the number of bundles b needed for each arc k. Basically, the initial b value can be set to be equal to the greater nearest integer of the root relaxation investment solution during the last time step;

c) Perform mixed integer optimization to get MILP solution;

d) If the problem is infeasible, increase all b values by 1 and go back to step c). If a feasible solution has been found, go to next step;

e) Check the investment decision solution for the last time step one by one. If on any arc k, the candidates have become saturated[7] at the last time step t, i.e., in the solution matrix, $x_{kb}(t)$ or $S_{kb}(t)$ becomes 1, increase b value by 1 for arc k. Update the MILP model using new b values then go to step c). If all arcs k are not

[6] The root relaxation solution is a linear programming solution, where variable integrality is relaxed

[7] "Saturated" means that all bundles on a certain route have been invested, thus, no additional circuit can be built on this candidate route anymore.

saturated, stop and the current MILP solution is the desired optimal solution for which at least one bundles was not utilized.

The process has been illustrated in Fig. 5.2 below:

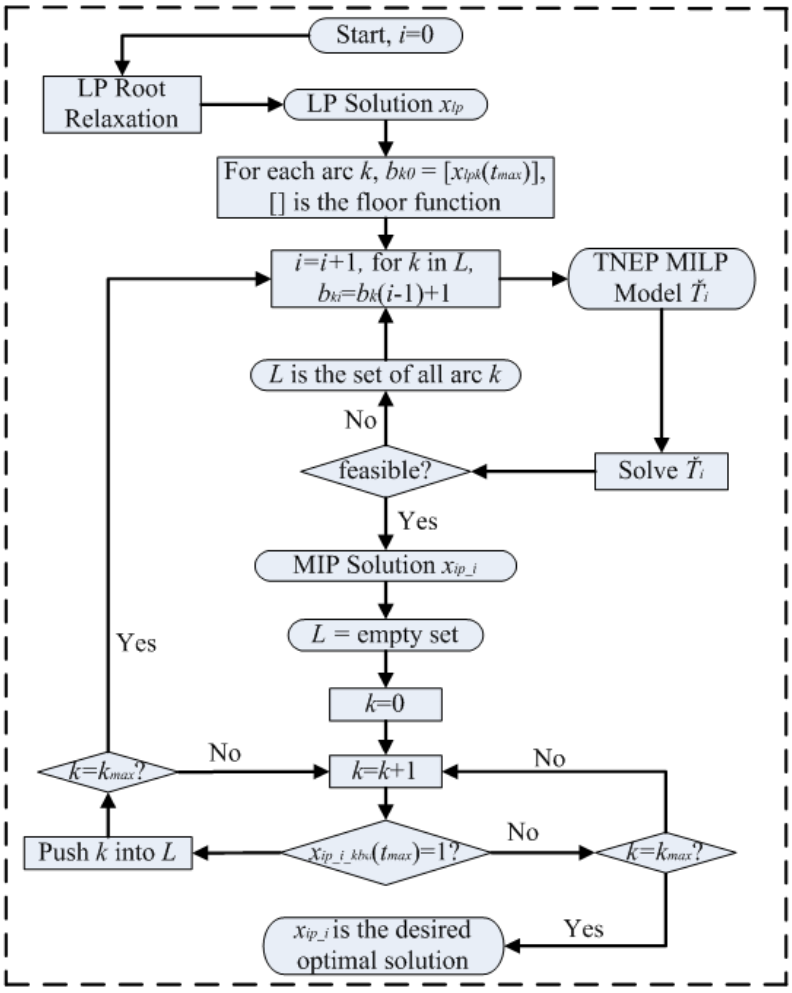

Fig. 5.2: Flow chart of optimal candidate number determination.

In Fig. 5.2, $x_{ip\_i\_kbki}(t_{max})$ is the investment decision solution value on arc k bundle b_{ki} during the last time step t of i_{th} TNEP MILP model. $x_{lpk}(t_{max})$ is the continuous investment decision solution value on arc k during the last time step t of root relaxation model. b_{ki} is the number of bundles for arc k in TNEP model i. We only examine the last

time step solution, because during the last time step, the number of newly added circuits will reach the maximum value during the whole planning horizon.

5.2.5 Multiple circuit type problem

In case there are multiple types of transmission circuit candidates to be invested in parallel, we may not implement model (5.42)–(5.51) directly, as the basic assumption of the decimal-binary disjunctive model is that all possible circuit additions should be of the same type of transmission on a certain candidate route. Hence, if there are more than one types of transmission circuit to be considered, we may duplicate the candidate route, one for each possible circuit type, to model different types of transmission technologies. Then, on each route, we may again use the decimal-binary disjunctive model to create a series of bundles for possible parallel circuit investments of the same type.

5.2.6 Value-based transmission planning

In Chapter 2 and Chapter 4, we have mentioned that transmission investment may have the effect to reduce generation production cost. The reason is straightforward: transmission investment may relief transmission congestions in existing network and in consequence to improve system operating efficiency, i.e., lower overall production cost. Recently there is a growing interest in value-based transmission planning, which considers both transmission investment cost and generation production cost in the planning model [25]–[27]. This planning approach considers the economic value of transmission, as well as reliability performance. Its execution can be greatly facilitated by computationally efficient TNEP optimization codes.

Here in this study, we implement this method into our decimal-binary disjunctive model, by making a change in the objective function:

$$Min_{\{x,\,f,\,g,\,\theta\}} \sum_{t\in \mathrm{H}inv} \sum_{k=1}^{k\max} \sum_{ii=1}^{bk} \beta(t) 2^{ii-1} c_I(k) x_{kii}(t) + \sum_{t\in \mathrm{H}} \beta(t) c_o g(t) \Delta(t) \tag{5.52}$$

All equality and inequality constraints remain the same. This model will be able to find the optimal balance between transmission investment and generation re-dispatch.

5.2.7 Transmission losses

In the previous model, all networks have been assumed to be lossless to maintain linearity. To precisely reflect transmission losses, one may need to use a full AC model, which is non-linear and thus is very challenging to solve for large systems, if not impossible. In order to improve model accuracy for the national planning problem without introducing excessive computational load, we design a method to incorporate a linearized loss function to the decimal-binary disjunctive model.

Generally speaking, there are two basic approaches to roughly estimate transmission losses in a linearized power flow model: one is to levelize them into transmission investment cost [62], and another is to assume a fixed loss ratio, say, 2%, for all circuits. Although both of them maintain linearity, the first one introduces significant error when the power flow on a certain line is quite different from the loading selected for levelization. And the second one fails to reflect loss rate variation among different types of transmission technologies. Here, we combine the two approaches together: we break the losses into two parts: fixed losses and variable losses. Variable loss increases linearly with branch flow, with a ratio of $1 - \eta_0$. It represents the losses of existing transmission and a portion of invested transmission. η_0 may be selected to be greater than the total transmission efficiency rate of all circuits. Fixed losses are related to transmission type and are proportional to line length l_{at}. They can be levelized into the

investment cost in the objective function by assuming the line loading is near its Surge Impedance Loading (SIL) . Then, the objective function of (5.52) needs to be updated to reflect this approach. The updated objective function is:

$$Min_{\{x,\,f,\,g,\,\theta\}} \sum_{t\in \mathrm{H}inv} \sum_{k=1}^{k_{\max}} \sum_{ii=1}^{bk} \beta(t) 2^{ii-1} c_I'(k) x_{kii}(t) + \sum_{t\in \mathrm{H}} \beta(t) c_o g(t) \Delta(t) + \sum_{t\in \mathrm{H}} \sum_{ij\in\Omega} \beta(t)(1-\eta_0)\Delta(t) E_r f_{ij}(t) \tag{5.53}$$

where E_r is the estimated average energy price. k_{max} is the total number candidate routes. $f_{ij}(t)$ is the total amount of power flow between node i and j on time step t. Note that the term c_I'(k) has been modified from $c_I(k)$ to account for the levelized transmission losses. Ω here represents all branches in network.

This combination approach provides an estimation of transmission losses in a linearized power flow model, without creating computing difficulties for large TNEP models. It takes into account of major influencing factors including circuit voltage level, circuit length and line loading. The variable losses, by properly selecting the η_0 value, will address the major part of losses which are subject to change to line loading. The remaining part of the losses will be calculated based on circuit type and length, and levelized into investment cost. For this particular high voltage bulk transmission system design in this thesis, this method considers more major influencing factors that the two basic methods and is likely to give more accurate loss estimation.

5.2.8 The implementation of Benders decomposition

For large systems having certain structure, Benders decomposition is often implemented to accelerate solution speed and improve solution accessibility. TNEP models are suitable for the implementation of Benders decomposition. J. F. Benders

introduced the Benders decomposition in 1962 to solve large mixed integer linear programming (MILP) problem [31]. Models which are suitable for Benders decomposition usually can be written into the following format [63]–[64]:

$$Min \quad z = c^T x + d^T y \tag{5.54}$$

Subject to

$$Ay \qquad \geq b \tag{5.55}$$

$$Ex + Fy \quad \geq h \tag{5.56}$$

$$x \geq 0, y \ \text{int}\, ergers \tag{5.57}$$

where x is the vector of continuous variables; y is the vector of integer variables; and A, E, F, c, and d are coefficient matrices. Since many TNEP problems for multi-stage bulk system planning tend to be of large size, and since they can be expressed in the above form, we consider employing the Benders decomposition algorithm to solve the previous model.

In this section, we derive the Benders decomposition formulation for large, difficult-to-solve models. We decouple the model into a master investment problem (MP0) and a few operational sub-problems (SP). The MP0 contains only binary variables, and SPs contain only continuous decision variables.

$$Min \quad Z_{lower} \qquad \text{MP0}$$

Subject to

$$Z_{lower} \geq \sum_{t \in \text{H}inv} \sum_{k=1}^{k\max} \sum_{ii=1}^{bk} \beta(t) 2^{ii-1} c_I'(k) x_{kii}(t) \tag{5.58}$$

$$\sum_{ii=1}^{b} 2^{ii-1} S_{ii}(t) = \sum_{j \in \text{H}inv,\, j \leq t} \sum_{ii=1}^{b} 2^{ii-1} x_{ii}(j) \tag{5.59}$$

$$x_{ii}(t), S_{ii}(t) \in \{0,1\}^m \tag{5.60}$$

For each operational time step t, we have a sub-problem SPt:

$$Min_{\{f,g,\theta\}} \sum_{t\in \mathrm{H}} \beta(t) c_o g(t) \Delta(t) + \sum_{t\in \mathrm{H}} \sum_{ij\in\Omega} \beta(t)(1-\eta_0)\Delta(t) E_r f_{ij}(t) \qquad \text{SP}t$$

Subject to

$$\sum_{k=(i,j)\, j\in\Omega_i^0} f_k(t) + \sum_{k=(i,j)\, j\in\Omega_i^+} \sum_{ii=1}^{bk} f_{kii}(t) - g_i(t) = d_i(t),\ i=1,n\ \forall t\in \mathrm{H} \tag{5.61}$$

$$f_k(t) - \gamma 0_k(\theta_i(t) - \theta_j(t)) = 0,$$

$$k=(i,j),\ j\in\Omega_i^0,\ i=1,n \quad \forall t\in \mathrm{H} \tag{5.62}$$

$$-M_{kii}(1-S_{kii}(t)) \le f_{kii}(t) - \gamma_k 2^{ii-1}(\theta_i(t) - \theta_j(t)) \le M_{kii}(1-S_{kii}(t)),$$

$$ii=1,b, \quad k=(i,j),\ j\in\Omega_i^+,\ i=1,n \quad \forall t\in \mathrm{H} \tag{5.63}$$

$$-f0_k^{\max}(t) \le f_k(t) \le f0_k^{\max}(t),$$

$$k=(i,j),\ j\in\Omega_i^0,\ i=1,n \quad \forall t\in \mathrm{H} \tag{5.64}$$

$$-2^{ii-1} f_k^{\max} S_{kii}(t) \le f_{kii}(t) \le 2^{ii-1} f_k^{\max} S_{kii}(t),$$

$$ii=1,b, \quad k=(i,j),\ j\in\Omega_i^+,\ i=1,n \quad \forall t\in \mathrm{H} \tag{5.65}$$

$$0 \le g_i(t) \le g_i^{\max}(t), \qquad i=1,n \quad \forall t\in \mathrm{H} \tag{5.66}$$

$$\theta_{ref}(t) = 0 \tag{5.67}$$

After building the model for a specific problem, MP0 and SPt can also be written in the format of (5.54)–(5.57). Benders decomposition algorithm is summarized below and illustrated in Fig. 5.3 as well.

a) It begins by solving MP0. If it is infeasible, then the original problem will also be infeasible. If feasible, we get an initial investment decision solution matrix x_{kB0};

b) For each of the t sub-problems, we solve it one-by-one, with investment decision variables being fixed to be x_{kB0} and S_{kB0}. If a SPt is feasible, continue with t+1 sub-problem. If SPt is infeasible, we add a feasibility cut to MP0 as follows:

$$(h-Fy)^T u^r \leq 0 \tag{5.68}$$

where u^r are the Lagrangian multipliers of constraints (5.69) below:

$$Min \quad \mathbf{1}^T s \tag{5.69}$$

Subject to

$$Ex+Is \geq h-Fy' \tag{5.70}$$

$$s, x \geq 0 \tag{5.71}$$

Here, s is an ancillary vector, and **1** is the unit vector. Variable y' is y with its value fixed to that of the previous MP solution.

c) After going through all sub-problems, solve the MP with added feasibility cuts. Obtain a new solution x_{kB1};

d) Go to step b, repeat the process until all sub-problems become feasible;

e) Solve the updated MP and check if the following optimality tolerance has been met:

$$| Z_{lower} - Z_{lower} | \leq \varepsilon, \tag{5.72}$$

$$Z_{upper} = d^T y' + (h-Fy')^T u^p \tag{5.73}$$

Z_{lower} is the objective value of previous MP solution. ε is the desired optimality

tolerance.

If the optimality tolerance has not been met, add the following optimality cut to MP. Solve the updated MP and check optimality tolerance again.

$$Z_{lower} \geq d^T y + (h - Fy)^T u^p \tag{5.74}$$

where u^p is the optimal dual solution of all sub-problems.

If the optimality tolerance has been met, the optimal solution has been found. Stop.

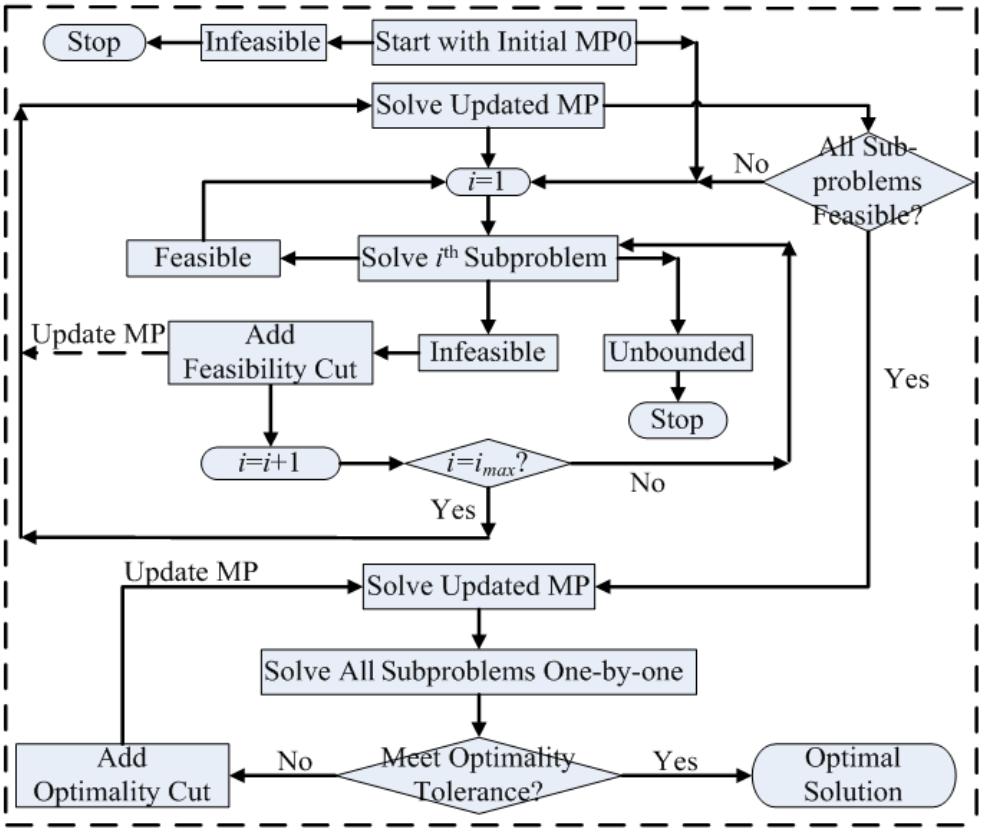

Fig. 5.3: Flow chart of Benders' decomposition.

CHAPTER 6. TREATMENT OF GLOBAL UNCERTAINTIES

6.1 The Concept of Flexibility and Adaptation Cost

Any kind of planning efforts inherently faces the problem of uncertainty treatment. In transmission planning there are numerous future uncertainties that can be influential in making planning decisions. The majority of these uncertainties include, but are not limited to, demand growth, fuel costs, generation expansion, renewable penetration, technology maturity and associated future investment cost, economic conditions, regulatory and legislative policies, and energy market trends. To select and design a cost-effective and robust transmission system to operate among different future scenarios is currently one of the most interesting topics in planning studies.

A traditional straightforward method is to conduct multiple case studies, to produce a planning decision under each scenario, and then integrate them using an appropriate weighted-average method. For example, the Midcontinent Independent System Operator (MISO)'s economic planning studies apply this approach to quantify transmission economic potential benefit of various proposals. In their Market Efficiency Planning Study [65], five futures were selected to reflect various natural gas prices, load growth, environmental policies, and economic conditions. Studies were performed for each future scenario to obtain the transmission solution's predicted economic benefit in terms of adjusted production cost (APC) savings. Finally, a weighted average among all

different APC_S under all futures was calculated to obtain a weighted average APC_S as the overall result from this method.

In this approach, the most controversial issue is to determine the appropriate weight for each future scenario. Under some conditions, the simple weighted average may not be sufficient, since the solutions for many problems are not always suitable for a weighted summation. A good example of this is the TNEP model introduced earlier, where transmission investment solutions are represented using binary variables. Such values would make little sense in terms of computing weighted averages for mixed integer solutions. Also, at a MISO's stakeholder meeting, representatives of some utilities raised the issue that a weighted average might cause a very attractive solution in terms of high occurrence probability that might be discarded because of outlier results associated with lower occurrence probabilities.

In recent years, there have been a few studies directed toward solving the multi-scenario problem by using the concept of "flexibility" or "adaptability". The concept of adaptation cost was used in [66] to represent the additional investment cost needed to make a particular investment plan become feasible under a different future scenario. This can be more clearly explained using Fig. 6.1.

x^*_i is the optimization results for the scenario i problem. As illustrated in Fig. 6.1, this solution may not be feasible under a different scenario j, and so additional investment in infrastructure, represented by y_{i-j} in Fig. 6.1 , is needed to make the original plan x^*_i become feasible under scenario j. The cost of y_{i-j}, is defined to be the adaptation cost from scenario i to scenario j.

In reference [66], the adaptation cost is calculated for each investment plan under

all possible futures, and the plan with the least total adaptation costs to all futures is selected as the most robust plan. This approach is an improvement over the weighted average method, but it splits the TNEP min-cost optimization and adaptation cost calculation into two separate steps and thus may not guarantee finding the most balanced solution between single-future optimality and multi-future robustness.

Reference [22] describes significant progress produced by introducing the method of flexibility design optimization, formulating a single optimization model to optimize both optimality and robustness. In this method, a core investment has been defined to represent those parts of investments that should occur in all future scenarios. Adaptation investment required by all these futures will be optimized together with the core investment in the objective function. This approach is guaranteed to find the best plan in terms of overall optimality and robustness performance, but in [22] it was applied to generation expansion using only a continuous linear programming model. In the next section, we will apply this method to the TNEP problem to formulate an MILP model, i.e., a flexibility design model for transmission expansion planning.

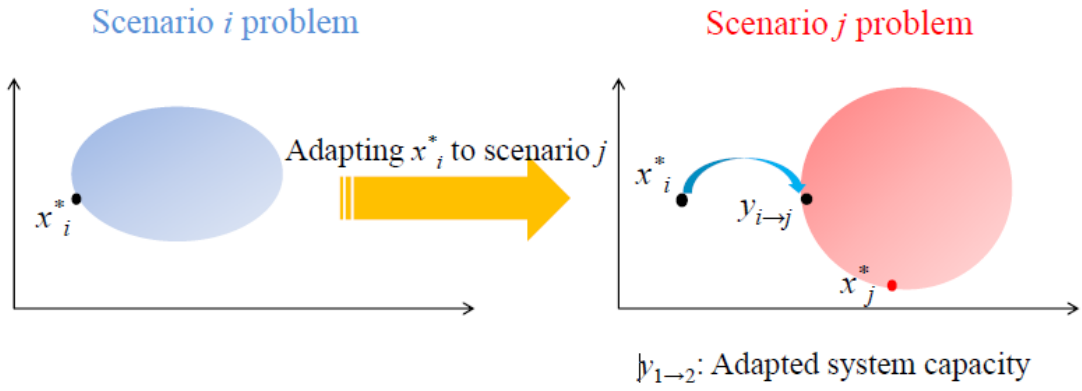

Fig. 6.1: The concept of adaptation cost (Source: [22]).

6.2 Flexibility Design Methodology and Problem Statement

Demand growth and future generation expansion are the two major factors that influence transmission needs and investment trends. There are more uncertainties in future generation's capacity, location, type, and timing than in demand change, so in this model we will treat future generation as the sole global uncertainty in the model. Demand will be assumed to be the same for each future, while generation dispatch may vary among different futures. Transmission investment as a decision variable will be split into core investment and several adaptation investments, one for each future. Similar to the approach described in reference [22], the objective function will consist of a core investment decision and *n* adaptation decision components. The operation costs and transmission losses will also only be contained in the adaptation cost in the objective function; they will not exist in the core investment cost. The constraints will be a combination of all linear constraints modeled under each future scenario. Using identical nomenclature from 5.1.3.1 and all additional variables introduced in another part of Chapter 5, we summarize the problem statement as follows:

$$
\begin{aligned}
Min_{\{x,\,f,\,g,\,\theta\}} \; & \sum_{t\in \mathrm{H}inv} \sum_{k=1}^{k\max} \sum_{ii=1}^{bk} \beta(t) 2^{ii-1} c_I(k) x_{kii}(t) + \\
& \sum_{\varsigma=1}^{\varsigma m} \rho_\varsigma \Big(\sum_{t\in \mathrm{H}inv} \sum_{k=1}^{k\max} \sum_{ii=1}^{bk} \beta(t) 2^{ii-1} c_I'(k) x_{\varsigma kii}(t) + \\
& \sum_{t\in \mathrm{H}} \beta(t) c_O g_\varsigma(t) \Delta(t) + \sum_{t\in \mathrm{H}} \sum_{ij\in \Omega_\varsigma} \beta(t)(1-\eta_0)\Delta(t) E_r f_{\varsigma ij}(t) \Big)
\end{aligned}
\tag{6.1}
$$

Subject to

For $\varsigma = 1, 2, \ldots, \varsigma m$:

$$\sum_{k=(i,j)\, j\in\Omega_i^0} f_{\varsigma k}(t) + \sum_{k=(i,j)\, j\in\Omega_i^+\cup\Omega_{\varsigma i}^+} \sum_{ii=1}^{bk} f_{\varsigma kii}(t) - g_{\varsigma i}(t) = d_i(t),\ i=1,n\ \forall t\in \mathrm{H} \tag{6.2}$$

$$f_{\varsigma k}(t) - \gamma 0_k(\theta_{\varsigma i}(t) - \theta_{\varsigma j}(t)) = 0,$$
$$k=(i,j),\ j\in\Omega_i^0,\ i=1,n\quad \forall t\in \mathrm{H} \tag{6.3}$$

$$-M_{kii}(1-S_{kii}(t)) \le f_{\varsigma kii}(t) - \gamma_k 2^{ii-1}(\theta_{\varsigma i}(t) - \theta_{\varsigma j}(t)) \le M_{kii}(1-S_{kii}(t)),$$
$$ii=1,b,\quad k=(i,j),\ j\in\Omega_i^+,\ i=1,n\quad \forall t\in \mathrm{H} \tag{6.4}$$

$$-M_{kii}(1-S_{\varsigma kii}(t)) \le f_{\varsigma kii}(t) - \gamma_k 2^{ii-1}(\theta_{\varsigma i}(t) - \theta_{\varsigma j}(t)) \le M_{kii}(1-S_{\varsigma kii}(t)),$$
$$ii=1,b,\quad k=(i,j),\ j\in\Omega_{\varsigma i}^+,\ i=1,n\quad \forall t\in \mathrm{H} \tag{6.5}$$

$$\sum_{ii=1}^{b} 2^{ii-1} S_{ii}(t) = \sum_{j\in \mathrm{H}inv,\, j\le t} \sum_{ii=1}^{b} 2^{ii-1} x_{ii}(j) \tag{6.6}$$

$$\sum_{ii=1}^{b} 2^{ii-1} S_{\varsigma ii}(t) = \sum_{j\in \mathrm{H}inv,\, j\le t} \sum_{ii=1}^{b} 2^{ii-1} x_{\varsigma ii}(j) \tag{6.7}$$

$$-f0_k^{\max}(t) \le f_{\varsigma k}(t) \le f0_k^{\max}(t),$$
$$k=(i,j),\ j\in\Omega_i^0,\ i=1,n\quad \forall t\in \mathrm{H} \tag{6.8}$$

$$-2^{ii-1} f_k^{\max} S_{kii}(t) \le f_{\varsigma kii}(t) \le 2^{ii-1} f_k^{\max} S_{kii}(t),$$
$$ii=1,b,\quad k=(i,j),\ j\in\Omega_i^+,\ i=1,n\quad \forall t\in \mathrm{H} \tag{6.9}$$

$$-2^{ii-1} f_k^{\max} S_{\varsigma kii}(t) \le f_{\varsigma kii}(t) \le 2^{ii-1} f_k^{\max} S_{\varsigma kii}(t),$$
$$ii=1,b,\quad k=(i,j),\ j\in\Omega_{\varsigma i}^+,\ i=1,n\quad \forall t\in \mathrm{H} \tag{6.10}$$

$$0 \le g_{\varsigma i}(t) \le g_{\varsigma_i}^{\max}(t), \qquad i=1,n\quad \forall t\in \mathrm{H} \tag{6.11}$$

$$\theta_{\varsigma ref}(t) = 0 \tag{6.12}$$

$$x_{ii}(t), S_{ii}(t), S_{\varsigma ii}(t) \in \{0,1\}^m \tag{6.13}$$

where

ς represents the index of future, with ςm being the total number of future generation scenarios considered. $\Omega_{\varsigma i}^{+}$ is the set of candidates in future ς. Ω_{ς} is the set of all branches in future ς. ρ_{ς} is a selected weight of cost for future ς.

Equation (6.2) represents nodal power balance; Equation (6.3) to (6.5) represent KVL for existing branches, candidate circuits for core investment and candidates for adaptation investment, respectively; Equations (6.6) and (6.7) relate transmission investment on each investment time step *t* and cumulative investment until time step *t* for multi-stage planning problem; Equations (6.8) to (6.10) are transmission capacity constraints for existing branches, candidate circuits for core investment and candidates for adaptation investment, respectively; Equation (6.11) is the generation output limits; Equation (6.12) sets the reference bus voltage angle to be 0; Equation (6.13) defines investment variables to be binary. All circuit resistances are neglected.

In the above model, the weights ρ_{ς} represent not only the occurrence probability of a future scenario ς, but they also reflect the importance of the adaptation cost under that scenario. If a future has low occurrence probability but requires a higher priority for reasons like, for example, significant impact on the existing system, significant requirement to change a current operating pattern, or avoidance of a worst-case scenario (in case this happens, severe reliability problems or others may occur and be extremely difficult or taxing to mitigate/adapt to), we may assign a higher ρ_{ς} value to this future, so values of ρ_{ς} for all scenarios do not necessarily sum to one. We can summarize some general relationships between core investment trends in true optimal solutions and ρ_{ς}

values, which should help in understanding core investment concepts.

1. If $\sum_{\varsigma=1}^{\varsigma m} \rho_{\varsigma} < 1$, it indicates that the solution will tend to de-emphasis core investments. Most investments will be for adaptation. This is because, under this situation, the cost for a core investment will be even higher than the total cost of building this line in every scenario. As a consequence, the optimization program will select to invest the line for the future under which it is needed, instead of building it in core investment which is more expensive. There could be some common parts among different futures.
2. If $\sum_{\varsigma=1}^{\varsigma m} \rho_{\varsigma} = 1$, it indicates that only if an investment is common in all futures, i.e., an investment which is needed for feasibility reasons under all futures, this investment may occur in the core investment as its cost now in core investment equals to the total cost of building this line in every scenario.
3. If $\sum_{\varsigma=1}^{\varsigma m} \rho_{\varsigma} >> 1$, $\rho_{\varsigma} < 1$, it means core investment is preferred if there is an investment needed under more than one future for feasibility reasons, because the core investment cost under this case tends to be still higher than the adaptation cost under a single future, but is likely to be less than the total cost under two or more different futures.
4. If $\rho_{\varsigma} > 1$, this indicates that there will only be core investment. No adaptation investment will be made in the solution, as core investment will be less expensive.

Based on this model, we perform studies for the national planning problem, to be introduced in Chapter 7 Section 8.

CHAPTER 7. U.S. TRANSMISSION DESIGN CASE STUDY

7.1 Available Bulk Power Transmission Technologies

For high-capacity inter-regional power transfer, there are a variety of transmission technologies available, including Extra High Voltage Alternative Current (EHVAC), High Voltage Direct Current (HVDC) circuits, underground cables, and others. Although underground cables have low ROW requirement and are not affected by weather conditions, their investment costs are typically much higher than those of overhead lines because of insulation requirements [67]. Thus, overhead cables are generally preferred mainly in metro and suburban regions where ROW is very expensive.

HVDC is suitable for long-distance, bulk-power transfer, because the DC line/cable cost per unit length is much lower even though the required converter station is expensive. In contrast, EHVAC is more economical for relatively short distance and lower capacity needs [68]. A typical cost comparison between AC and DC options is shown in Fig. 7.1. Generally, the typical break-even distance for these two approaches is about 400 miles or 600 km. Additionally, HVDC serves like a sort of bridge between a power source and a sink and thus wouldn't be able to pick up the resources or serve the load at some intermediate point on a route. At the same time, since we are discussing national-level transmission design, synchronization between different interconnections requires a DC link or back-to-back DC stations. There is a perspective that a hybrid

AC/DC overlay will better satisfy needs with lower total cost [7], but that perspective is not universally accepted, and in fact, many organizations believe that overlays should be completely DC [69].

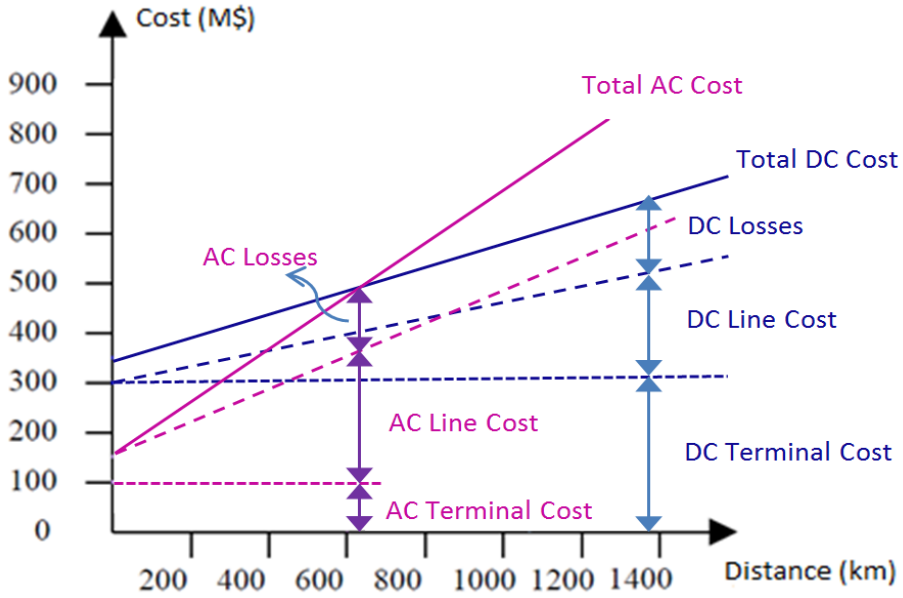

Fig. 7.1: Cost comparison between AC and DC options.

In this study, we select four types of high voltage transmission circuits, which are today's most mature and cost-effective technologies for bulk power transfer. The four technologies include: 765kV EHVAC, 500kV EHVAC, 600kV HVDC and 800kV HVDC. We summarize their cost, loadability and losses data in the next section.

7.2 Cost, Loadability and Losses

7.2.1 Investment cost

Equations (7.1)–(7.4) below express the investment cost per circuit. Data are listed in Table 7.1 ([70]–[62]). In the remainder of this Chapter, we assign index numbers

1, 2, 3 and 4 to 765kV AC, 500kV AC, 600kV DC and 800kV DC circuits, respectively.

$$\text{765kV AC: } CT_{1t} = 3.49 l_{at} m_t + 16.14 \times [\frac{l_{at} + 2l_0}{l_0}] + 170 n_{at} TC_{1t} \quad (7.1)$$

$$\text{500kV AC: } CT_{2t} = 2.75 l_{at} m_t + 12.57 \times [\frac{l_{at} + 2l_0}{l_0}] + 155 n_{at} TC_{2t} \quad (7.2)$$

$$\text{600kV DC: } CT_{3t} = 1.8 l_{at} m_t + 2 \times 155 TC_{3t} + 155 n_{it} TC_{3t} \quad (7.3)$$

$$\text{800kV DC: } CT_{4t} = 1.95 l_{at} m_t + 2 \times 170 TC_{4t} + 170 n_{it} TC_{4t} \quad (7.4)$$

l_0 is the estimated typical distance between intermediate stations for AC lines. We choose l_0 to be 200miles in this study. $[\frac{l_{at} + 2l_0}{l_0}]$ represents the number of AC substations needed ([] is the integer function). Particularly, we add two other types of cost to these functions, as shown in the last term of (7.1)–(7.4). n_{at} is the number of back to back DC substations for synchronization of different interconnections, and n_{it} is the number of DC substations for resource integration purposes, which is needed on arcs with DC circuits that have major resources at some middle point along the route. The two types of additional costs have been expressed to be proportional to total transmission capacity addition on arc t in (7.1)–(7.4).

7.2.2 Loadability

Line loadability is estimated based on St. Clair Curves [71], as approximated by the function $f(l_{at}) \approx 43.261 l_{at}^{-0.6678}$. We select a typical rating for a single circuit of each technology, listed in Table 7.1. For EHVAC options, we use Surge Impedance Loading (SIL) values. Equations (7.5)–(7.8) express the location-specified loadability data.

$$\text{765kV AC: } TC_{1t} = SIL_1 f(l_{at}) \quad (7.5)$$

500kV AC: $TC_{2t} = SIL_2 f(l_{at})$ (7.6)

600kV DC: $TC_{3t} = 3$ (7.7)

800kV DC: $TC_{4t} = 6$ (7.8)

7.2.3 Losses

We used the method introduced in 5.2.7 to approximate transmission losses, by adding a new term $40(\sum_{s=1}^{4} \Delta_s)(\eta_0 - \eta_{kt})TC_{kt}E_r$ into each of (7.1)–(7.4), where

$\eta_{kt} = 1 - w_k l_{at}$ (7.9)

Values for the parameter w_k for all circuit types are listed in Table 7.1. Loss data are estimated from [62] and [72]. In this study, we assume η_0 to be 0.99 and average energy price E_r to be 0.0089M$/GWhr.

Table 7.1: Basic data for transmission technologies.

Technology	765kV	500kV	600kV	800kV
Typical Rating(GW)	SIL=2.25@300mile	SIL=1@300mile	3GW	6GW
Circuit Breaker(M$)	2.88	2.27	–	–
Transformer(M$)	9.02	6.8	–	–
Voltage Control(M$)	4.24	3.5	–	–
Converter(M$/MW)	–	–	0.155	0.17
Line Cost (M$/mile)	3.49	2.75	1.8	1.95
ROW (ft.)	200	200	250	270
($w_k l_{at}$) losses@SIL(10^{-5})	6.47l_{at}	12.6 l_{at}	6.58 l_{at}	4.58 l_{at}
X for AC (Ω/mile)	0.5069	0.5925	–	–

7.3 Problem Statement

We implement the decimal-binary disjunctive model described in Chapter 5 to model the national transmission overlay design problem. To clearly describe the problem,

we re-write the nomenclature and problem statement in this chapter.

7.3.1 Nomenclature

$y/s/g/h$	Year/load step/node/generation type number
$k/t/b$	Transmission type/arc number/branch index
$N_y/N_s/N_g$	Number of year/load step/node in the model
N_h/N_k	Number of generation/transmission type
N_t/N_b	Number of candidate arcs/parallel branches
N_{inv}	Set of years which allow transmission expansion
η_0	Efficiency of existing transmission system
η_{kt}	Efficiency of type *k* new transmission on arc *t*
E_r	Average energy price (M$/GWhr)
r	Discount rate: 0.02
Δ_s	Time duration for step *s* in each year (hour)
$v(y)$	Residual value factor for year *y*
P_{ysgh}	Generation output of type *h* unit on node *g* during year *y* step *s* (GW)
D_{ysg}	Active load on node *g* during year *y* step *s* (GW)
A	Incidence matrix
CG_{gh}	Type *h* unit production cost on node *g* (M$/GWhr)
CT_{kt}	Type *k* transmission investment cost on arc *t* (M$)
x_{yktb}	Number of type *k* circuits invested on arc *t* branch *b* during year *y*
S_{yktb}	Cumulative number of type *k* circuits invested on arc *t* branch *b* till year *y*
B_{yst}	Total power flow on arc *t* on year *y* step *s* (GW)

B_{yst0} Branch flow on existing transmission on arc *t* year *y* step *s* (GW)

B_{ystkb} Branch flow on arc *t* type *k* transmission branch *b* on year *y* step *s* (GW)

CF_{gh} Renewable capacity factor for type *h* unit on *g*

PC_{ygh} Generation capacity of type *h* unit on node *g* during year *y* (GW)

θ_{ysg} Voltage angle on bus *g* on year *y* step *s* (radians)

$X0_{ty}$ Reactance of existing transmission on arc *t* year *y*

X_{tkb} Reactance of type *k* circuit addition on arc *t* branch *b*

UB_{ysktb} Disjunctive coefficient for year *y* step *s* type *k* trans-mission arc *t* branch *b*

G A large number

TC_{kt} Type *k* transmission loadability on arc *t* (GW)

$TC0_t$ Existing transmission capacity on arc *t* (GW)

l_{mt} Investment equivalent distance on arc *t* (mile)

l_{at} Actual route distance on arc *t* (mile)

l_0 Typical distance between AC substations (mile)

w_k Linear coefficient between loss and distance for type *k* circuit (mile^{-1})

S_k Type *k* circuit Surge Impedance Loading (SIL) (GW)

$f(l_{at})$ Approximation function of St. Clair Curve

7.3.2 Problem statement

$$Min \sum_{y=1}^{Ny}\sum_{s=1}^{Ns}\sum_{g=1}^{Ng}\sum_{h=1}^{Nh}(1+r)^{-y} P_{ysgh}\Delta_s CG_{gh} + \sum_{\substack{y=1 \\ y\in N_{inv}}}^{Ny}\sum_{k=1}^{Nk}\sum_{t=1}^{Nt}\sum_{b=1}^{Nb} 2^{b-1}(1+r)^{-y} v(y) CT_{kt}\, x_{ysktb} + \sum_{y=1}^{Ny}\sum_{s=1}^{Ns}\sum_{t=1}^{2Nt}(1+r)^{-y}(1-\eta_0)\Delta_s E_t B_{yst}$$

(7.10)

Subject to

$$\sum_{h=1}^{Nh} P_{ysgh} - D_{ysg} = \sum_{t=1}^{2Nt} A^T(g,t) B_{yst} \tag{7.11}$$

$$\sum_{i=1}^{y} \sum_{b=1}^{Nb} 2^{b-1} x_{iktb} = \sum_{b=1}^{Nb} 2^{b-1} S_{yktb} \tag{7.12}$$

$$B_{yst} = B_{yst0} + \sum_{k=1}^{Nk} \sum_{b=1}^{Nb} B_{ystkb} \tag{7.13}$$

$$\theta_{ysgi} - \theta_{ysgj} = X0_{ty}(B_{yst0} - B_{ys(t+Nt)0}) \tag{7.14}$$

$$\theta_{ysgi} - \theta_{ysgj} = X_{tkb}(B_{ystkb} - B_{ys(t+Nt)kb}) + (S_{yktb} - 1)G + UB_{ysktb} \tag{7.15}$$

$$0 \le UB_{ysktb} \le 2(1 - S_{yktb})G \tag{7.16}$$

$$0 \le B_{ysktb} \le 2^{b-1} S_{yktb} TC_{kt} \tag{7.17}$$

$$0 \le B_{yst0} \le TC0_{ty} \tag{7.18}$$

$$0 \le P_{ysgh} \le CF_{gh} PC_{ygh} \tag{7.19}$$

Constraints (7.1)–(7.8) (7.20)

Binary

$$S_{yktb},\ x_{yktb}$$

Here, $v(y) = (N_y + 1 - y)/40$ is the residual value factor for each year. (7.11) is the power balance constraints on each node. (7.12) is the relationship between yearly and accumulative investments, derived from reference [14]'s modeling approach. (7.13) is the branch flow decomposition. (7.14)–(7.16) are the disjunctive DC flow constraints (i, j are the beginning/end node for arc t). (7.17)–(7.18) are circuit capacity limits. (7.19) is the generation output limits. All costs have been discounted to 2010$.

7.4 Reference Case

Based on the assumptions in Chapter 3, Section 4, we considered the following four generation futures using NETPLAN: reference, high offshore wind, high solar and high geothermal. The reference case models significant inland wind and only a relatively low amount of other renewables. The generation portfolio is summarized in Table 7.2 and Fig. 7.2. The penetration level of inland wind increases to 50.61% at year 40, and at that time most current coal and oil generation facilities will undoubtedly be retired and will not be rebuilt. IGCC and geothermal also show significant predicted increase, while other types of conventional generation are predicted to slowly increase. Figure 7.3 shows the location and capacity of major inland wind power facilities. Generation investments are optimized on a yearly basis, as introduced in Chapter 3.

Table 7.2: Generation capacity vs. year for reference case.

Capacity (GW) at Year / Generation Type	1	10	20	30	40	Final Penetration
Nuclear	107.4	132.3	159.1	146.5	118.1	5.20%
Pulverized Coal	332.1	210.9	39.4	28.8	13.1	0.58%
NGCC	240.0	275.6	310.8	208.8	251.4	11.07%
CT	219.5	285.9	241.8	256.8	274.4	12.09%
Hydro	98.5	96.0	90.5	86.7	79.0	3.48%
IGCC	0.6	32.2	83.9	157.7	205.9	9.07%
IPCC	0.0	0.0	0.0	0.0	0.0	0.00%
Oil	56.7	52.8	5.1	1.2	1.2	0.05%
Geothermal	0.0	0.8	43.1	135.8	178.1	7.84%
Offshore Wind	0.0	0.0	0.0	0.0	0.0	0.00%
Inland Wind	37.5	366.9	570.1	829.5	1,149	50.61%
Solar Thermal	0.5	0.1	0.1	0.0	0.0	0.00%
Solar PV	0.4	0.4	0.4	0.4	0.0	0.00%
OTEC	0.0	0.0	0.0	0.0	0.0	0.00%

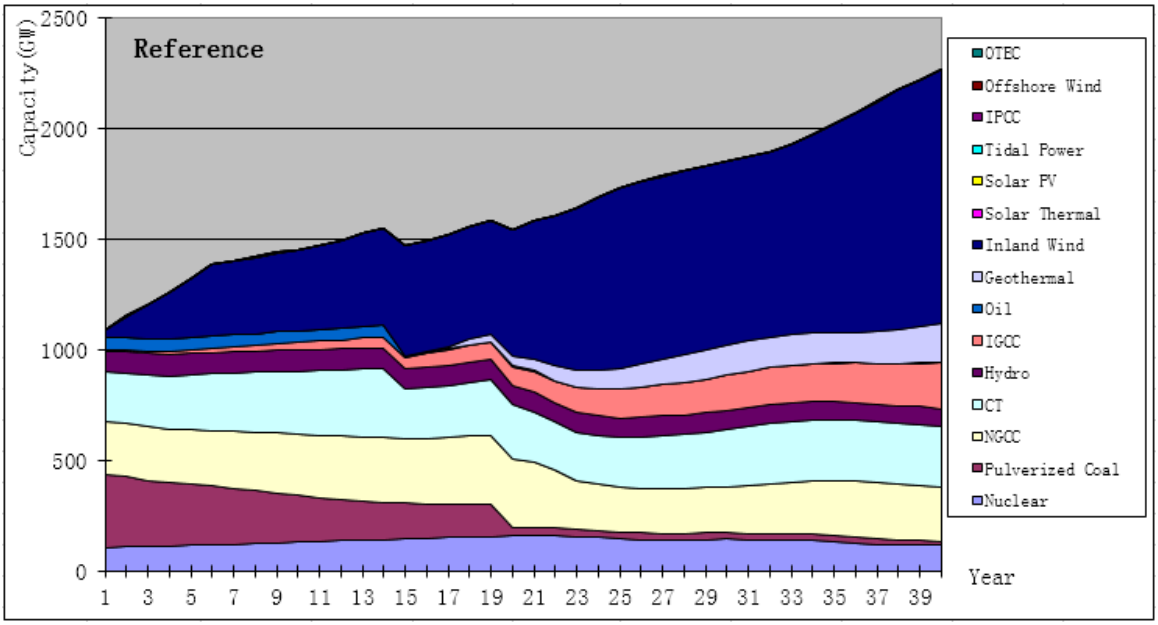

Fig. 7.2: Generation capacity vs. year for reference case.

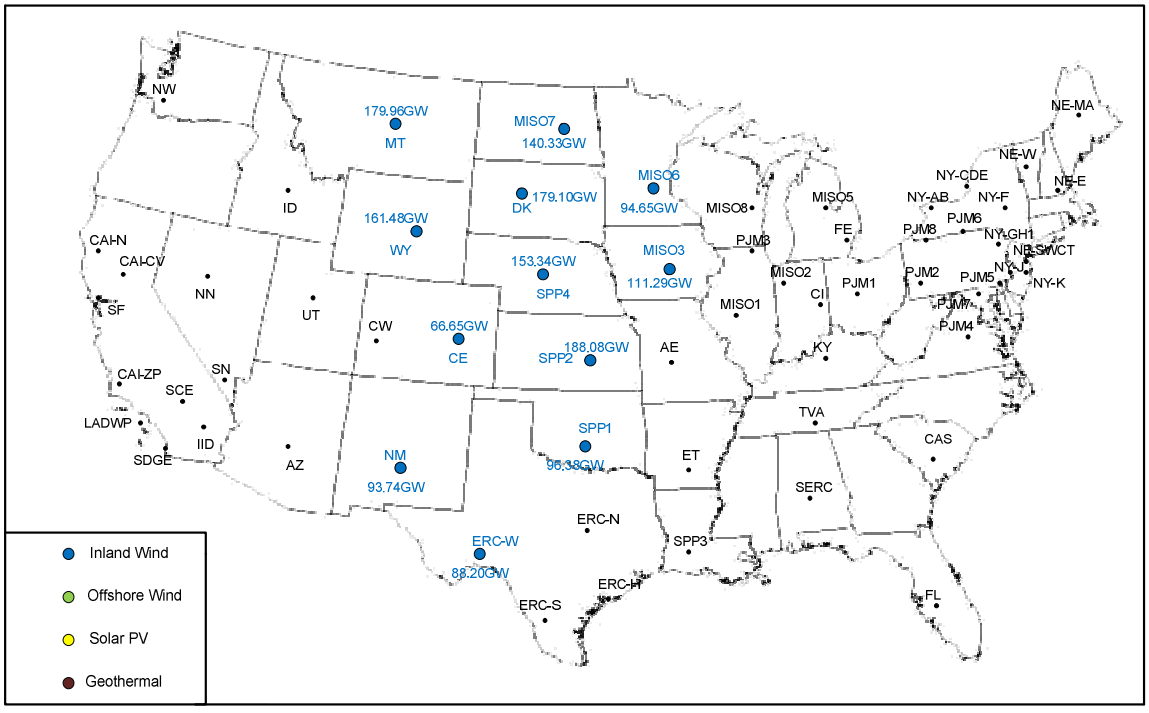

Fig. 7.3: Major inland wind generation location for reference case.

Based on this generation scenario, we selected years 1 and 16 for transmission investment, and we assume peak and off-peak load steps for each year; all four extra high-voltage transmission technologies previously discussed in this chapter have been modeled. We allow 2 parallel bundles for most transmission candidates, representing an upper limit of 3 parallel circuit additions for each technology. For the 19 (of all 383) arcs that tend to have large transmission needs, we allow 5 bundles, equivalent to a maximum of 31 parallel circuits. These 19 arcs have been selected based on a large number of previous simulations. The TNEP model has been coded in MATLAB R2012b and solved in CPLEX v12.5 on a server with 24 2.67MHz CPUs and 47GB memory, located in the Department of Electrical and Computer Engineering at Iowa State University. Problem and solution information is summarized in Table 7.3 below.

Table 7.3: Reference case model description and solution details.

Number of Variables	1,858,904
Number of Binaries	138,264
Number of Equality Constraints	215,132
Number of Inequality Constraints	1,703,128
Number of Total Linear Constraints	1,918,260
Model Generation Time (sec.)	1,157.45
Solution Time (sec.)	468,439.96
MIP Gap	4.94%
Number of Total Iterations	1,981,678
Number of Circuit Additions at Year 1	63
Number of Circuit Additions at Year 16	341
Total Cost (Gen. Inv. Cost Excluded) (2010B$)	1,557.853
Total Transmission Investment Cost (2010B$)	472.1436
Total Circuit Miles Invested	140,366.9

Figure 7.4 and 7.5 display transmission overlay design on the map for year 15 and year 40, respectively, to give a simple illustration of the network investment trend. Lines in these maps are for illustration purpose only, which do not represent actual route.

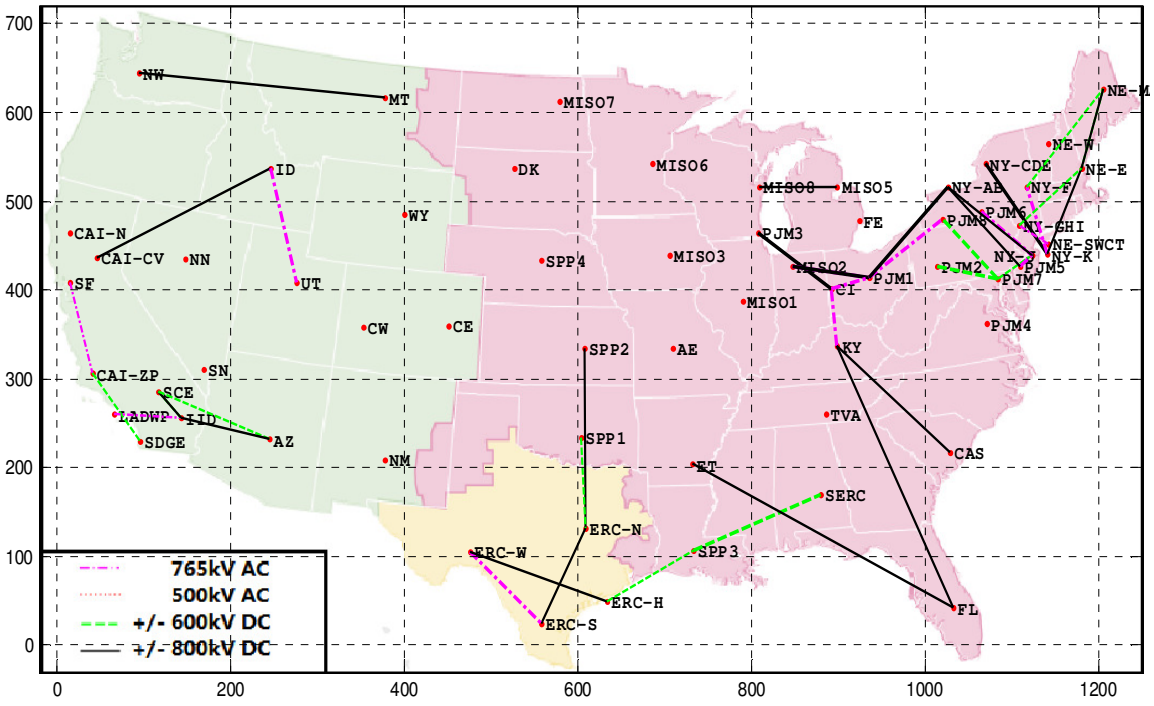

Fig. 7.4: Transmission overlay design for reference case at year 15.

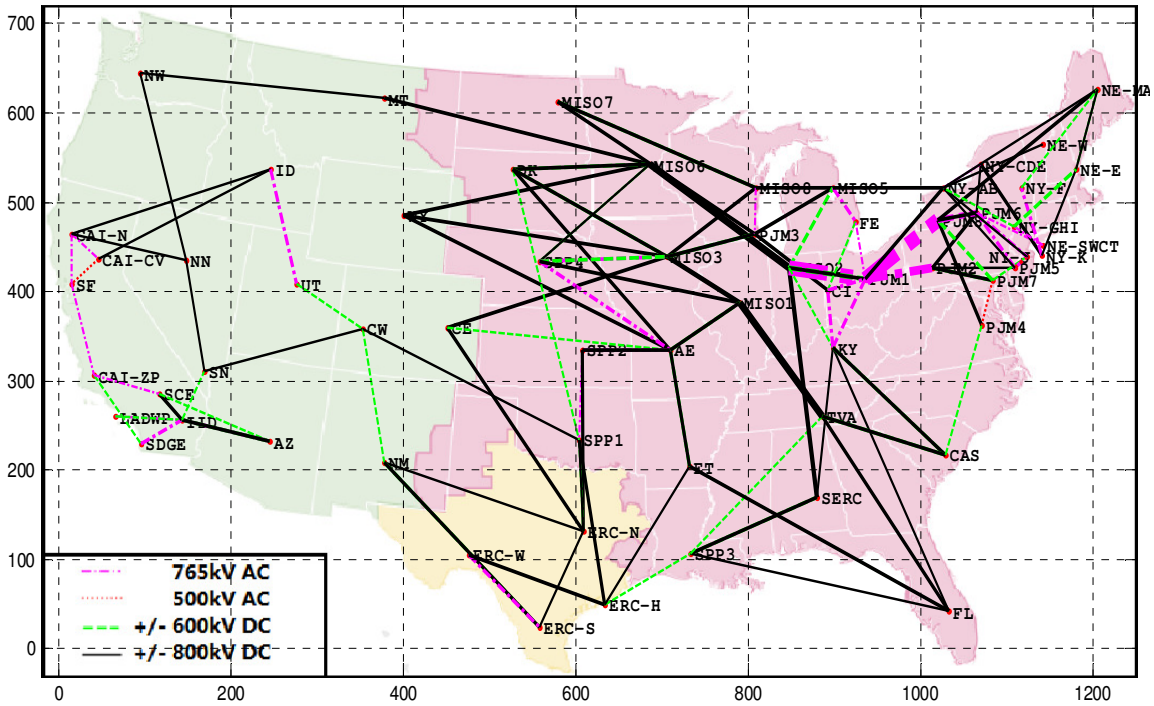

Fig. 7.5: Transmission overlay design for reference case at year 40.

Table 7.4 below shows the details of a selected portion of major new transmission, while Table 7.5 shows the investment amount of each technology.

Table 7.4: Major transmission investments for reference case.

Year	Tech	From	To	# of Ckt. Added	Length (mile)	Capacity per Ckt. (GW)	Cost per Circuit (2010M$)
1	765kV	M2	P1	4	176.0	3.1	675.0
1	600kV	S3	SE	2	472.0	3.0	2240.5
1	800kV	N6	N2	2	290.0	6.0	2885.1
16	765kV	M2	P1	16	176.0	3.1	675.0
16	765kV	M2	P1	8	176.0	3.1	675.0
16	765kV	P1	P2	8	205.0	2.8	827.5
16	765kV	P1	P8	16	185.0	3.0	712.1
16	765kV	P1	P8	8	185.0	3.0	712.1
16	765kV	P8	P6	8	204.0	2.8	787.8
16	500kV	P7	P4	1	107.0	1.9	472.2
16	600kV	M1	TV	8	338.0	3.0	1,705.5
16	600kV	M2	P1	8	176.0	3.0	1,269.2
16	800kV	M1	TV	8	338.0	6.0	2,858.9
16	800kV	M3	M1	8	339.0	6.0	2,802.4
16	800kV	M6	M2	8	610.0	6.0	3,960.8
1	600kV	S3	SE	2	472.0	3.0	2,240.5

Table 7.5: Investment amount of each technology for reference case.

Technology / Metrics	765kV	500kV	600kV	800kV
Total Circuit Miles	24,442.8	296.9	29,437.0	86,190.2
# of Circuit	137	5	82	180
Total Capacity (GW)	435.19	13.09	246.00	1,080.00
Total Cost (2010B$)	54.73	0.56	87.04	329.82

From the table we can see that, in this case, in order to carry wind power from the Midwest and Great Basin to load centers in the East, major transmission requirements become pronounced near the south region of the Great Lakes after year 2025. There is also a requirement for significant transmission between SPP and ERCOT, and MISO and TVA. The design is a hybrid AC/DC network, and 800kV HVDC is the preferred type.

7.5 High Offshore Wind Case

The high offshore wind case projects a relatively high amount of offshore wind generation used to replace a portion of inland wind. Other types of renewable and conventional generation have capacities similar to that of the reference case. In general, this case is similar to the reference case and thus is expected to require similar overlay design. The generation portfolio for this case is summarized in Table 7.6 and Fig. 7.6. The penetration level of offshore wind increases by 11.81% at year 40. As for the reference case, most coal and oil generation facilities are expected to be retired and will not be rebuilt, while IGCC and geothermal facilities show significant increase. Other types of conventional generation increase slowly as well. Figure 7.7 shows the location and capacity of major offshore wind.

Table 7.6: Generation capacity vs. year for high offshore wind case.

Capacity (GW) at Year / Generation Type	1	10	20	30	40	Final Penetration
Nuclear	107.4	132.3	159.1	146.5	118.1	5.24%
Pulverized Coal	332.1	210.9	39.4	28.8	13.1	0.58%
NGCC	240.0	273.2	308.4	206.4	251.4	11.15%
CT	219.5	285.9	241.8	256.8	274.4	12.17%
Hydro	98.5	96.0	90.5	86.7	79.0	3.51%
IGCC	0.6	26.3	73.6	139.2	178.6	7.92%
IPCC	0.0	0.0	0.0	0.0	0.0	0.00%
Oil	56.7	52.8	5.1	1.2	1.2	0.05%
Geothermal	0.0	0.6	32.7	125.0	171.6	7.61%
Offshore Wind	0.0	92.2	194.6	266.3	266.3	11.81%
Inland Wind	37.5	270.9	349.5	571.8	900.9	39.96%
Solar Thermal	0.5	0.1	0.1	0.0	0.0	0.00%
Solar PV	0.4	0.4	0.4	0.4	0.0	0.00%
OTEC	0.0	0.0	0.0	0.0	0.0	0.00%

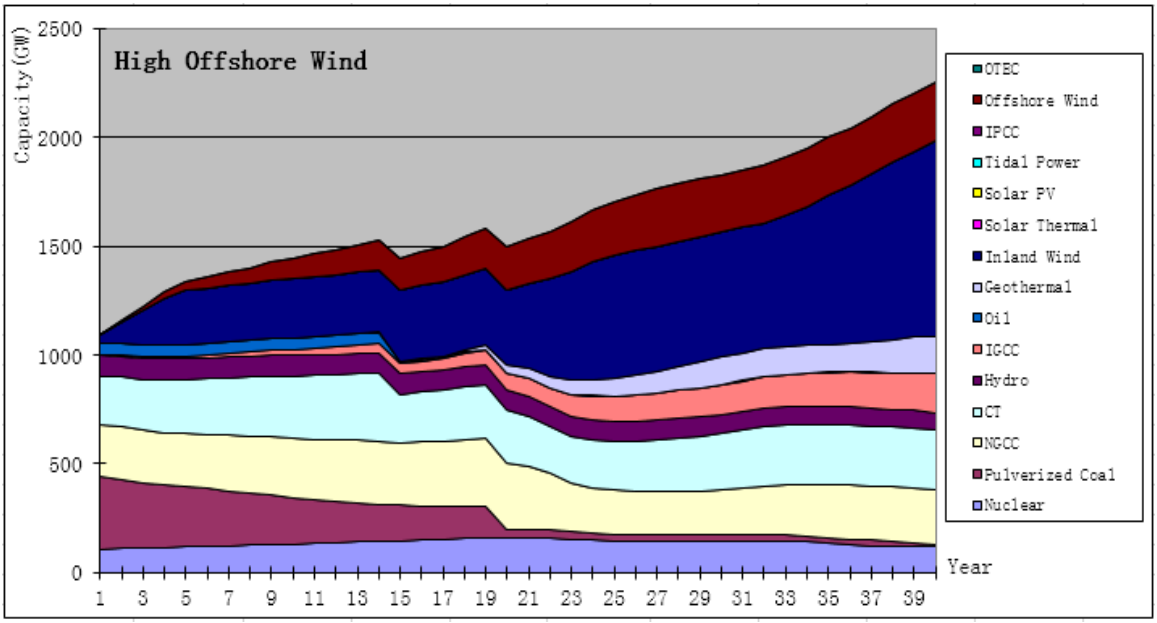

Fig. 7.6: Generation capacity vs. year for high offshore wind case.

Fig. 7.7: Major offshore wind generation location for high offshore wind case.

All modeling parameters remain consistent with the reference case introduced in the last section. Problem and solution information for this case are summarized in Table 7.7. Figure 7.8 and 7.9 display transmission design for this case for years 15 and 40, respectively.

Table 7.7: High offshore wind case model description and solution details.

Number of Variables	1,858,904
Number of Binaries	138,264
Number of Equality Constraints	215,132
Number of Inequality Constraints	1,703,128
Number of Total Linear Constraints	1,918,260
Model Generation Time (sec.)	1100.64
Solution Time (sec.)	537,283.85
MIP Gap	9.49%
Number of Total Iterations	1,634,319
Number of Circuit Additions at Year 1	89
Number of Circuit Additions at Year 16	351
Total Cost (Gen. Inv. Cost Excluded) (2010B$)	1,572.069
Total Transmission Investment Cost (2010B$)	478.2649
Total Circuit Miles Invested	139,773.0

Table 7.8: Major transmission investments for high offshore wind case.

Year	Tech	From	To	# of Ckt. Added	Length (mile)	Capacity per Ckt. (GW)	Cost per Circuit (2010M$)
1	765kV	P1	P8	4	185.0	3.0	712.1
1	500kV	CI	P1	8	107.0	1.9	339.7
1	600kV	N6	NI	1	443.0	3.0	2,840.1
1	800kV	M3	M1	8	339.0	6.0	2,802.4
16	765kV	CI	P1	8	107.0	4.3	405.7
16	765kV	M2	P1	16	176.0	3.1	675.0
16	765kV	P1	P8	16	185.0	3.0	712.1
16	765kV	P3	M2	16	183.0	3.0	847.6
16	500kV	M2	CI	8	112.0	1.9	387.3
16	600kV	M2	P1	8	176.0	3.0	1,269.2
16	800kV	M1	TV	8	338.0	6.0	2,858.9
16	800kV	M3	M1	8	339.0	6.0	2,802.4
16	800kV	M6	M2	8	610.0	6.0	3,960.8

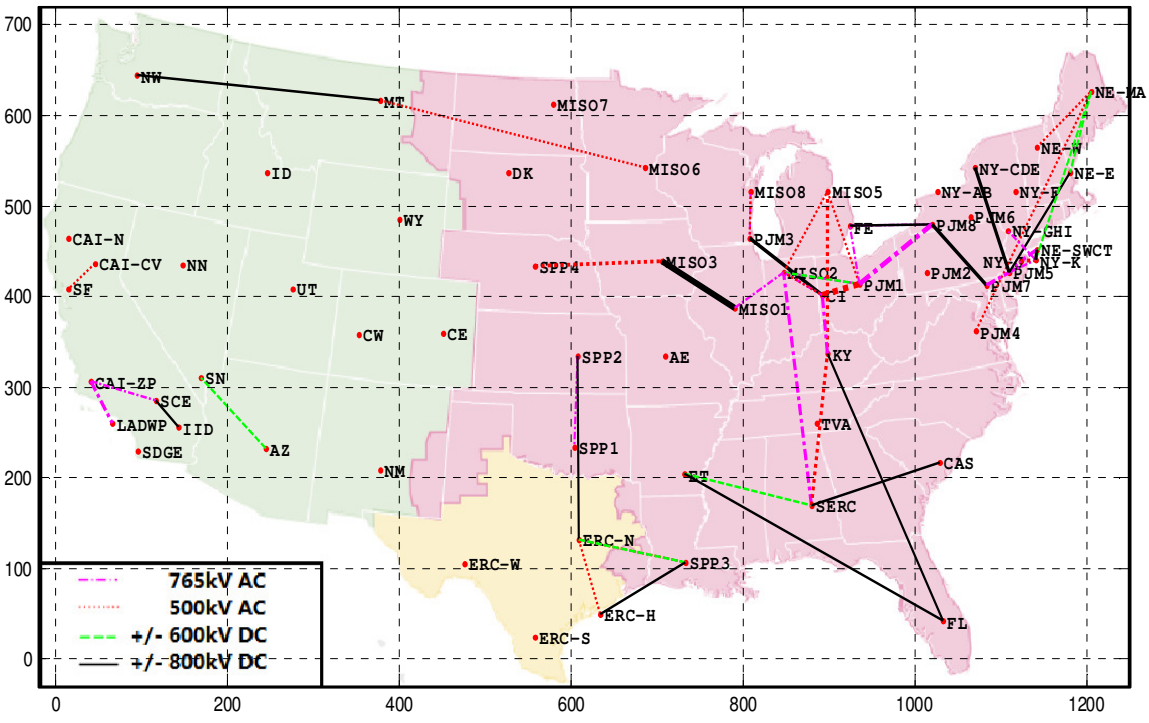

Fig. 7.8: Transmission overlay design for high offshore wind case at year 15.

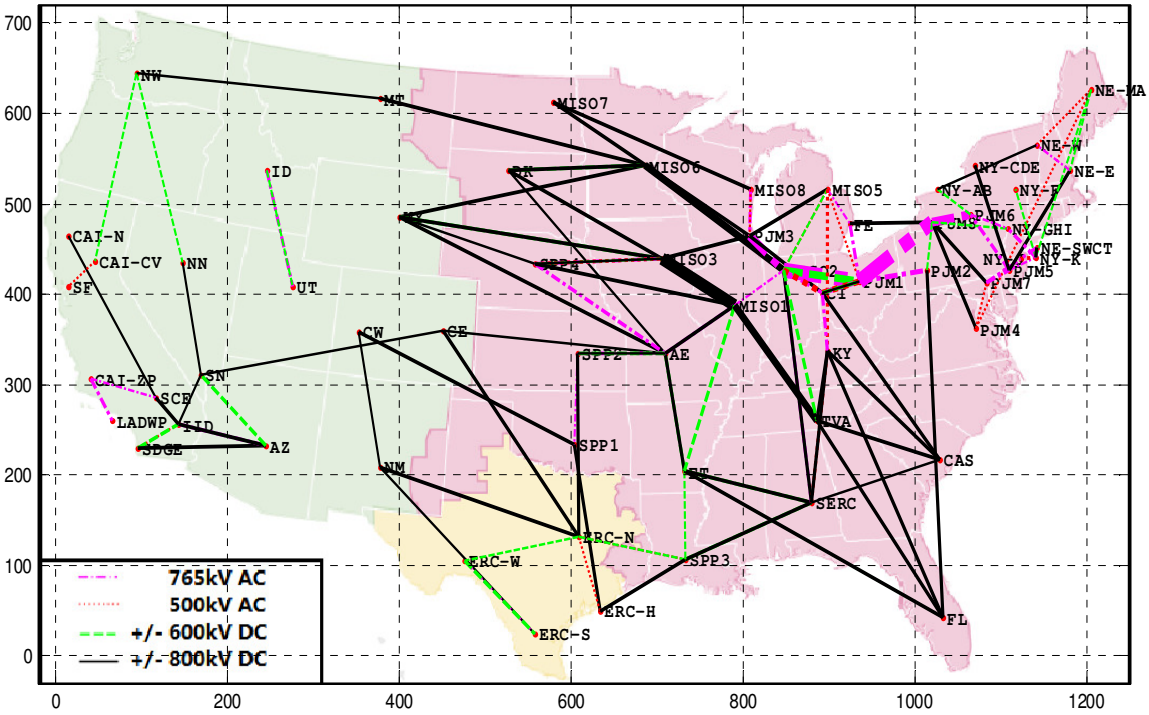

Fig. 7.9: Transmission overlay design for high offshore wind case at year 40.

Table 7.9: Investment amount of each technology for high offshore wind case.

Metrics \ Technology	765kV	500kV	600kV	800kV
Total Circuit Miles	28,239.2	8,020.0	19,750.0	83,763.8
# of Circuit	161	41	61	177
Total Capacity (GW)	526.73	66.31	183.00	1,062.00
Total Cost (2010B$)	66.54	29.16	57.32	325.24

Table 7.8 provides details for a selected portion of major new transmission, while Table 7.9 gives each technology's required investment. A few observations can be made based on these results. First, there is a slight increase in transmission investment before year 15 and the amount is very close to that of the reference case. Although the high offshore wind case requires slightly more circuits to be built and a higher total investment cost, the total circuit miles invested drops a little from the reference case value. The reason for this is that, compared to inland wind, offshore wind resources are located closer to major load centers along the East and West coasts, as discussed in Table 3.6 in Chapter 3. Also, this design is indeed quite similar in topology compared to the design for the reference case, with only slight differences in technology selection. There is more 500kV AC and less 600kV DC, but 800kV HVDC remains the type of circuit most heavily invested. Similarly, very significant transmission needs are predicted after year 2025 near the south region of the Great Lakes area, where the preferred technology used to carry wind power from the Midwest and Great Basin to the East is still 765kV EHVAC. Other main investment trends remain consistent with the reference case. Finally, with respect to computational performance, this case required slightly more computation time with less number of iterations, and produced slightly lower solution quality than the reference case, but still was within a 10% MIP gap tolerance.

7.6 High Solar Case

In the high solar case, a significant difference from the previous cases is that solar PV generation increases rapidly during the planning horizon, replacing more than 300GW's of inland wind power and reaching up to 15.28% penetration in the last year. It also models with about a 7% penetration of geothermal generation. Other types of generation, like coal, oil, IGCC, etc., all have a similar trend in capacity change as previous cases. The generation portfolio is summarized in Table 7.10 and Fig. 7.10. Figure 7.3 shows the location and capacity of major solar generation, mostly located in Arizona, New Mexico, and Colorado, in good agreement with the distribution patterns of the Chapter 3 resource maps. Since future solar PV generation is pretty concentrated and at great distance from the loads, it can be expected to require more transmission investment in the overlay design.

Table 7.10: Generation capacity vs. year for high solar case.

Capacity (GW) at Year / Generation Type	1	10	20	30	40	Final Penetration
Nuclear	107.4	132.3	159.1	146.5	118.1	4.89%
Pulverized Coal	332.1	210.9	39.4	28.8	13.1	0.54%
NGCC	240.0	274.0	309.2	207.2	251.4	10.41%
CT	219.5	285.9	241.8	256.8	274.4	11.36%
Hydro	98.5	96.0	90.5	86.7	79.0	3.27%
IGCC	0.6	32.1	83.1	155.3	201.4	8.34%
IPCC	0.0	0.0	0.0	0.0	0.0	0.00%
Oil	56.7	52.8	5.1	1.2	1.2	0.05%
Geothermal	0.0	0.8	43.1	132.4	178.9	7.41%
Offshore Wind	0.0	0.0	0.0	0.0	0.0	0.00%
Inland Wind	37.5	301.6	406.0	628.7	928.4	38.44%
Solar Thermal	0.5	0.1	0.1	0.0	0.0	0.00%
Solar PV	0.4	107.6	226.6	345.7	369.1	15.28%

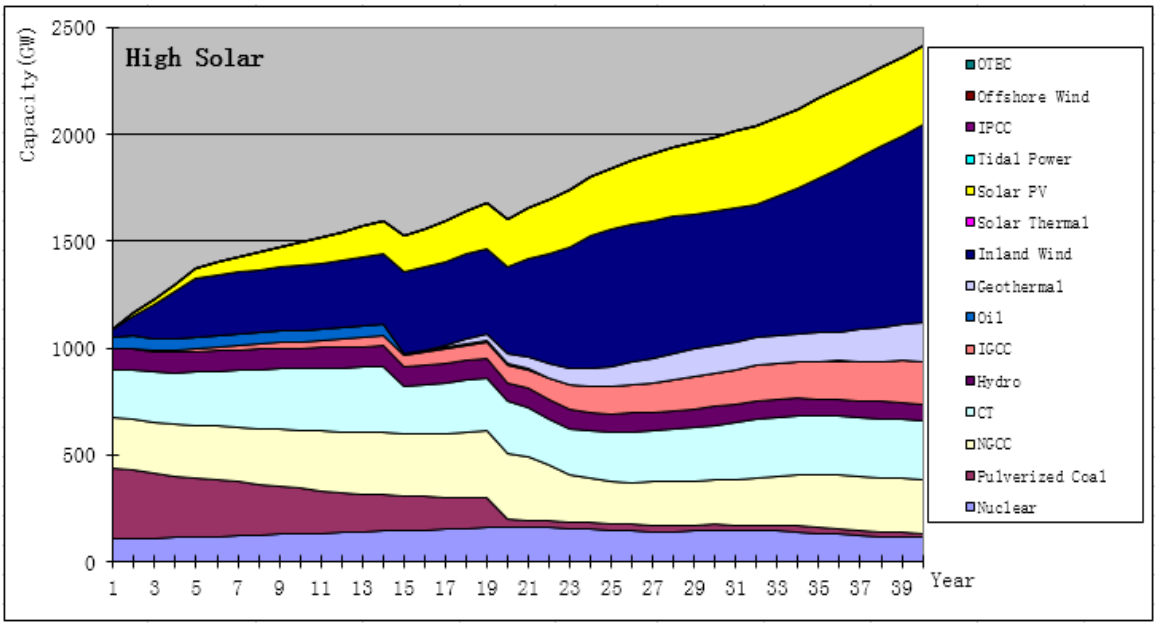

Fig. 7.10: Generation capacity vs. year for high solar case.

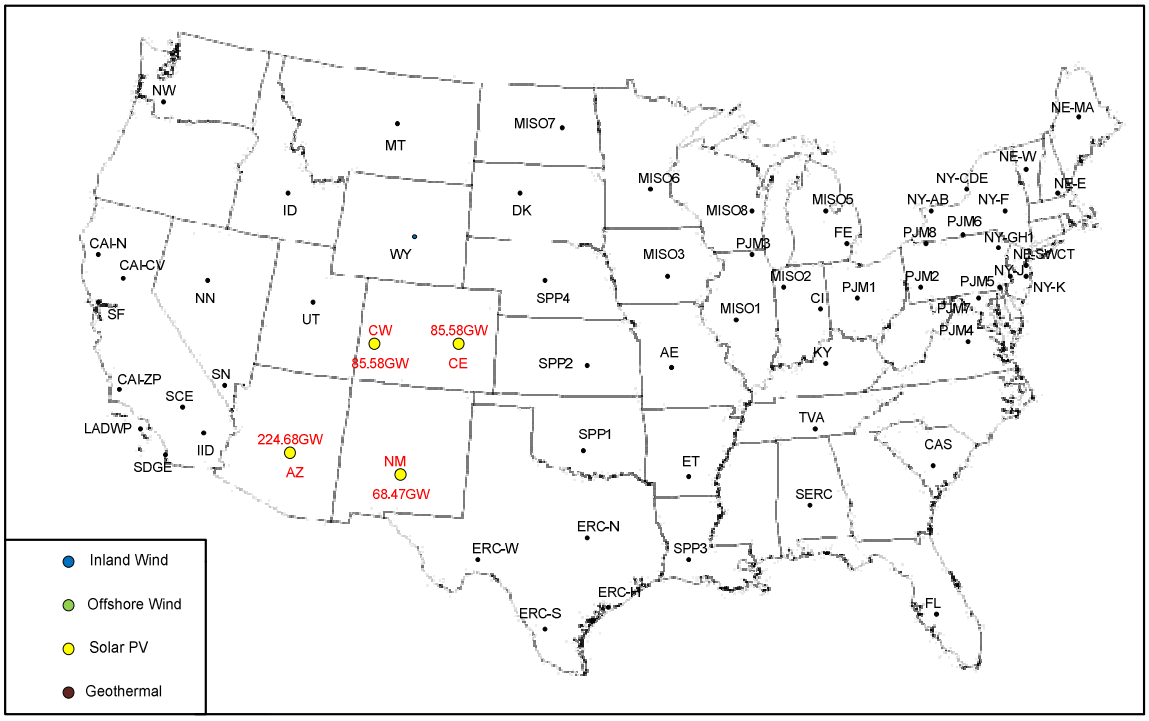

Fig. 7.11: Major solar generation location for high solar case.

All modeling parameters remain consistent with previous cases. Problem and solution information for this case is summarized in Table 7.11. Figure 7.12 and 7.13 display transmission design for years 15 and 40, respectively.

Table 7.11: High solar case model description and solution details.

Number of Variables	1,858,904
Number of Binaries	138,264
Number of Equality Constraints	215,132
Number of Inequality Constraints	1,703,128
Number of Total Linear Constraints	1,918,260
Model Generation Time (sec.)	1,142.21
Solution Time (sec.)	120,491.46
MIP Gap	5.81%
Number of Total Iterations	1,144,854
Number of Circuit Additions at Year 1	97
Number of Circuit Additions at Year 16	349
Total Cost (Gen. Inv. Cost Excluded) (2010B$)	1,582.110
Total Transmission Investment Cost (2010B$)	498.9853
Total Circuit Miles Invested	147,926.5

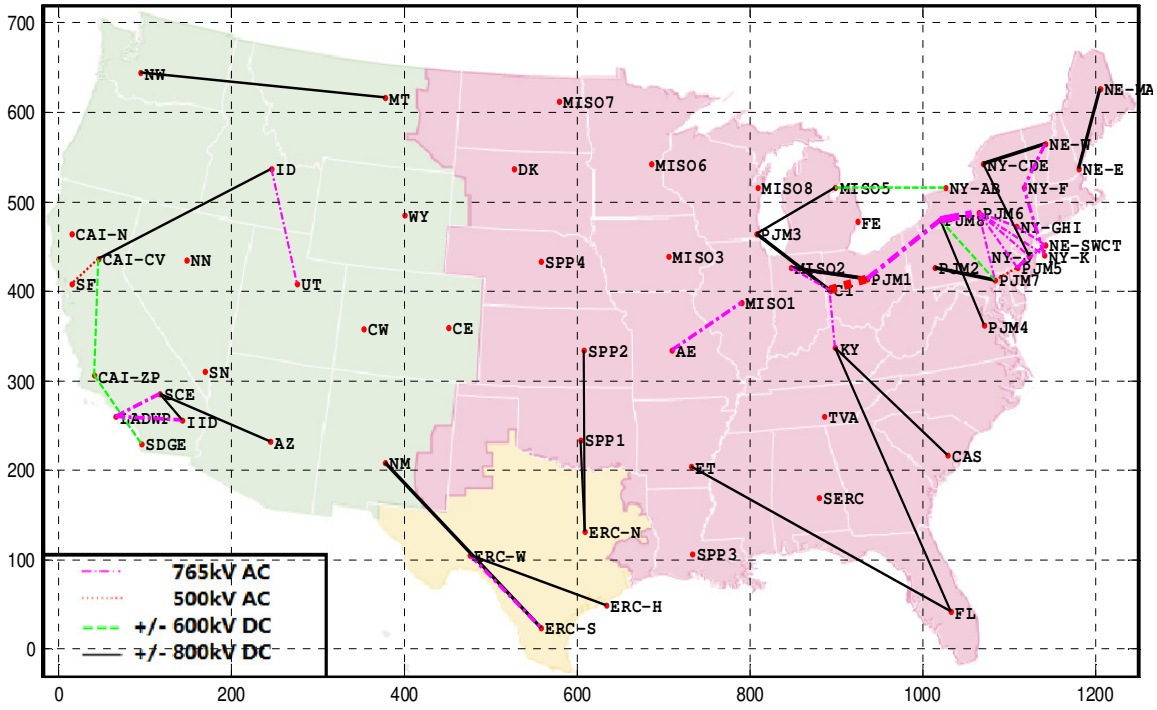

Fig. 7.12: Transmission overlay design for high solar case at year 15.

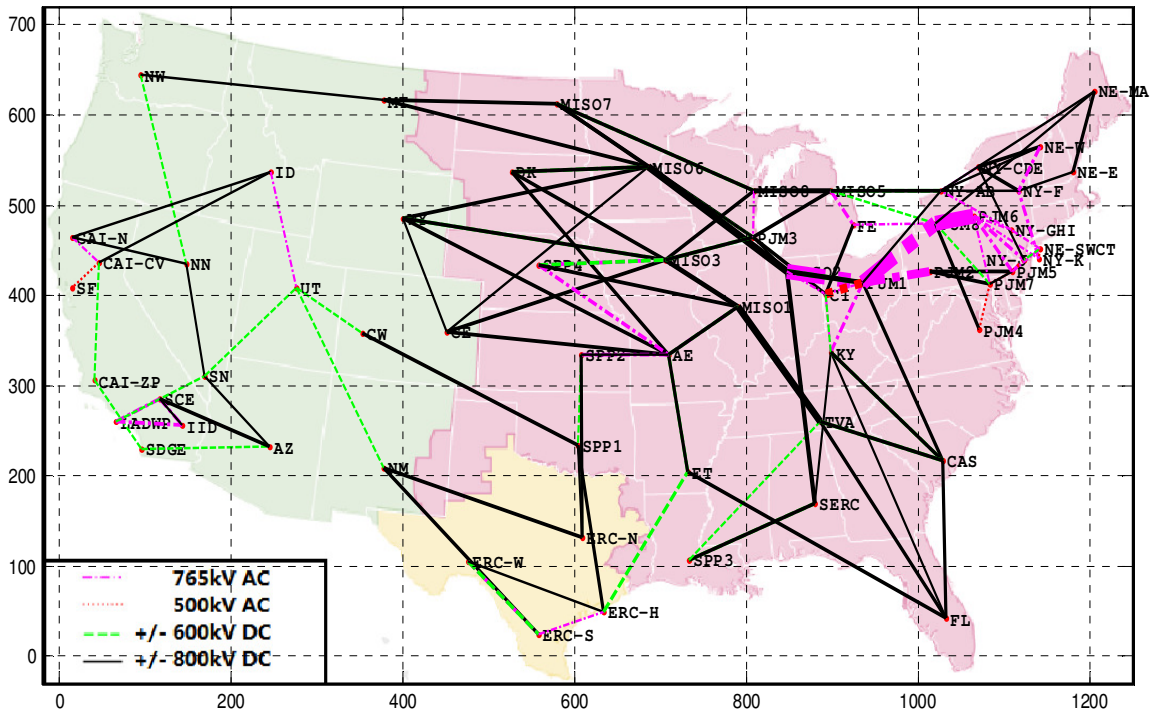

Fig. 7.13: Transmission overlay design for high solar case at year 40.

Table 7.12 below shows the details of a selected portion of major new transmission, while Table 7.13 shows the investment amount of each technology.

Table 7.12: Major transmission investments for high solar case.

Year	Tech	From	To	# of Ckt. Added	Length (mile)	Capacity per Ckt. (GW)	Cost per Circuit (2010M$)
1	765kV	P8	P6	8	204.0	2.8	787.8
1	500kV	CI	P1	16	107.0	1.9	339.7
1	800kV	NM	ES	2	729.0	6.0	4,018.8
16	765kV	M2	P1	16	176.0	3.1	675.0
16	765kV	P1	P2	8	205.0	2.8	827.5
16	765kV	P1	P8	16	185.0	3.0	712.1
16	765kV	P8	P6	16	204.0	2.8	787.8
16	500kV	P5	N5	2	34.0	3.0	137.3
16	600kV	M2	P1	8	176.0	3.0	1,269.2
16	800kV	M1	TV	8	338.0	6.0	2,858.9
16	800kV	M3	M1	8	339.0	6.0	2,802.4
16	800kV	M6	M2	8	610.0	6.0	3,960.8
16	800kV	SE	M2	4	589.0	6.0	3,930.8

Table 7.13: Investment amount of each technology for high solar case.

Metrics \ Technology	765kV	500kV	600kV	800kV
Total Circuit Miles	29,839.7	2,146.8	24,122.0	91,818.0
# of Circuit	165	23	65	193
Total Capacity (GW)	517.88	48.38	195.00	1,158.00
Total Cost (2010B$)	75.57	6.76	61.55	355.11

It can also be observed the major transmission needs for this case persist near the south region of the Great Lakes area after year 2025. The topology is slightly changed from the reference case along the East coast, in the Dakotas, and particularly in the WECC region where solar generation is expected to influence transmission design. The transmission circuits invested and their total cost also increase dramatically from the reference case, as anticipated. From Table 7.13 we can also observe that 500kV EHVAC circuits are only invested on short arcs of about 100 miles or less, while 600kV HVDC and 765kV EHVAC are invested on longer arcs. 800kV HVDC is used only for very long arcs, usually at least 300 miles long.

7.7 High Geothermal Case

This case models a higher amount of geothermal investment, and the generation portfolio is summarized in Table 7.14 and Fig. 7.14. The penetration level of geothermal power increases to 14.97% at year 40. Figure 7.15 shows the location and capacity of geothermal resources, and we can see the geothermal resources actually spread out in the WECC area, remote from the loads, indicating that this case would represent the greatest transmission needs.

Table 7.14: Generation capacity vs. year for high geothermal case.

Capacity (GW) at Year / Generation Type	1	10	20	30	40	Final Penetration
Nuclear	107.4	132.3	159.1	146.5	118.1	5.13%
Pulverized Coal	332.1	210.9	39.4	28.8	13.1	0.57%
NGCC	240.0	250.9	286.1	184.1	238.5	10.37%
CT	219.5	285.9	241.8	256.8	274.4	11.93%
Hydro	98.5	96.0	90.5	86.7	79.0	3.44%
IGCC	0.6	23.8	68.7	123.8	143.8	6.25%
IPCC	0.0	0.0	0.0	0.0	0.0	0.00%
Oil	56.7	52.8	5.1	1.2	1.2	0.05%
Geothermal	0.0	33.8	137.3	240.8	344.3	14.97%
Offshore Wind	0.0	0.0	0.0	0.0	0.0	0.00%
Inland Wind	37.5	370.2	555.0	818.5	1,087	47.28%
Solar Thermal	0.5	0.1	0.1	0.0	0.0	0.00%
Solar PV	0.4	0.4	0.4	0.4	0.0	0.00%
Tidal Power	0.0	0.0	0.0	0.0	0.0	0.00%
OTEC	0.0	0.0	0.0	0.0	0.0	0.00%

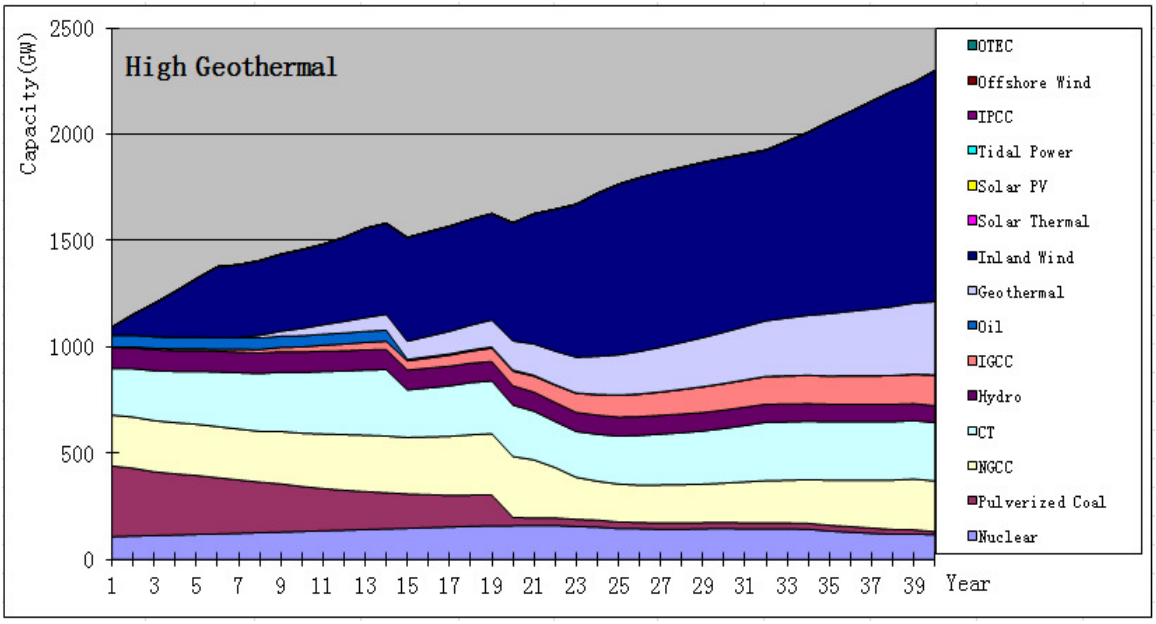

Fig. 7.14: Generation capacity vs. year for high geothermal case.

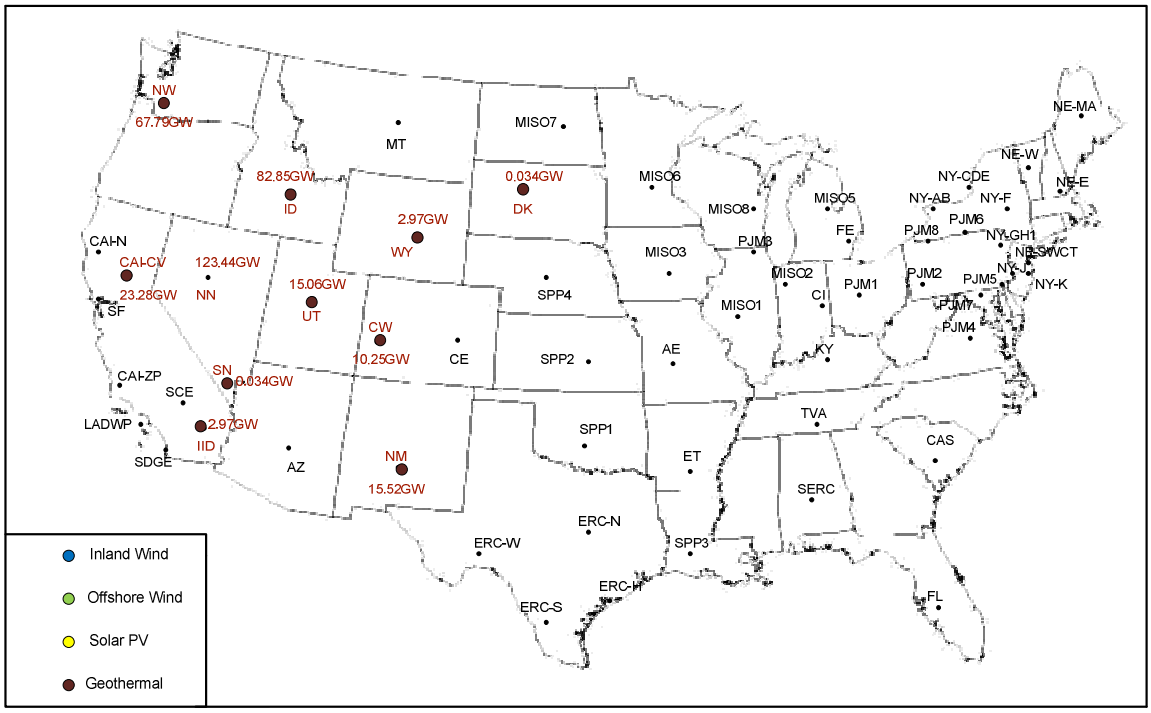

Fig. 7.15: Major geothermal generation location for high geothermal case.

All modeling parameters keep consistent with previous cases. Problem and solution information for this case are summarized in Table 7.15.

Table 7.15: High geothermal case model description and solution details.

Number of Variables	1,858,904
Number of Binaries	138,264
Number of Equality Constraints	215,132
Number of Inequality Constraints	1,703,128
Number of Total Linear Constraints	1,918,260
Model Generation Time (sec.)	1,068.14
Solution Time (sec.)	139,312.57
MIP Gap	4.36%
Number of Total Iterations	2,031,709
Number of Circuit Additions at Year 1	70
Number of Circuit Additions at Year 16	358
Total Cost (2010B$)	1,599.838
Total Transmission Investment Cost (2010B$)	509.0788
Total Circuit Miles Invested	153,799.5

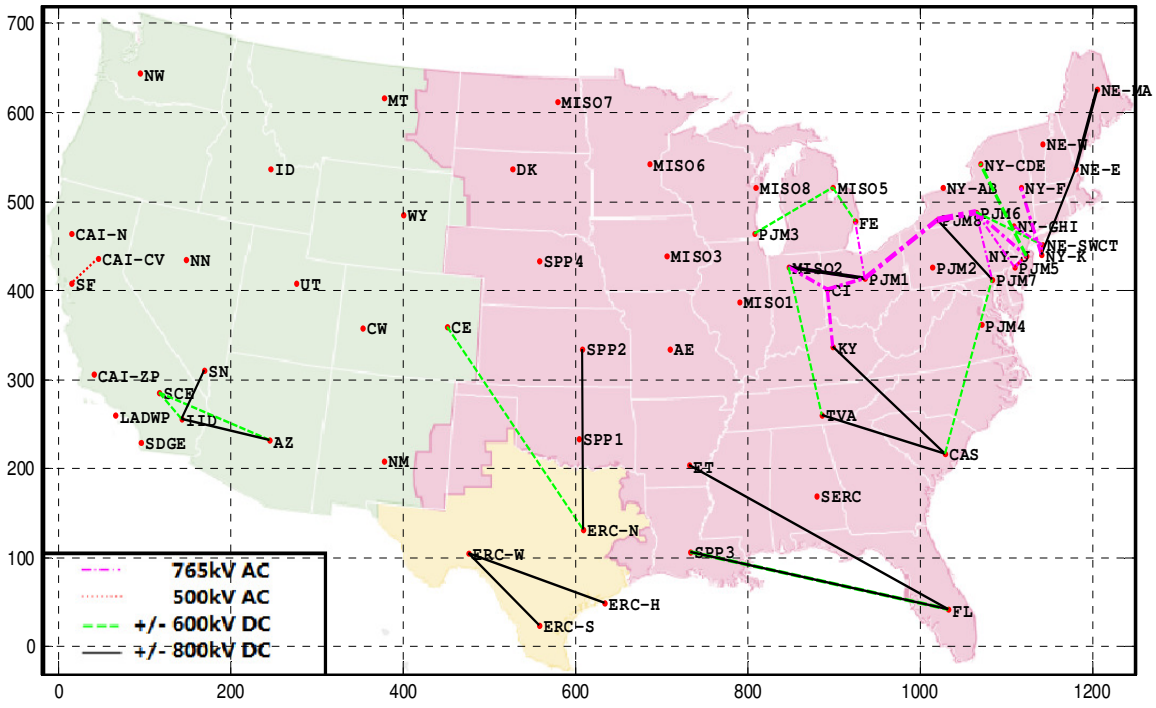

Fig. 7.16: Transmission overlay design for high geothermal case at year 15.

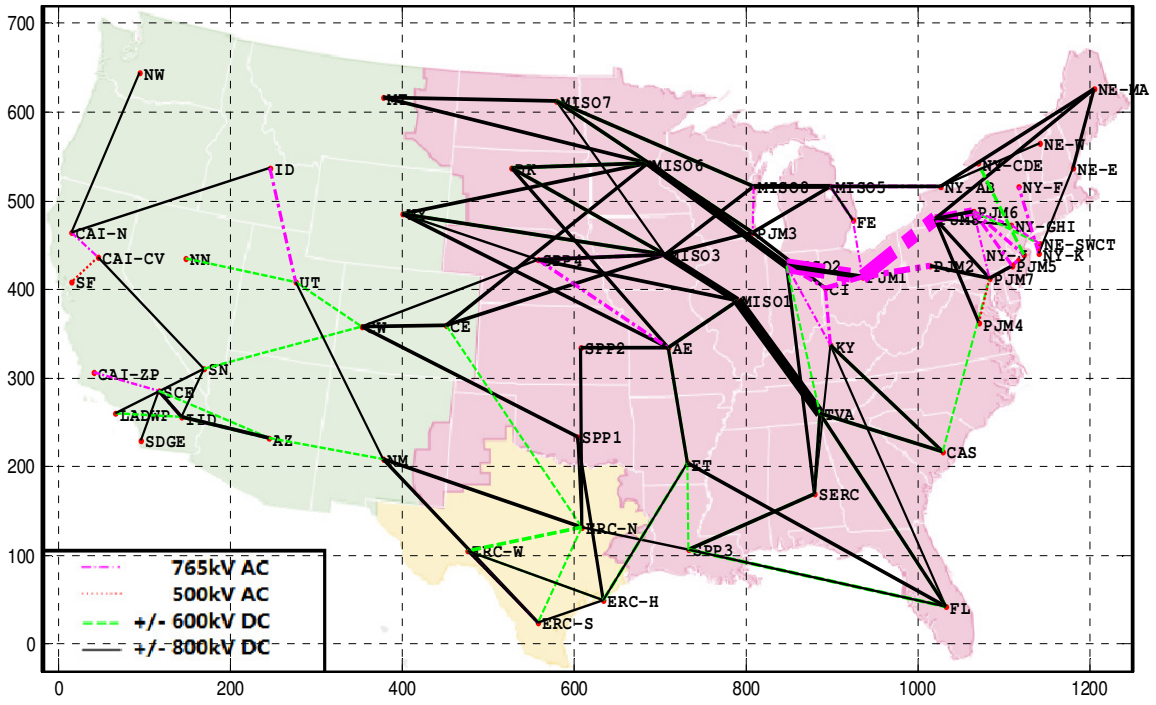

Fig. 7.17: Transmission overlay design for high geothermal case at year 40.

Table 7.16: Major transmission investments for high geothermal case.

Year	Tech	From	To	# of Ckt. Added	Length (mile)	Capacity per Ckt. (GW)	Cost per Circuit (2010M$)
1	1	P1	P8	8	185.0	3.0	712.1
1	1	P8	P6	8	204.0	2.8	787.8
1	3	S3	FL	2	1,280.0	3.0	5,067.4
1	4	NI	NE	2	223.0	6.0	3,000.5
16	1	M2	P1	16	176.0	3.1	675.0
16	1	P1	P2	8	205.0	2.8	827.5
16	1	P1	P8	16	185.0	3.0	712.1
16	2	P5	N5	2	34.0	3.0	137.3
16	3	FL	TV	2	686.0	3.0	2,817.0
16	4	M1	TV	16	338.0	6.0	2,858.9
16	4	M3	M1	8	339.0	6.0	2,802.4
16	4	M6	M2	8	610.0	6.0	3,960.8

Table 7.17: Investment amount of each technology for high geothermal case.

Technology / Metrics	765kV	500kV	600kV	800kV
Total Circuit Miles	25,019.7	312.8	30,039.0	98,428.0
# of Circuit	143	6	64	215
Total Capacity (GW)	463.13	16.09	192.00	1,290.00
Total Cost (2010B$)	60.07	0.91	82.16	365.95

From the above results, we can see that, in this case, transmission investment cost and circuit miles built are much greater than for the other cases, confirming that the distribution pattern of geothermal resources requires the greatest transmission investment. Compared to the reference case, although we do see some differences in topology and technology chosen in the WECC region, the major transmission investment trend changes only a little, since the main renewable resource is still inland wind. Also, in all cases, the three interconnections: Eastern, Texas and WECC are all connected at different places using HVDC links. This indicates that synchronizing all the different interconnections may lower the overall energy costs by enabling more frequent power exchange.

7.8 Flexible Design among Four Scenarios

In this section, we implement the flexibility design method introduced in Chapter 6 to design a national transmission overlay that is not only cost-effective but also robust with respect to all four futures introduced earlier. To reduce the computational burden without losing too much generality and model accuracy, we only allowed a single HVDC circuit addition on each route to provide adaptation investment, and all transmissions are expanded only at year 1. The problem statement has been re-written for this particular problem using the nomenclature in 7.3.1 and necessary additional variables:

$$\begin{aligned} Min \quad & \sum_{\substack{y=1 \\ y\in N_{inv}}}^{Ny}\sum_{k=1}^{Nk}\sum_{t=1}^{Nt}\sum_{b=1}^{Nb} 2^{b-1}(1+r)^{-y}v(y)CT_{kt}x_{yktb} + \\ & \sum_{\varsigma=1}^{4}\rho_{\varsigma}\Big(\sum_{\substack{y=1 \\ y\in N_{inv}}}^{Ny}\sum_{k=Nac+1}^{Nk}\sum_{t=1}^{Nt}(1+r)^{-y}v(y)CT_{kt}x_{\varsigma ykt} + \\ & \sum_{y=1}^{Ny}\sum_{s=1}^{Ns}\sum_{g=1}^{Ng}\sum_{h=1}^{Nh}(1+r)^{-y}P_{\varsigma ysgh}\Delta_s CG_{gh} + \sum_{y=1}^{Ny}\sum_{s=1}^{Ns}\sum_{t=1}^{2Nt}(1+r)^{-y}(1-\eta_0)\Delta_s E_r B_{\varsigma yst}\Big) \end{aligned} \tag{7.21}$$

Subject to

For scenario ς , ς =1, 2, 3, and 4:

$$\sum_{h=1}^{Nh} P_{\varsigma ysgh} - D_{ysg} = \sum_{t=1}^{2Nt} A^T(g,t)B_{\varsigma yst} \tag{7.22}$$

$$\sum_{i=1}^{y}\sum_{b=1}^{Nb} 2^{b-1}x_{iktb} = \sum_{b=1}^{Nb} 2^{b-1}S_{yktb} \tag{7.23}$$

$$\sum_{i=1}^{y} x_{\varsigma ikt} = S_{\varsigma ykt}, \quad k=3,4 \tag{7.24}$$

$$B_{\varsigma yst} = B_{\varsigma yst0} + \sum_{k=1}^{Nk}\sum_{b=1}^{Nb} B_{\varsigma ystkb} + \sum_{k=Nac+1}^{Nk} \bar{B}_{\varsigma ystk} \tag{7.25}$$

$$\theta_{\varsigma ysg_i} - \theta_{\varsigma ysg_j} = X0_{ty}(B_{\varsigma yst0} - B_{\varsigma ys(t+Nt)0}) \tag{7.26}$$

$$\theta_{\varsigma ysg_i} - \theta_{\varsigma ysg_j} = X_{tkb}(B_{\varsigma ystkb} - B_{\varsigma ys(t+Nt)kb}) + (S_{yktb} - 1)G + UB_{\varsigma ysktb} \tag{7.27}$$

$$0 \le UB_{\varsigma ysktb} \le 2(1 - S_{yktb})G \tag{7.28}$$

$$0 \le B_{\varsigma ysktb} \le 2^{b-1} S_{yktb} TC_{kt} \tag{7.29}$$

$$0 \le B_{\varsigma yst0} \le TC0_{ty} \tag{7.30}$$

$$0 \le \bar{B}_{\varsigma ystk} \le S_{\varsigma ykt} TC_{kt}, \quad k = 3,4 \tag{7.31}$$

$$0 \le P_{\varsigma ysgh} \le CF_{gh} PC_{\varsigma ygh} \tag{7.32}$$

Constraints (7.1)–(7.8) (7.33)

$$\theta_{\varsigma ysg_{ref}} = 0 \tag{7.34}$$

Binary

S, x

Where

$v(y) = \dfrac{N_y + 1 - y}{40}$ is the residual value factor for each year.

Equation (7.22) is the power balance constraints on each node. Equation (7.23), (7.24) are the relationship between yearly investments and accumulative investments. Equation (7.25) is the branch flow decomposition. Equation (7.26)–(7.28) are the disjunctive DC flow constraints (*i*, *j* are the beginning and end node for arc *t*). Equation (7.29)–(7.31) are transmission capacity constraints. Equation (7.32) is the generation output limits. All costs have been discounted to 2010$. Only DC options are allowed for adaptation

investments. Yearly active load has been modeled for this problem. We utilize the CPLEX solver on the same server to get the optimization results. Problem and general solution information are summarized in Table 7.18, and a portion of main transmission investment results are displayed in Table 7.19. Table 20 displays the investment amount for each technology. Figure 7.18 to 7.22 plot the transmission overlay design maps for core expansion and adaptation for each future. We select ρ_s values to be 0.4, 0.25, 0.1 and 0.25 for reference, high offshore, high solar and high geothermal case, respectively.

Table 7.18: Flexibility design model description and solution details.

Number of Variables	2,287,636
Number of Binaries	138,036
Number of Equality Constraints	724,020
Number of Inequality Constraints	1,745,760
Number of Total Linear Constraints	2,469,780
Model Generation Time (sec.)	2,381.77
Solution Time (sec.)	115,890.90
MIP Gap	4.79%
Number of Total Iterations	1,268,561
Number of Circuit Additions in Total	214
Number of Circuit Additions in Core Investment	109
Number of Circuit Additions in Reference Adaptation	30
Number of Circuit Additions in High Offshore Adaptation	17
Number of Circuit Additions in High Solar Adaptation	17
Number of Circuit Additions in High Geothermal Adaptation	33
Total Cost (2010B$)	1,322.355
Total Transmission Investment Cost (2010B$)	205.0738
Transmission Investment Cost for Core (2010B$)	129.9226
Transmission Investment Cost for Reference Case (2010B$)	81.4302
Transmission Investment Cost for High Offshore Wind Case (2010B$)	47.0013
Transmission Investment Cost for High Solar Case (2010B$)	74.9698
Transmission Investment Cost for High Geothermal Case (2010B$)	93.3271
Total Circuit Miles Invested	58,997.3
Circuit Miles Invested for Core Investment	21,222.1
Circuit Miles Invested for Reference Case Adaptation	10,046.9
Circuit Miles Invested for High Offshore Wind Case Adaptation	5,479.8
Circuit Miles Invested for High Solar Case Adaptation	9,373.7
Circuit Miles Invested for High Geothermal Case Adaptation	12,874.8

Table 7.19: Major transmission investments for flexibility design model.

Scenario	Tech	From	To	# of Ckt. Added	Length (mile)	Capacity per Ckt. (GW)	Cost per Circuit (2010M$)
Core	1	CI	P1	8	107.0	4.3	405.7
Core	1	M2	CI	4	112.0	4.2	462.2
Core	1	M2	P1	8	176.0	3.1	675.0
Core	1	M8	P3	4	100.0	4.5	398.7
Core	1	P1	P8	8	185.0	3.0	712.1
Core	2	M2	CI	4	112.0	1.9	387.3
Core	3	M2	CI	2	112.0	3.0	1151.8
Core	4	FL	KY	2	870.0	6.0	4996.9
Core	4	KY	CA	2	418.0	6.0	3502.2
Core	4	S3	SE	2	472.0	6.0	3463.5
Core	4	UT	CW	2	284.0	6.0	3161.2
Reference	3	M2	CI	1	112.0	3.0	1151.8
Reference	4	CA	P2	1	467.0	6.0	3801.6
Reference	4	CV	UT	1	649.0	6.0	3856.1
Reference	4	P8	NI	1	789.0	6.0	4847.6
High Off.	3	SE	KY	1	380.0	3.0	1922.7
High Off.	4	FL	KY	1	870.0	6.0	4996.9
High Solar	3	NI	NE	1	223.0	3.0	1856.0
High Solar	4	FL	KY	1	870.0	6.0	4996.9
High Solar	4	FL	P7	1	851.0	6.0	4778.9
High Solar	4	P8	NI	1	789.0	6.0	4847.6
High Geo.	3	ET	S3	1	396.0	3.0	2075.3
High Geo.	3	ET	SE	1	383.0	3.0	2017.4
High Geo.	3	S3	SE	1	472.0	3.0	2240.5
High Geo.	4	ET	FL	1	779.0	6.0	4625.8
High Geo.	4	FL	KY	1	870.0	6.0	4996.9
High Geo.	4	FL	P4	1	790.0	6.0	4600.2
High Geo.	4	P8	NI	1	789.0	6.0	4847.6
High Geo.	4	S3	FL	1	1280.0	6.0	6676.6

Table 7.20: Investment amount of each technology for flexibility design.

Technology / Metrics	765kV	500kV	600kV	800kV
Total Circuit Miles	10,711.20	813.00	6,376.60	41,096.50
# of Circuit	73	8	27	106
Total Capacity (GW)	266.78	16.02	81.00	636.00
Total Cost (2010B$)	44.50	28.01	41.28	33.81

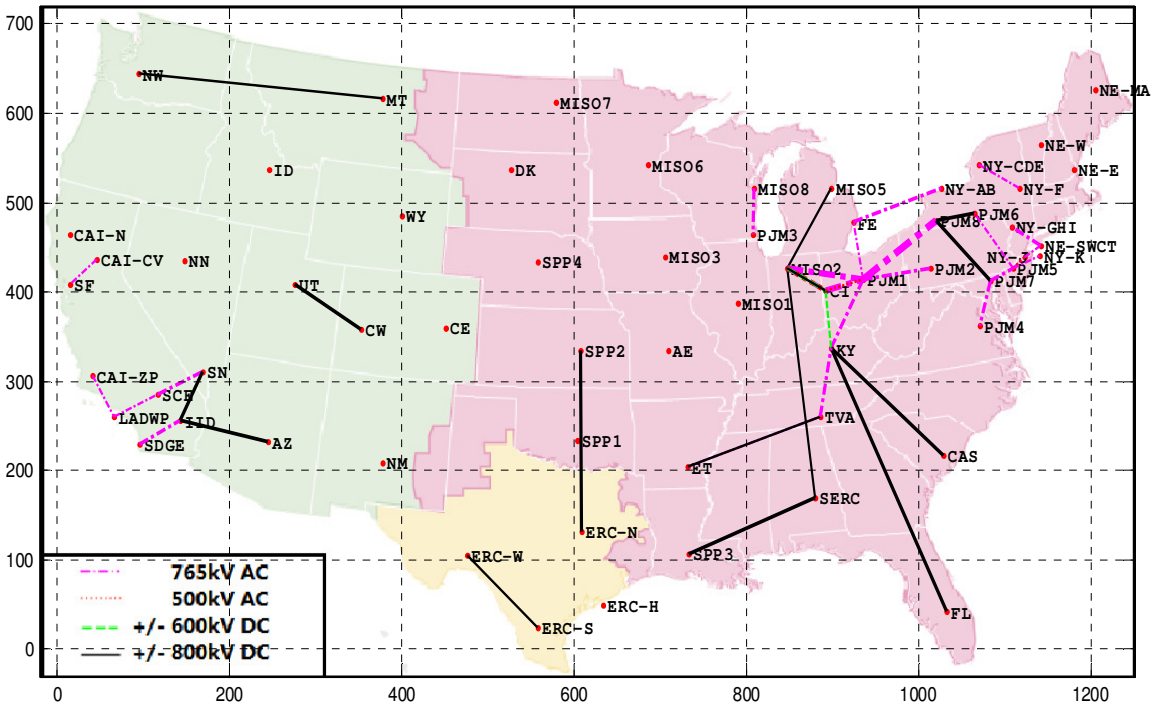

Fig. 7.18: Transmission overlay design map of core investments.

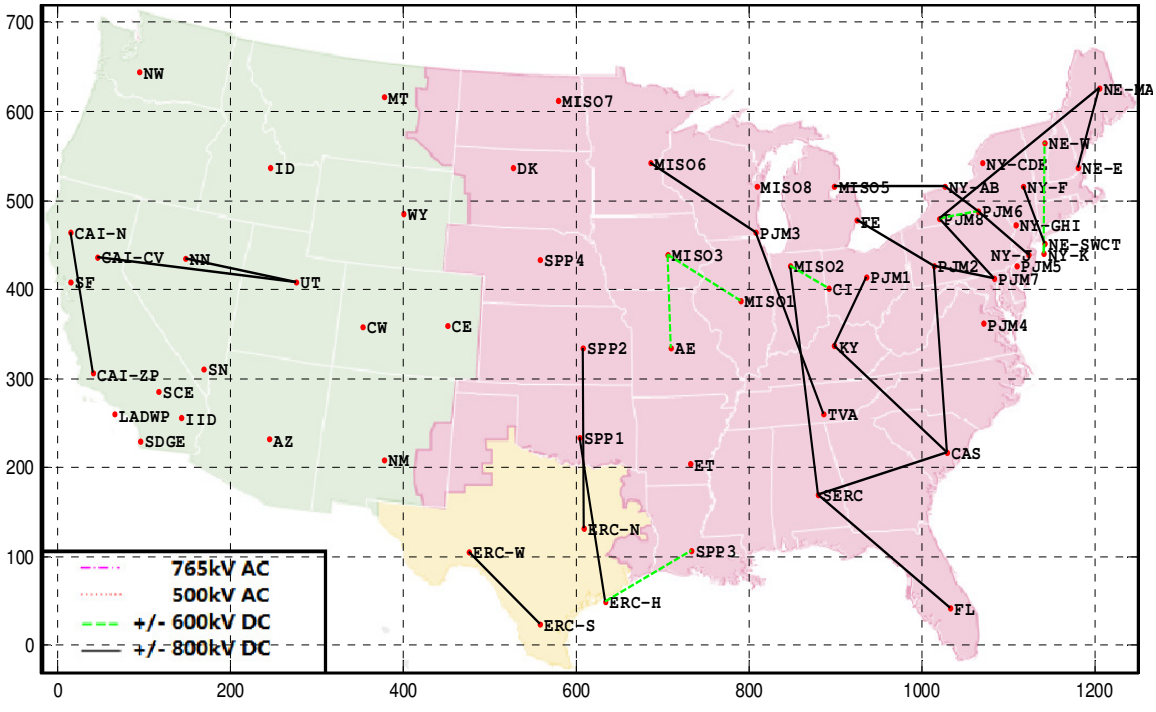

Fig. 7.19: Transmission overlay design of reference case adaptation.

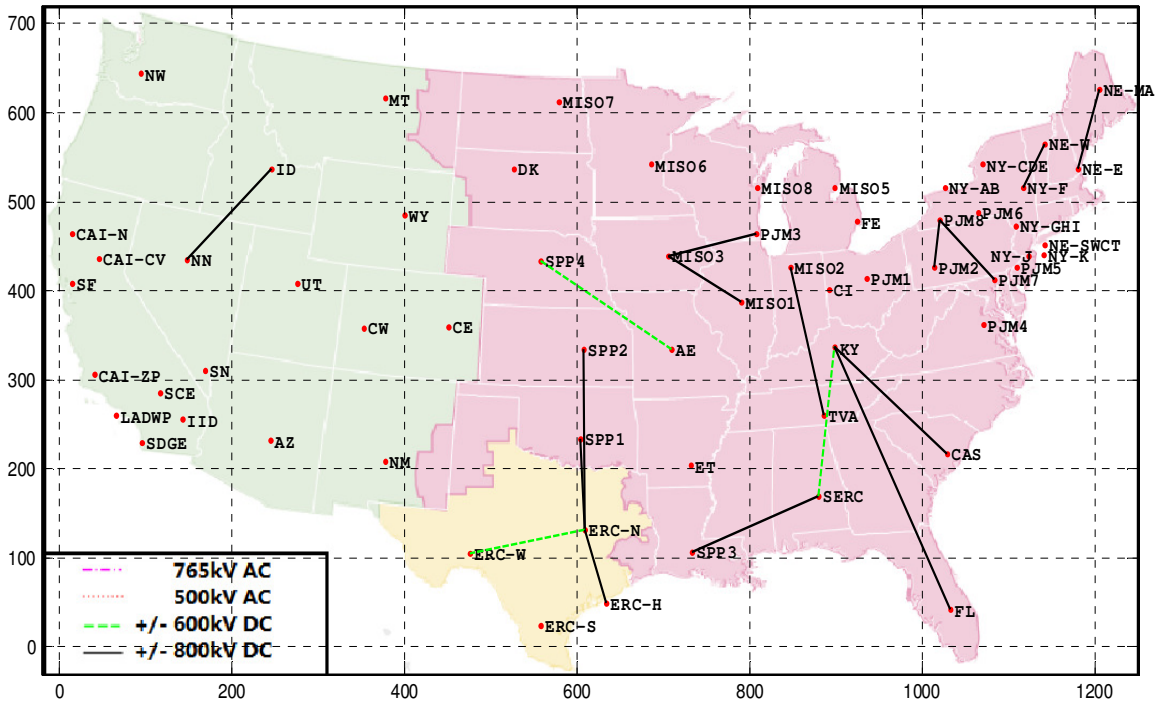

Fig. 7.20: Transmission overlay design of high offshore wind case adaptation.

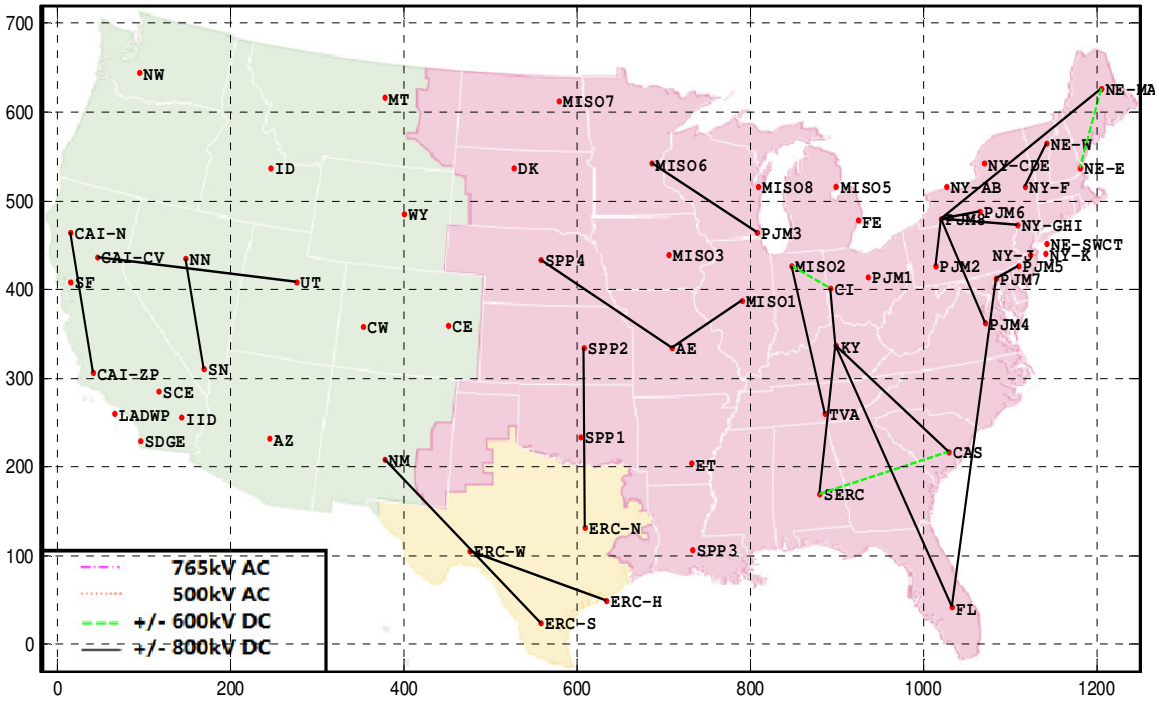

Fig. 7.21: Transmission overlay design of high solar case adaptation.

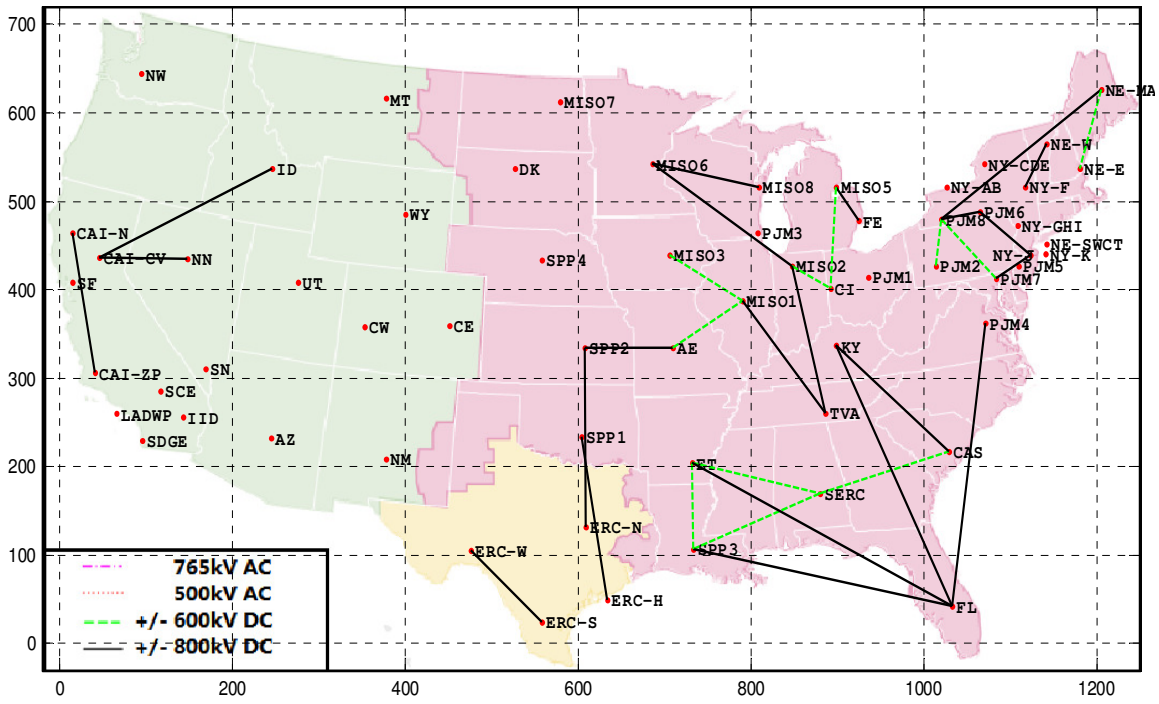

Fig. 7.22: Transmission overlay design of high geothermal case adaptation.

From these results, we can see that most observations in the individual TNEP optimization results hold true in this study. First, the main transmission needs persist near the Great Lakes, from MISO/TVA to SERC, and in New York, New England and California. For each future, the adaptation investments appear to be the part of transmission expansion that occurs in its individual TNEP results but does not occur in the core investment results. Thus, by combining the core design and adaptation design for a certain future, it produces results quite similar to the individual TNEP results for that future. However, individual TNEP design for one future is an optimal result, which will generally be different from the combination of core design and adaptation investments for that future, which is only a feasible result. Secondly, the most favorable technology is still 800kV DC, and the high solar and high geothermal cases require more adaptation

transmission investments than the high offshore wind case, once again confirming the previous summary of the relationship between renewable type and transmission needs.

Also, when we select the ρ_s values such as to produce a summation of 1, a major component of transmission expansion tends to occur in the core investment part, indicating that there are significant similarities in transmission needs among all four cases. Also, overall cost and transmission investment costs become lower in the flexibility design case than in any of the individual TNEP cases.

One issue to be pointed out is that the flexibility design approach, requiring the network expansion to satisfy all constraints under all futures together, is actually similar to combining all models under each future, and will inherently dramatically increase problem dimensions. Due to limitations of computing capability, it is difficult to keep all modeling assumptions consistent with the pre10ious individual TNEP optimization. For example, the load data used here for flexibility design is yearly, but the individual TNEP uses a 2-step load for each year. Such differences in modeling may influence the final results, so at this stage, while we can make effective qualitative comparisons among the results, more work must be done to resolve the computational burden before we can perform comprehensive quantitative analysis.

CHAPTER 8. STEADY STATE BENEFIT QUANTIFICATION

As stated before and in reference [2], a national transmission overlay may bring benefit to the overall U.S. electric system. In general, such benefits mainly include, but are not limited to, overall production and investment cost reduction, greenhouse gas emission reduction, energy price decreases, and creation of employment opportunities. There may be other types of important benefits, like reliability performance, system robustness, etc., but here we focus on four types of benefits that can be clearly quantified to demonstrate the advantage of a national transmission overlay.

The most straightforward and effective method to quantify such benefits is to conduct comparison studies between cases both with and without a transmission overlay. In Chapter 7, we designed several overlays using mathematical optimization methods and, to quantify their benefits, each overlay design was fed back into its original generation optimization model from which the respective generation scenario was designed in step 1 of the study process to evaluate its operating performance. Since transmission and generation have been separately optimized in this study, additional generation may be re-invested to make the model feasible and further reduce total costs, so the objective function is to minimize production and additional generation investment cost. The additional generation investment cost here is actually another form of adaptation cost discussed in Chapter 6. There will be no additional transmission investment in this step, i.e., the transmission topology and capacity are fixed. To avoid redundancy, we will not

repeat the problem statement here. From the optimization results, we can calculate the total cost, emission, energy price and job creation metrics, and compare them to the case results without a national transmission overlay. We will discuss the results in the next two sections.

8.1 Cost and CO_2 Emissions Metrics.

We have performed 16 pairs of comparison studies, each designed for all futures, to illustrate the benefits of transmission overlays. Comparisons between the system performance with and without a national transmission overlay, in terms of cost (in 2010 trillion $) and emissions (in trillion short ton CO_2) metrics, are summarized in Table 8.1. The generation investment cost for each technology has also been converted back to the reference case's value to provide a fair comparison of costs between different cases, since some investment costs, including offshore wind, solar PV, and geothermal, have been discounted to reflect technology maturity in different futures. The scenario cost in the table represents the original generation investment cost in step 1, and the generation investment cost in the table represents the cost of additional generation investment associated with adapting an overlay design to each of the four futures.

To better illustrate the numbers, we also plotted the bar charts in Fig. 8.2 to Fig. 8.5 for each design under its particular scenario and compared these to the fixed existing transmission system's performance. A weighted average of cost and emission metrics of designs among all futures is summarized in Fig. 8.1 and Table 8.2 to provide a rough illustration of their overall performance.

Table 8.1: Steady state benefit comparison with/without transmission overlays.

(a) Reference case transmission design.

W/ or w/o Transmission \ Study Case		Reference	High Offshore	High Solar	High Geothermal
Transmission Overlay from Reference Case	Gen. Prod. Cost (T$)	1.0837	1.0926	1.0827	1.0891
	Gen. Inv. Cost (T$)	0.0000	0.0107	0.0175	0.0214
	Trans. inv. Cost (T$)	0.4721	0.4721	0.4721	0.4721
	Gen.+ Trans. Cost (T$)	1.5559	1.5754	1.5724	1.5826
	Scenario Cost (T$)	2.6850	2.9345	4.5308	2.6678
	Total Cost (T$)	4.2409	4.5099	6.1032	4.2504
	CO_2 (T short ton)	0.0918	0.0959	0.0891	0.0865
Fixed Current Transmission System	Gen. Prod. Cost (T$)	1.1294	1.1212	1.1125	1.1343
	Gen. Inv. Cost (T$)	0.4638	0.5166	0.5438	0.5692
	Trans. inv. Cost (T$)	0.0000	0.0000	0.0000	0.0000
	Gen.+ Trans. Cost (T$)	1.5933	1.6378	1.6563	1.7035
	Scenario Cost (T$)	2.6850	2.9345	4.5308	2.6678
	Total Cost (T$)	4.2783	4.5723	6.1871	4.3713
	CO_2 (T short ton)	0.0954	0.0967	0.0955	0.0940
Cost Savings & CO_2 Reduction	Gen. Prod. Cost (T$)	0.0457	0.0286	0.0298	0.0452
	Gen. Inv. Cost (T$)	0.4638	0.5059	0.5263	0.5478
	Trans. inv. Cost (T$)	-0.4721	-0.4721	-0.472	-0.4721
	Total Cost (T$)	0.0374	0.0624	0.0839	0.1209
	CO_2 (T short ton)	0.0036	0.0008	0.0064	0.0075

(b) High offshore wind case transmission design.

W/ or w/o Transmission \ Study Case		Reference	High Offshore	High Solar	High Geothermal
Transmission Overlay from High Offshore Wind Case	Gen. Prod. Cost (T$)	1.0865	1.0931	1.0851	1.0912
	Gen. Inv. Cost (T$)	0.0455	0.0000	0.0444	0.0535
	Trans. inv. Cost (T$)	0.4783	0.4783	0.4783	0.4783
	Gen.+ Trans. Cost (T$)	1.6102	1.5713	1.6077	1.6230
	Scenario Cost (T$)	2.6850	2.9345	4.5308	2.6678
	Total Cost (T$)	4.2952	4.5058	6.1385	4.2908
	CO_2 (T short ton)	0.0922	0.0952	0.0897	0.0871
Fixed Current Transmission System	Gen. Prod. Cost (T$)	1.1294	1.1212	1.1125	1.1343
	Gen. Inv. Cost (T$)	0.4638	0.5166	0.5438	0.5692
	Trans. inv. Cost (T$)	0.0000	0.0000	0.0000	0.0000
	Gen.+ Trans. Cost (T$)	1.5933	1.6378	1.6563	1.7035
	Scenario Cost (T$)	2.6850	2.9345	4.5308	2.6678
	Total Cost (T$)	4.2783	4.5723	6.1871	4.3713
	CO_2 (T short ton)	0.0954	0.0967	0.0955	0.0940

Table 8.1 (b). (Continued).

Cost Savings & CO_2 Reduction	Gen. Prod. Cost (T$)	0.0429	0.0281	0.0274	0.0431
	Gen. Inv. Cost (T$)	0.4183	0.5166	0.4994	0.5157
	Trans. inv. Cost (T$)	-0.4783	-0.4783	-0.478	-0.4783
	Total Cost (T$)	-0.0169	0.0665	0.0486	0.0805
	CO_2 (T short ton)	0.0032	0.0015	0.0058	0.0069

(c) High solar case transmission design.

W/ or w/o Transmission \ Study Case		Reference	High Offshore	High Solar	High Geothermal
Transmission Overlay from High Solar Case	Gen. Prod. Cost (T$)	1.0850	1.0934	1.0816	1.0899
	Gen. Inv. Cost (T$)	0.0170	0.0181	0.0000	0.0299
	Trans. inv. Cost (T$)	0.4990	0.4990	0.4990	0.4990
	Gen.+ Trans. Cost (T$)	1.6009	1.6105	1.5806	1.6188
	Scenario Cost (T$)	2.6850	2.9345	4.5308	2.6678
	Total Cost (T$)	4.2859	4.5450	6.1114	4.2866
	CO_2 (T short ton)	0.0907	0.0949	0.0883	0.0856
Fixed Current Transmission System	Gen. Prod. Cost (T$)	1.1294	1.1212	1.1125	1.1343
	Gen. Inv. Cost (T$)	0.4638	0.5166	0.5438	0.5692
	Trans. inv. Cost (T$)	0.0000	0.0000	0.0000	0.0000
	Gen.+ Trans. Cost (T$)	1.5933	1.6378	1.6563	1.7035
	Scenario Cost (T$)	2.6850	2.9345	4.5308	2.6678
	Total Cost (T$)	4.2783	4.5723	6.1871	4.3713
	CO_2 (T short ton)	0.0954	0.0967	0.0955	0.0940
Cost Savings & CO_2 Reduction	Gen. Prod. Cost (T$)	0.0444	0.0278	0.0309	0.0444
	Gen. Inv. Cost (T$)	0.4468	0.4985	0.5438	0.5393
	Trans. inv. Cost (T$)	-0.4990	-0.4990	-0.499	-0.4990
	Total Cost (T$)	-0.0076	0.0273	0.0757	0.0847
	CO_2 (T short ton)	0.0047	0.0018	0.0072	0.0084

(d) High geothermal case transmission design.

W/ or w/o Transmission \ Study Case		Reference	High Offshore	High Solar	High Geothermal
Transmission Overlay from High Geothermal Case	Gen. Prod. Cost (T$)	1.0847	1.0929	1.0829	1.0900
	Gen. Inv. Cost (T$)	0.0106	0.0027	0.0106	0.0000
	Trans. inv. Cost (T$)	0.5091	0.5091	0.5091	0.5091
	Gen.+ Trans. Cost (T$)	1.6045	1.6047	1.6026	1.5991
	Scenario Cost (T$)	2.6850	2.9345	4.5308	2.6678
	Total Cost (T$)	4.2895	4.5392	6.1334	4.2669
	CO_2 (T short ton)	0.0914	0.0953	0.0885	0.0861

Table 8.1 (d). (Continued).

Fixed Current Transmission System	Gen. Prod. Cost (T$)	1.1294	1.1212	1.1125	1.1343
	Gen. Inv. Cost (T$)	0.4638	0.5166	0.5438	0.5692
	Trans. inv. Cost (T$)	0.0000	0.0000	0.0000	0.0000
	Gen.+ Trans. Cost (T$)	1.5933	1.6378	1.6563	1.7035
	Scenario Cost (T$)	2.6850	2.9345	4.5308	2.6678
	Total Cost (T$)	4.2783	4.5723	6.1871	4.3713
	CO_2 (T short ton)	0.0954	0.0967	0.0955	0.0940
Cost Savings & CO_2 Reduction	Gen. Prod. Cost (T$)	0.0447	0.0283	0.0296	0.0443
	Gen. Inv. Cost (T$)	0.4532	0.5139	0.5332	0.5692
	Trans. inv. Cost (T$)	-0.5091	-0.5091	-0.509	-0.5091
	Total Cost (T$)	-0.0112	0.0331	0.0537	0.1044
	CO_2 (T short ton)	0.0040	0.0014	0.0070	0.0079

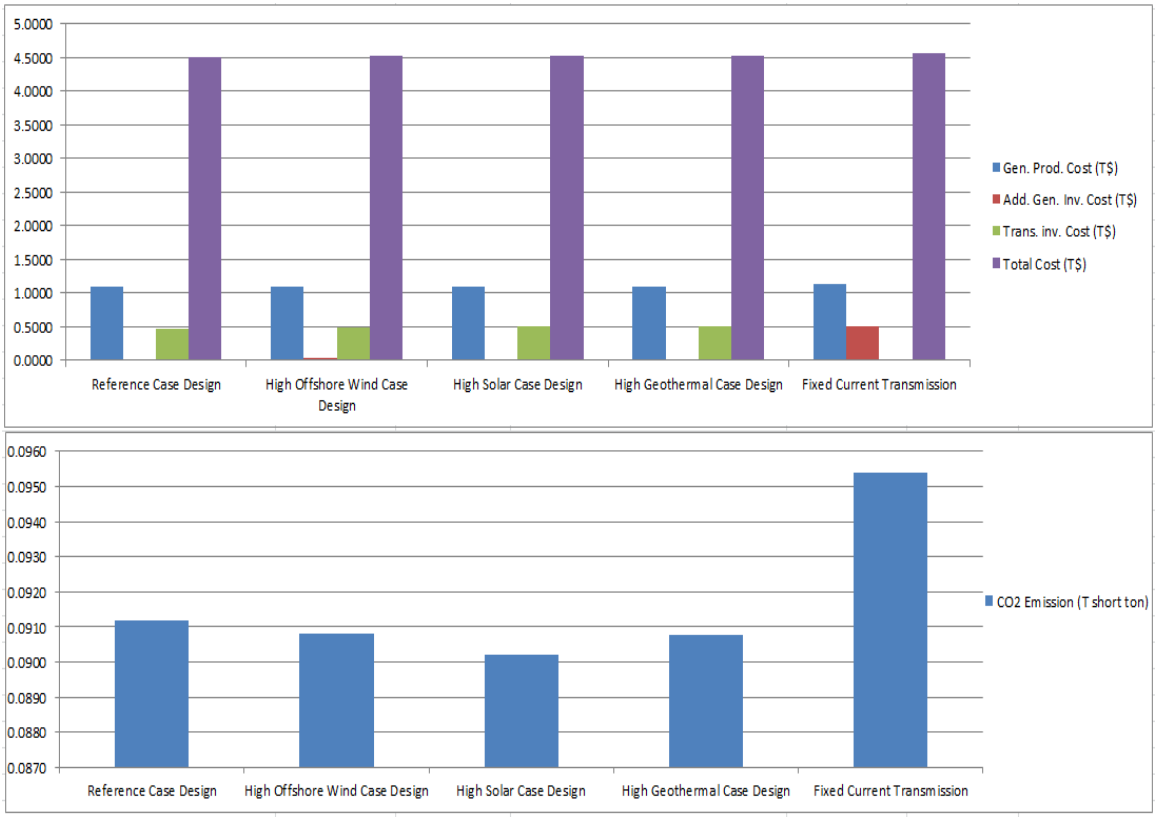

Fig. 8.1: Weighted average cost and emission metrics comparison among all cases.

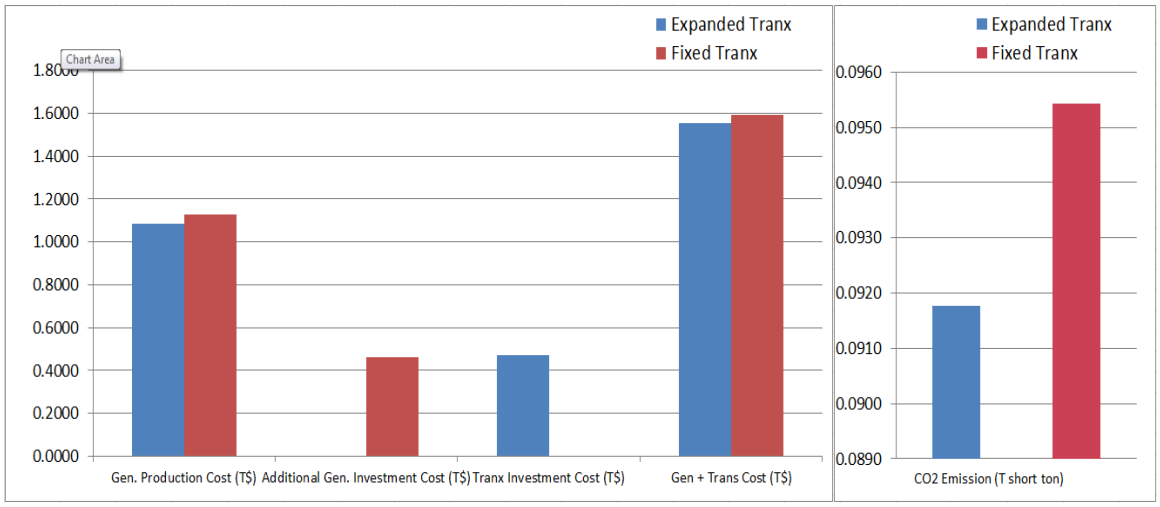

Fig. 8.2: Cost and emission metrics comparison for reference case.

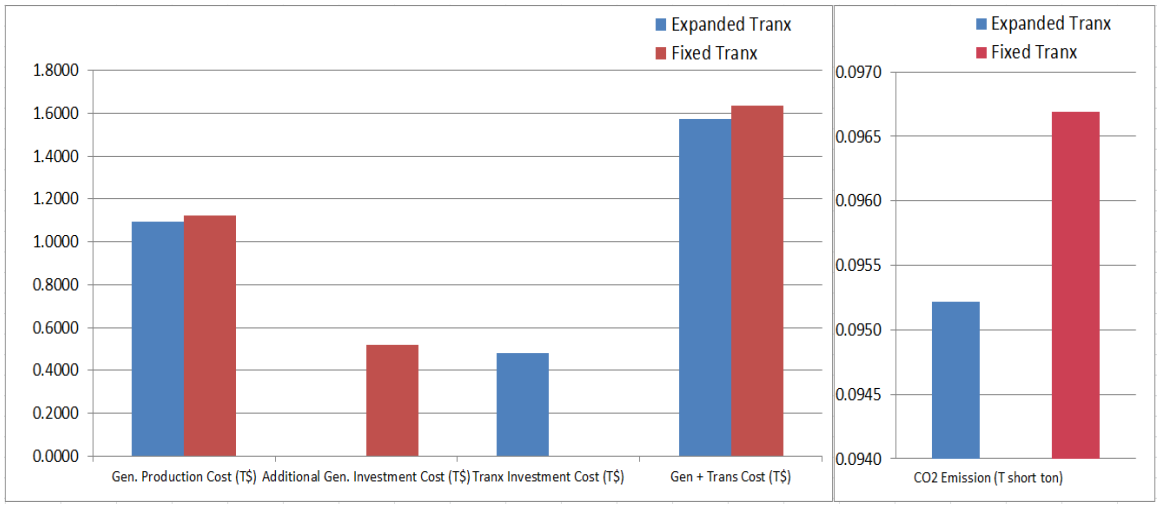

Fig. 8.3: Cost and emission metrics comparison for high offshore wind case.

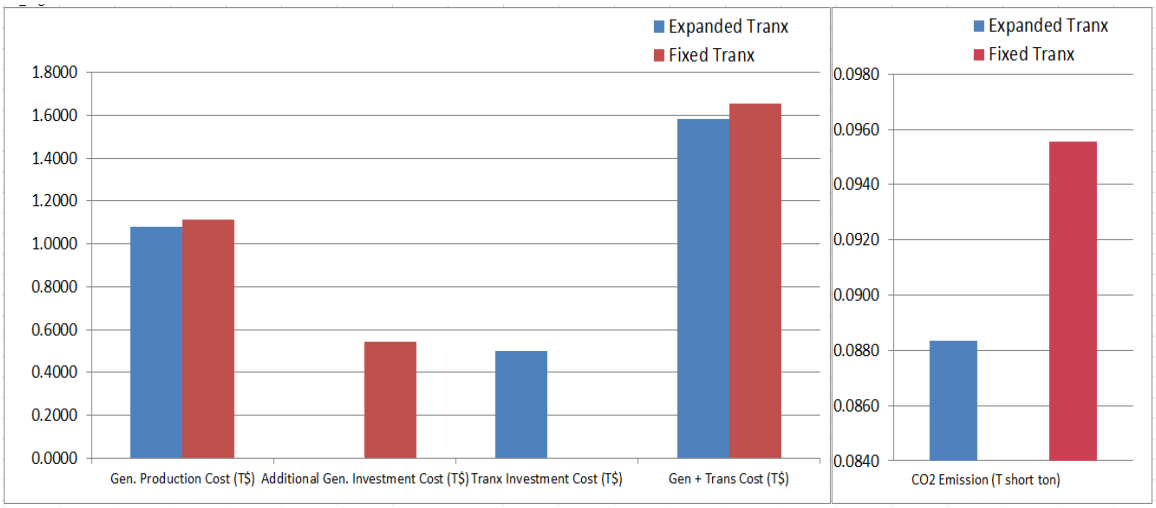

Fig. 8.4: Cost and emission metrics comparison for high solar case.

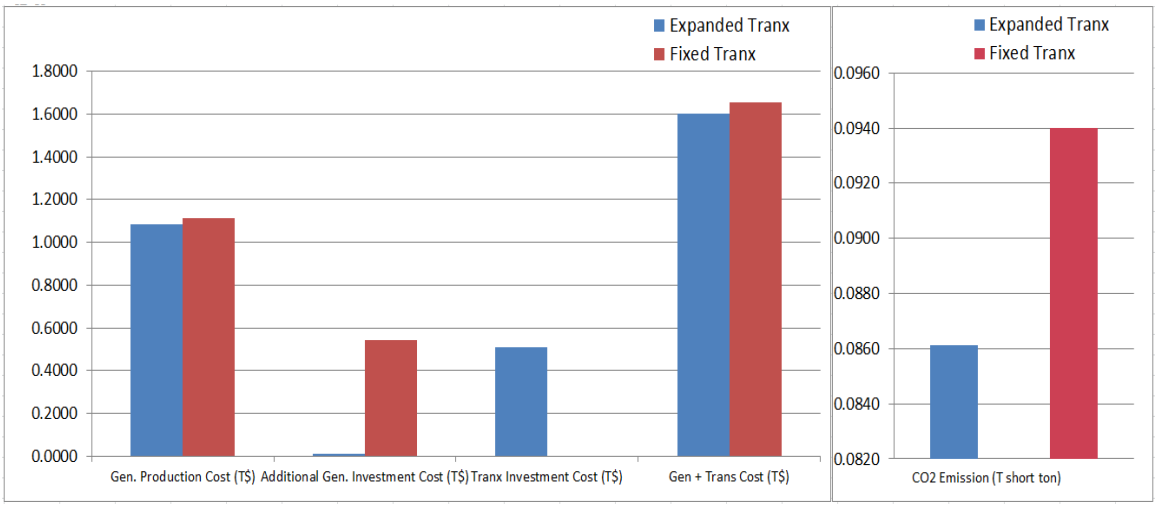

Fig. 8.5: Cost and emission metrics comparison for high geothermal case.

From the above results, we can observe that the presence of a national transmission overlay lowers both cost and emissions in all four high-renewable futures, except that there is a slight cost increase for the high offshore wind, high solar, and high geothermal cases design with respect to the reference case scenario. Particularly, except

for the reference overlay, a certain transmission overlay design performs best or at least second best for the scenario from which it has been designed, showing a significant advantage in the direction of fixed existing transmission. The reference case shows a simultaneous 37.4 billion dollars (in 2010$) cost savings and 3.6 billion dollar short ton CO_2 emission reduction. Under most situations, the transmission investment costs from building the overlay has been over-compensated by production cost reduction and generation investment cost savings.

In general, we can see from the above tables that the high geothermal case benefits the most from a transmission overlay. This is because, as discussed earlier, the high geothermal case has the greatest transmission needs when compared to other futures, so any of the four overlay designs will perform well for this case, bringing significant higher cost benefits than other futures.

To give an estimation of how well a certain design performs under all futures, we show the weighted average cost and emission metrics for each design among all futures in Table 8.2 and the bar chart in Fig 8.1, together with the fixed existing transmission. The weights have been selected to be identical with the ρ_{ξ} values used in flexibility design in the previous chapter, i.e., 0.4, 0.25, 0.1, and 0.25 for the reference case, the high offshore wind case, the high solar case, and the high geothermal case, respectively. It can be observed that the reference case design has the lowest average cost, and the high solar case has the lowest average emissions. The fixed current transmission case has the highest cost and emissions, confirming the benefits of an overlay design.

Table 8.2: Weighted average performance among all futures for each design.

Average Performance Metrics	Reference Design	High Off. Design	High Solar Design	High Geo. Design	Current Transmission
Gen. Prod. Cost (T$)	1.0872	1.0892	1.0880	1.0879	1.1269
Gen. Inv. Cost (T$)	0.0098	0.0360	0.0188	0.0060	0.5114
Trans. Inv. Cost (T$)	0.4721	0.4783	0.4990	0.5091	0.0000
Scenario Cost (T$)	2.9277	2.9277	2.9277	2.9277	2.9277
Total Cost (T$)	4.4968	4.5311	4.5334	4.5306	4.5659
CO_2 Emission (T short ton)	0.0912	0.0908	0.0902	0.0908	0.0954

8.2 Tradeoff between Job Opportunities and Energy Prices

In the previous section, we discussed the cost and environmental benefits from a national transmission overlay design. These benefits actually can be observed from an overall system point of view, indicating how much cost or emission can be reduced for the whole nation. In this section, we will talk about the influences on a certain region produced by a national transmission overlay.

From a power system engineering and market perspective, the benefit (or loss) to a certain region in energy systems may be expressed by energy price change and job creation opportunity in that region. Employment opportunity creation is produced by the investment of infrastructure, mainly renewable generation expansion facilitated by transmission overlay design. The energy price can be simply illustrated by the Locational Marginal Price (LMP) [73]. Hence, in the next two parts, we will calculate the number of jobs created by renewable generation expansion and the LMP change due to transmission overlays.

8.2.1 Employment opportunities

Compared to fossil fuels, which rely heavily on expensive pieces of production equipment, renewables tend to be a more labor-intensive energy source when considered on a per-MW basis. Currently, about 2.3 million people worldwide work either directly in renewables or indirectly in supplier industries. Given incomplete data, this is in all likelihood a conservative figure. The wind power industry employs some 300,000 people, the solar photovoltaic (PV) sector accounts for an estimated 170,000 jobs, and the solar thermal industry, at least 624,000. More than 1 million jobs are found in the biomass and biofuels sector [74].

In the United States, federal policies have been inconsistent over recent years, leaving leadership to individual state governments. Still, a study for the American Solar Energy Society found that the U.S. renewables sector employed close to 200,000 people directly in 2006 and another 246,000 indirectly [75].

Below are a few estimations on job creation by renewable generation expansion:

a) In-land and Offshore Wind: 4.55 jobs per MW expansion [76];

b) Solar PV: 9.76 jobs per MW expansion [77];

c) Geothermal: 8.92 jobs per MW expansion [78].

The numbers of jobs here all refer to permanent employment. Based on these estimations and renewable generation investment capacities, we calculated the total job creation numbers at each node during the next 40 years, with the results shown in Fig. 8.6 through Fig. 8.9, one for each future. In these figures, the numbers of job opportunities created are marked on the side of each node name, in units of one thousand jobs.

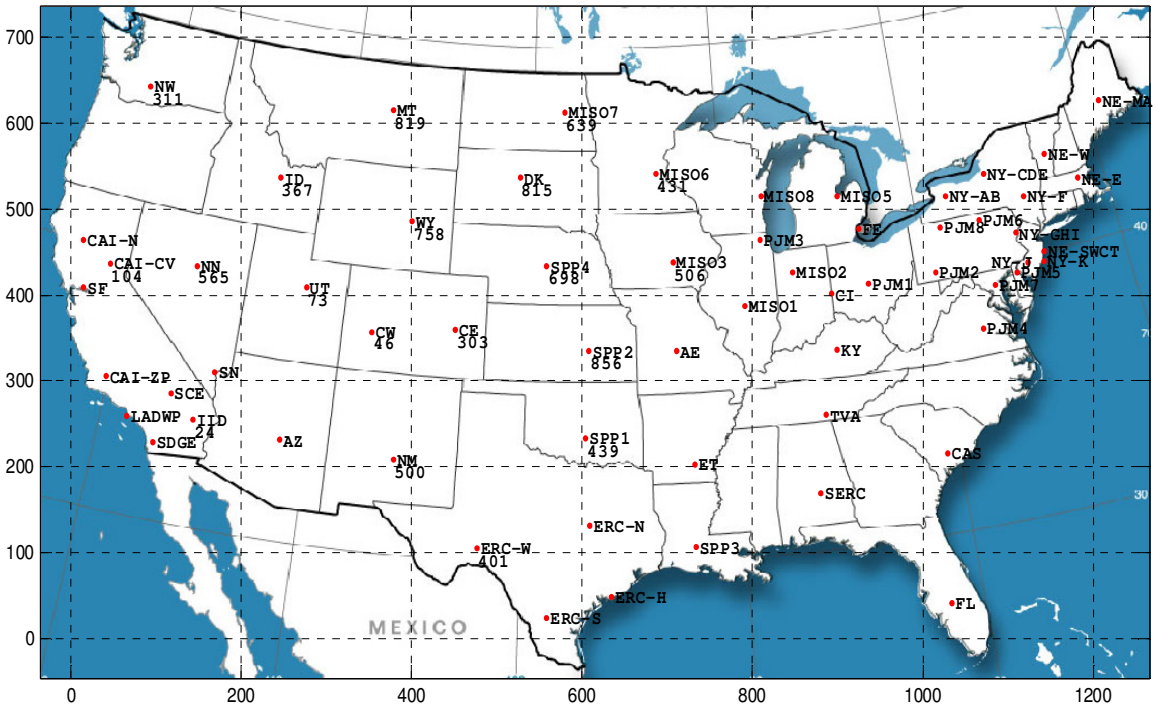

Fig. 8.6: Jobs created for reference case.

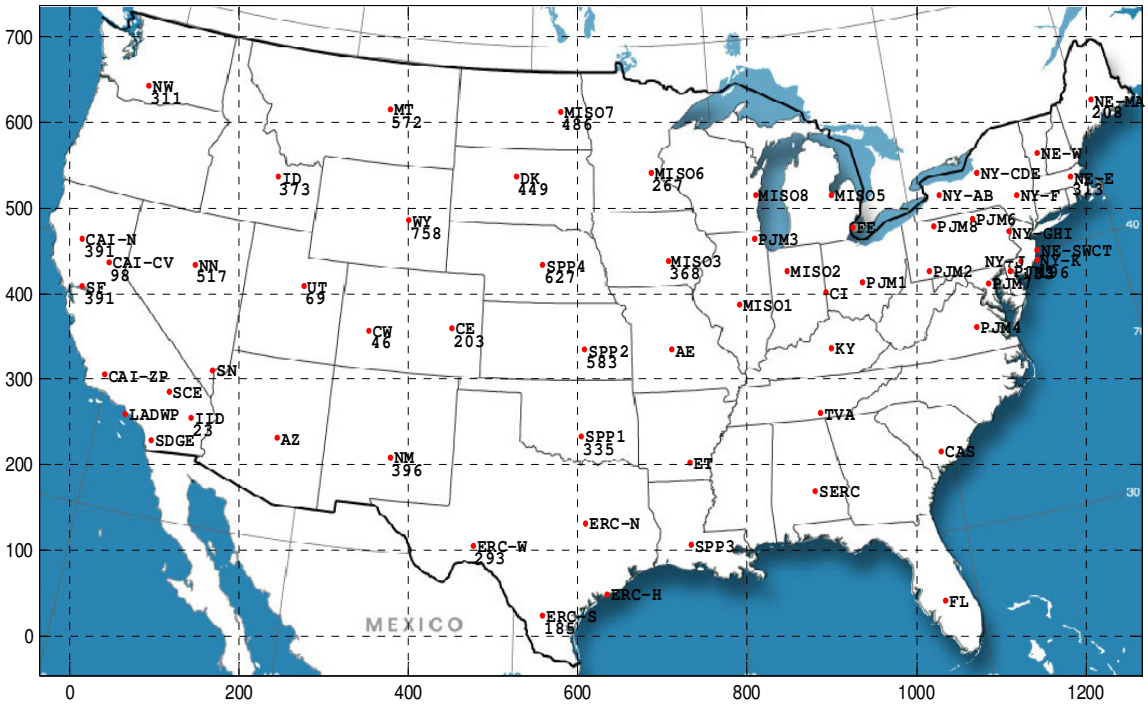

Fig. 8.7: Jobs created for high offshore wind case.

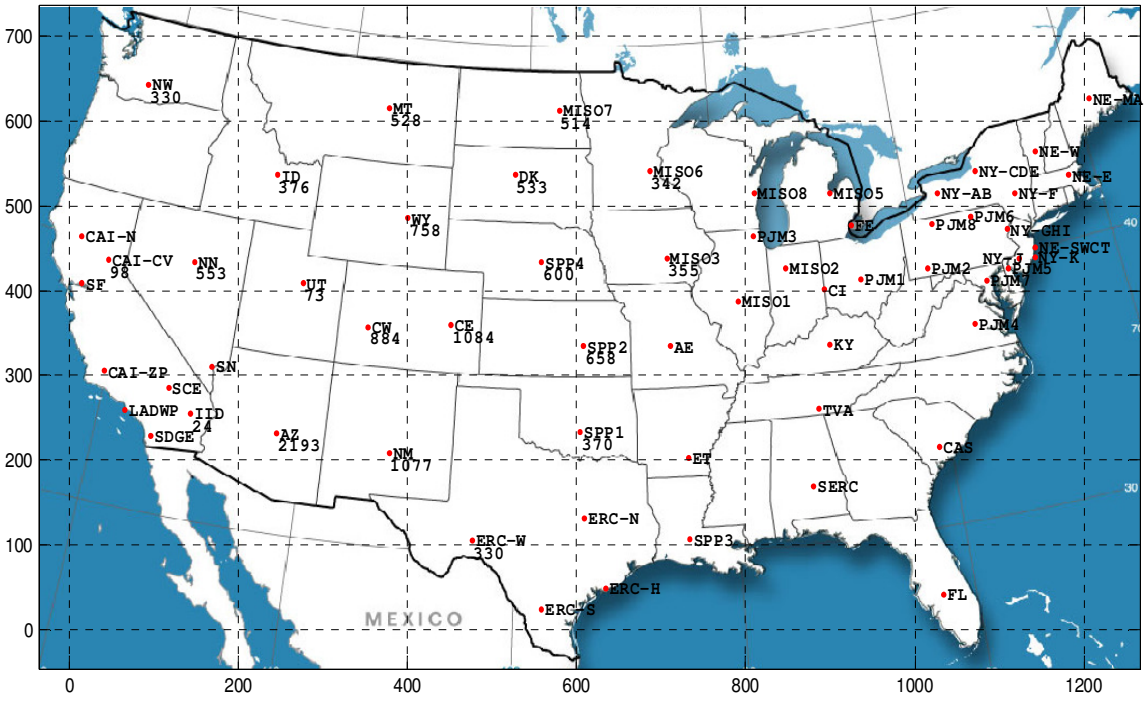

Fig. 8.8: Jobs created for high solar case.

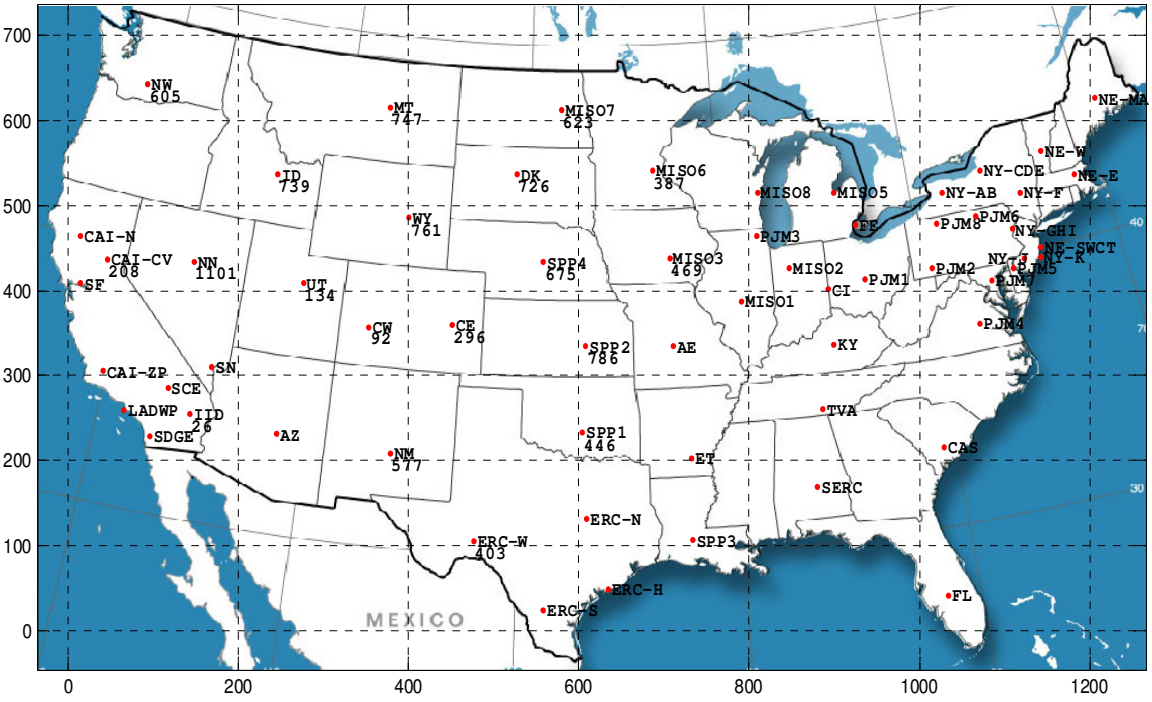

Fig. 8.9: Jobs created for high geothermal case.

From the results we can see the employment opportunities created are mainly located in SPP, Midwest and WECC, where the inland/off shore wind, solar, and geothermal resources are mainly located. The total number of jobs created in a particular region varies between tens of thousands to over several million. In the reference case, we can see a total of 8,655,000 jobs created in the renewable energy sector. In other cases, 8,591,000, 11,683,000 and 9,801,000 jobs are created in the high offshore wind case, the high solar case, and the high geothermal case. Solar PV and geothermal tend to produce more jobs based on the previous estimation and thus will result in more jobs created for the last two cases. Transmission investment will also create a certain number of jobs, but since these are mostly temporary and minimal compared to renewable generation jobs, we will not include them here.

8.2.2 LMP change

Similarly, we calculated the LMP changes from TNEP optimization results. Maps of LMP changes (in M$/GW) for all scenarios are shown in Fig. 8.10 through 8.13. The green numbers indicate a decrease of LMP, while red numbers indicate an energy price increase.

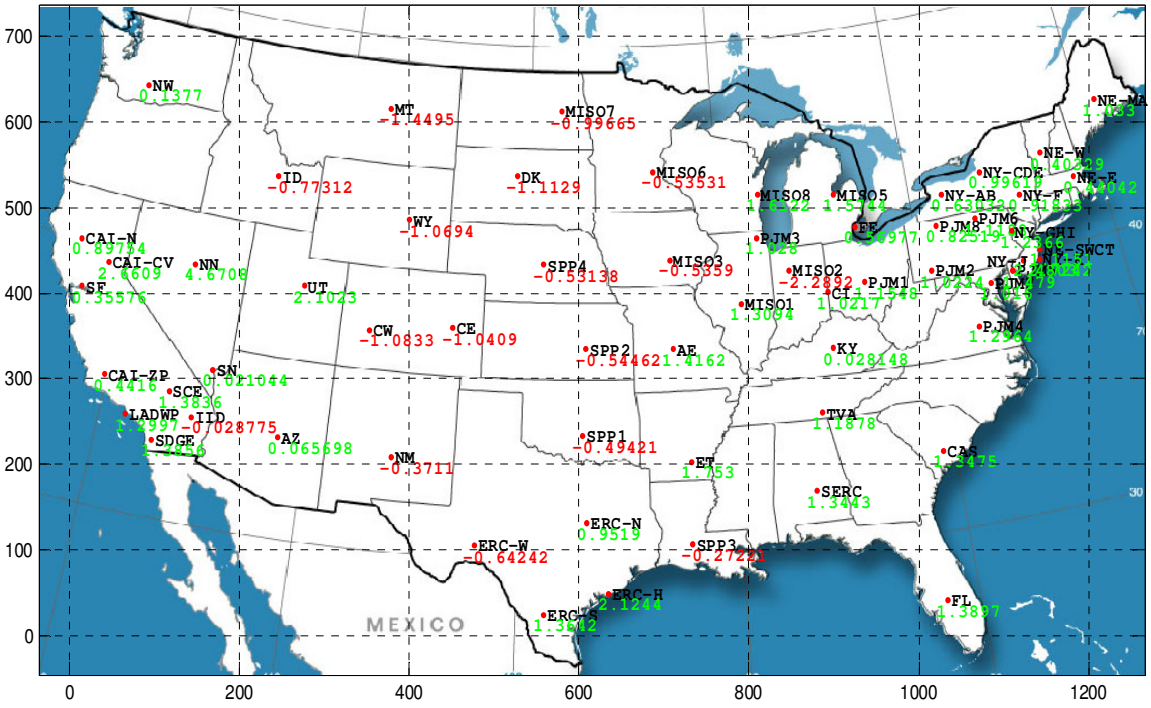

Fig. 8.10: LMP change between reference case and fixed current transmission.

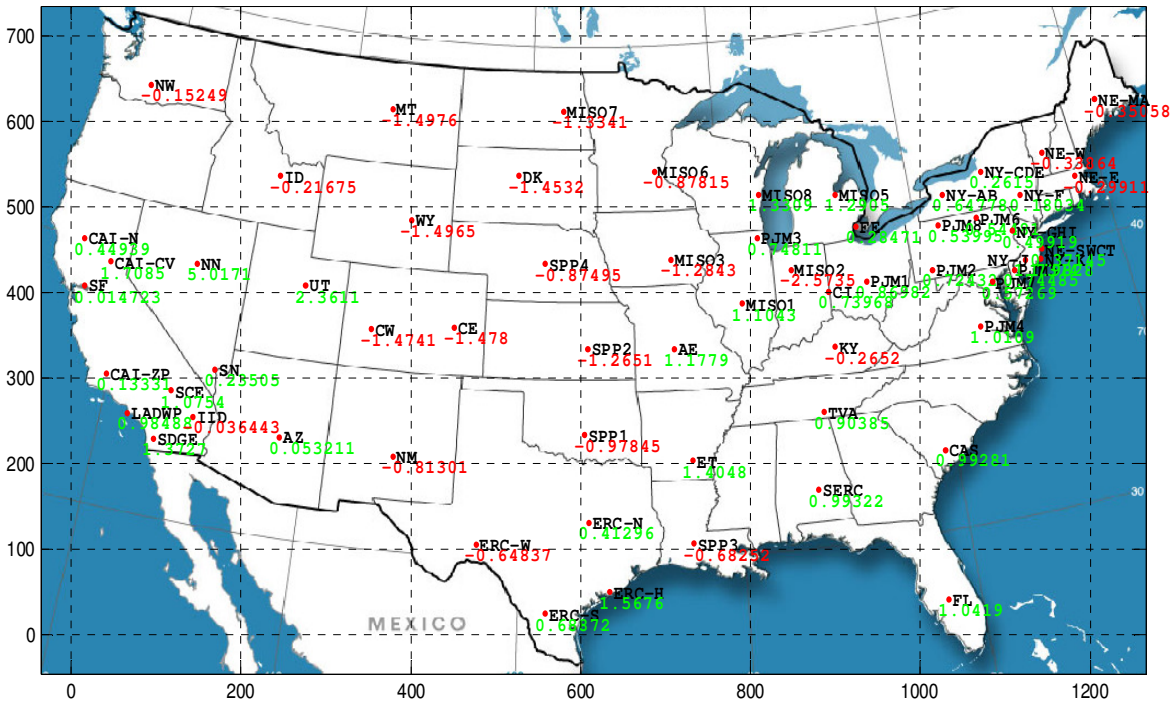

Fig. 8.11: LMP change between high offshore wind case and fixed current transmission.

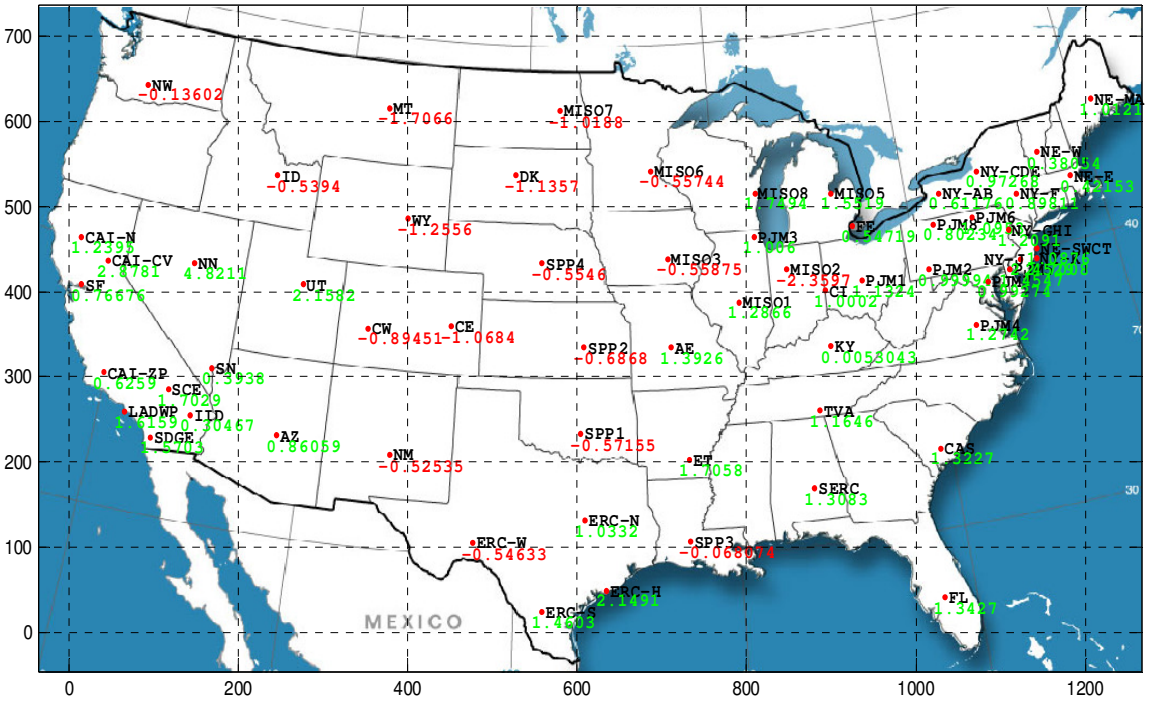

Fig. 8.12: LMP change between high solar case and fixed current transmission.

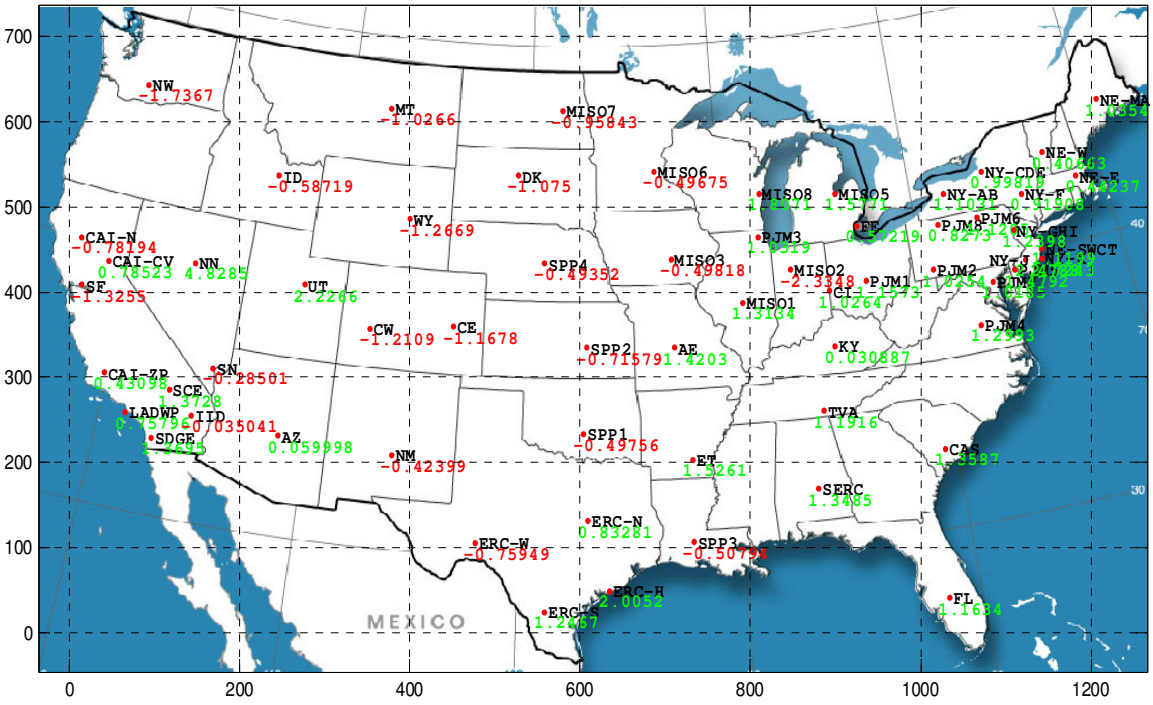

Fig. 8.13: LMP change between high geothermal case and fixed current transmission.

These results show that the LMP decreases for the overall continental U.S. Comparing Fig. 8.6 to Fig. 8.9, it is easy to observe that, in the areas where LMP increases, there will be large number of employment opportunities created. In contrast, in those areas (mainly load centers) where LMP decreases, few jobs are created. This is actually an effect of bulk transmission, i.e., leveling out LMP differences in different areas. In regions where renewable generation is invested, bulk transmission will transfer the energy out, so compared to the case without transmission, the LMP will increase. This result indicates a benefit trade-off between energy price and jobs. In most areas, the disadvantage of losing jobs (or having higher electricity bills) will be compensated for by the other types of benefits.

CHAPTER 9. CONCLUSION AND FUTURE WORK

9.1 Conclusion

This thesis introduces a study framework and methodology of long term transmission design at the national level. The framework has been implemented on the U.S. national electric system to design overlays to facilitate different types of future renewable generation. We developed innovative transmission candidate selection algorithm (IRMST algorithm) and efficient decimal-binary disjunctive modeling approach for TNEP problem. The IRMST algorithm converges fast for this case, resulting in a 383-arc candidate set used for mathematical optimization. The decimal binary disjunctive modeling method, also introduced in [14], has been applied to model the national transmission expansion optimization problem and increase modeling efficiency. Based on the study results and analysis in Chapter 7 and 8, we summarize the following observations and conclusions at high level:

a. A national transmission overlay benefits the U.S. overall system, by reducing cost and CO_2 emissions. The designed overlays perform better under their particular future from which they have been optimized from. This validates our design approach to some extent;
b. A national transmission overlay lowers overall energy price. It may increase LMP at certain region;

c. A national transmission overlay facilitates the growth of renewable generation, including inland and offshore wind, solar and geothermal. In consequence, large amount of employment opportunities may be created by the infrastructure investment;

d. In general, due to the transmission overlay, energy price tends to increase in regions with bulk new renewable generation, while large number of jobs can be created in these regions as a sort of compensation of benefit. Vice versa.

e. 800kV HVDC is the preferred technology in most regions in these designs, with significant number of 765kV AC circuit added as well;

f. All optimized overlays are hybrid AC/DC networks, confirming that hybrid AC/DC network may better satisfy needs at lower total costs;

g. More transmission is needed to facilitate geothermal; less transmission is needed to facilitate offshore wind. This is reflected in the transmission investment amount under each future. Different type of future renewable generation may change overlay design in topology and capacity needs;

h. Transmission needs are heaviest after years 2015;

i. Major transmission needs are pronounced near the Great Lakes for all cases, which is consistent with results in [36]. 765kV EHVAC is preferred there. There are significant transmission needs from MISO to TVA to SERC, between SPP and ERCOT, and along East and West coasts;

j. From preliminary analysis, transmission design for the reference case has the best overall performance among all futures. However, this will need further investigation; the flexibility design approach, when properly select the ρ_s

values, could potentially lower overall cost and achieve better balance between optimality and adaptability among various futures, thus is worth further investigation.

The work presented in this thesis is a step forward from the PSERC White paper [2], by using a more granular model and a higher-fidelity study methodology especially designed for this problem. The above high-level conclusions and observations made may provide insight for future studies on investment of high capacity inter-regional transmission. In doing so reliability and uncertainty issues should be addressed comprehensively as well. Although overlay design differs from conventional transmission planning, some methods described here may be applicable to conventional planning as well. The IRMST transmission candidate selection method may provide useful reference for candidate routing, and the decimal binary disjunctive model may be used to improve modeling efficiency for extra-large real power systems. To sum up, the contributions of this dissertation, as stated in Chapter 1 Section 2, mainly include: (a) A well-articulated study framework for national level transmission design; (b) A transmission candidate selection method based on graph theory, combined with industry experience in transmission cost estimation; (c) The decimal-binary disjunctive model for TNEP, which extends the traditional disjunctive model to efficiently model multiple parallel circuit additions on a single transmission corridor. We also developed methods to determine the ideal number of parallel candidates needed, handle multiple circuit type problem, and implement Benders decomposition, to further enhance the ability to model large-sized problems; (d) Hybrid AC/DC transmission expansion planning (TEP) model: This thesis develops a TEP formulation which enables multiple AC transmission levels

and multiple DC transmission levels for circuit selection, with appropriate representation of AC capacity dependence on length and corresponding cost of substations, and with appropriate representation of terminal costs for DC circuits; (e) Transmission overlay designs for the contiguous U.S from the systematic optimization and evaluation approach; (f) Quantification of national transmission overlay's economic and environmental benefits, confirming the conclusion of reference [2] that a national transmission overlay benefits the overall system economically and environmentally, using more granular national electric system model; (g) Extend the flexibility design approach from [22] to transmission planning optimization problems, and design a single transmission overlay balancing both optimality and flexibility to different scenarios.

9.2 Future Work

Transmission planning has never been conducted before on such a large geographical region. The national transmission overlay design problem is a relatively new topic, and it will no doubt face many new issues and challenges. The work in this thesis should be viewed as a preliminary investigation on this problem from a pure engineering perspective. In the future, while there are many more research aspects that should address, we only list a few of them below that we feel are particularly consistent with the content of this thesis.

1. Design with reliability performance consideration. In step 3 in Fig. 2.2, N-1 security constraints may be added to the TNEP model. However, due to computing ability, very limited reliability concerns have been made in this thesis'

studies. In the future, improvements on this point could be made from two paths:

a) Perform N-1 power flow studies for the time step when the overall system is under heaviest stress, and refine transmission investment plan based on violation results;

b) Identify a few critical contingencies which will bring post-contingency thermal overload that cannot be mitigated by generation re-dispatch only. Then, append new constraints for these critical contingencies and repeat optimization. This approach is generally computational intense, requiring extensive knowledge of the model and select effective and limited number of outage events;

2. Utilize "co-optimization". In Chapter 2, we have discussed the interdependencies between transmission and generation system. From intuitive and a few previous study results we have conducted, it is believed that co-optimization between both transmission and generation systems (perhaps also with natural gas and other energy systems) may potentially achieve better overall solutions. Again, the modeling and solving of co-optimization is limited by the computing ability, due to the very large problems size of a single co-optimization model. An alternative approach is to repeat step 1–3 in Fig. 2.2 for a few iterations. The whole iterative design process of "generation-transmission-generation" will then represent some level of coordination between generation and transmission planning, without introducing excessive computational burden. Using this approach, one can repeat generation forecast with optimized transmission plan from previous iteration, and compare the previous and updated generation

portfolio to see how big the difference is. If the mismatch has reached within a reasonable tolerance, then it means that we have found the desired optimal solution for the overall generation-transmission system.

3. We have implemented reference [22]'s flexibility design approach to find transmission overlay design with better overall optimality and adaptability performance. The limitation of computing capability has limited us to relatively low modeling granularity. A possible approach to solve this problem is to design a decomposition method to break down the huge model by futures. Meanwhile, the relatively slow branch and cut solving progress might indicate that parallel computing could be one of the possible measures to enhance computational capability, since the decimal binary disjunctive model has already sped up the root relaxation process by reduced model size.

Despite the benefits, interregional transmission is difficult to build in the U.S. One reason for this is the balkanization of authority. Most lines in each design are long, often routing through the lands of two or more states. Because states have siting authority for electric transmission, a state may reject a transmission project through its lands and would likely do so if it does not perceive sufficient benefit to its own populace (operating companies could also impede transmission development through their service area, but recently, FERC Order 1000 lifted an operating company's right of first refusal for circuit development in their service area). Another reason why interregional transmission is difficult to build is resource parochialism, where a state or region may prefer to forgo economic benefits of inexpensive energy made available by interregional transmission, electing instead to build more expensive generation locally. Such a choice may seem

justified based on economic development resulting from building local generation; however, such a perspective does not consider the net benefit of transmission from lowered energy prices in the receiving region and the economic development in the sending region, a benefit that may be significantly greater than what can be obtained by building local generation.

In [2, 20], we describe three distinct paths that could be pursued to realize continent-wide interregional transmission design: market driven investment, federal initiative, and interregional coordination. There are elements of each of these three approaches ongoing today. The market-driven approach has appeared via several recent efforts towards building merchant transmission, and in several recent FERC rulings on such proposals. An initial movement towards the federal initiative approach can be observed in Section 1221 of the Energy Policy Act of 2005 giving some authority to FERC to site interstate transmission lines, although no transmission siting applications have yet to be approved as a result of this authority. Interregional coordination is ongoing via the DOE-funded interconnection-wide planning efforts, and these kinds of activities are receiving support from at least two governor's associations as well as the recent FERC Order 1000. Ultimately, a hybrid approach may be most effective, where an interregional transmission system is designed by a multiregional collaborative stakeholder group of industry, states, advocacy organizations, and DOE, with input from governors associations. Impasses would be addressed by federally-appointed arbiters. Merchant transmission developers are incentivized to build consistent with the design; what merchant developers will not or cannot build is federalized, but with careful Federal-State coordination and cooperation.

9.3 Publications

Publications related to this topic, produced during the work of this dissertation:

[1] Y. Li, H. Villegas, J. McCalley, and D. Aliprantis, "A national transmission overlay," in Proc. 2013 PSERC Industry Advising Board Meeting, Madison, WI, May 29-31, 2013.

[2] Y. Li, J. McCalley, "Design of a high capacity interregional transmission overlay for the U.S.," accepted by IEEE transactions on power systems on May, 2014.

[3] Y. Li, J. McCalley, "A decimal-binary disjunctive model for value-based bulk transmission expansion planning," submitted to IET Generation, Transmission and Distribution.

[4] J. McCalley, Y. Li, "Interregional transmission design and benefit assessment," CIGRE Paper, Houston, TX, October, 2014.

Publications in progress and to be prepared:

[5] Y. Li, J. McCalley, "Implementation of Benders decomposition to the decimal binary disjunctive model," under preparation for PES Letter.

[6] Y. Li, J. McCalley, "Co-optimization between transmission and generation systems: modeling and solution for the U.S. national electric system," under preparation for journal submission.

[7] Y. Li, J. McCalley, "Flexible transmission design among global uncertainties in future generation," under preparation for journal submission.

[8] Y. Li, J. McCalley, "High capacity inter-regional transmission design for the U.S. with reliability considerations," under preparation for conference submission.

BIBLIOGRAPHY

[1] U.S. DOE, "National electric transmission congestion study," Dec. 2009.

[2] J. McCalley, J. Bushnell, V. Krishnan, and S. Cano, "Transmission design at the national level: Benefits, risks, and possible paths forward," PSERC, White paper Jan. 2012.

[3] GE Energy, "Western wind and solar integration study," Prepared for National Renewable Energy Laboratory under subcontract # AAM-8-77557-01, May 2010.

[4] EnerNex Corporation, "Eastern wind integration and transmission study: executive summary and project overview", National Renewable Energy Laboratory, subcontract No. AAM-8-88513-01. Knoxville, TN: EnerNex, 2010.

[5] M. Heyeck. (2008, Apr.). Interstate electric transmission: enabler for clean energy. American Electric Power Company. [Online]. Available: http://www.aep.com/about/transmission/docs/EnablerforCleanEnergy-presentation.pdf.

[6] American Superconductor, "Superconductor electricity pipelines: carrying renewable electricity across the U.S.", American Superconductor White Paper. Devens, MA: American Superconductor, May 2009.

[7] J. A. Fleeman, R. Gutman, M. Heyeck (American Electric Power), M. Bahrman, and B. Normark (ABB), "EHVAC and HVDC transmission working together to integrate renewable power," CIGRE Paper 978-2-85873-080-3, 2009.

[8] National Oceanic and Atmospheric Administration (NOAA), "Cost-optimized national electric power system," [Online]. Available: http://www.noaa.gov/.

[9] D. Osborn, T. Paul, M. Waight, A. Figueroa, D. Orser, "HVDC network concept," internal presentation at MISO, Eagan, MN, July 2014.

[10] Wikipedia, "European super grid," [Online]. Available: http://en.wikipedia.org/wiki/European_super_grid.

[11] E. Ibáñez, J. McCalley, D. Aliprantis, R. Brown, K. Gkritza, A. Somani, and L. Wang, "National energy and transportation systems: interdependencies within a long term planning model," in Proc. of IEEE Energy 2030 Conf., Atlanta, Georgia, Nov. 2008.

[12] J. McCalley, E. Ibáñez, Y. Gu, K. Gkritza, D. Aliprantis, L. Wang, A. Somani and R. Brown, "National long-term investment planning for energy and transportation systems," in 2010 IEEE Power and Energy Society General Meeting, 25-29 July 2010.

[13] Y. Li, J. McCalley, "Design of a high capacity inter-regional transmission overlay for the U.S.," accepted by IEEE Trans. on Power System, May 2014.

[14] Y. Li, J. McCalley, "A decimal-binary disjunctive model for value-based bulk transmission expansion planning," submitted to IET Generation, Transmission and Distribution.

[15] CAISO (May 2012). Participating transmission owner per unit costs, Folsom, CA. [Online]. Available: http://www.caiso.com/informed/Pages/StakeholderProcesses/ParticipatingTransmissionOwnerPerUnitCosts.aspx.

[16] Thomas H. Cormen, Charles E. Leiserson, Ronald L. Rivest, and Clifford Stein, Introduction to Algorithms, Second Edition. MIT Press and McGraw-Hill, 2001. ISBN 0-262-03293-7. Section 23.2: The algorithms of Kruskal and Prim, pp. 567–574.

[17] J. L. Gross and J. Yellen, Handbook of Graph Theory, CRC Press, 2004, page 314.

[18] J. M. Areiza, G. Latorre, R. D. Cruz, and A. Villegas, "Classification of publications and models on transmission expansion planning," IEEE Trans. Power Syst., vol. 18, no. 02, pp. 938–946, May 2003.

[19] R. Romero, A. Monticelli, A. Garcia and S. Haffner, "Test systems and mathematical models for transmission network expansion planning," in Proc. 2002 IEE Generation Transmission Distribution, vol. 149, No. 1.

[20] R. Villanasa, "Transmission network planning using linear and mixed linear integer programming," Ph.D. dissertation, Rensselaer Polytechnic Institute, 1984.

[21] L. Bahiense, G. C. Oliveira, M. Pereira, and S. Granville, "A mixed integer disjunctive model for transmission network expansion," IEEE Trans. Power Syst., vol. 16, no. 3, pp. 560–565, Aug. 2001.

[22] D. Mejia, "Robust and Flexible Planning of Power System Generation Capacity," Doctoral thesis, Iowa State University, Ames, Iowa, 2012.

[23] L. S. Moulin, M. Poss, and C. Sagastizabal, "Transmission expansion planning with re-design," Energy Syst., vol. 1, no. 2, pp. 113 – 139, Feb. 2010.

[24] Wang, X., and McDonald, J. R., Modern Power System Planning, McGraw-Hill, 1994.

[25] S. Siddiqi and M. Baughman, “Value-based transmission planning and the effects of network models,” Power Systems, IEEE Transactions on, vol. 10, no. 4, pp. 1835 – 1842, Nov. 1995.

[26] L. Hecker, Z. Zhou, D. Osborn, and J. Lawhorn, "Value based transmission planning process for joint coordinated system plan," in Power & Energy Society General Meeting, 2009. PES '09. IEEE, 2009, pp. 1-6.

[27] Prabhakar, A.J.; Rauch, L.; Hecker, L.; Lawhorn, J., "Business case justification for multi-value projects in the MISO Midwest region," Power and Energy Society General Meeting (PES), 2013 IEEE, vol., no., pp.1, 5, 21-25 July 2013.

[28] Genesi, C.; Marannino, P.; Montagna, M.; Rossi, S.; Siviero, I., "Power flow based indices for the coordination of transmission and generation system planning," PowerTech, 2009 IEEE Bucharest, vol., no., pp.1, 7, June 28 2009-July 2 2009.

[29] Alizadeh, B.; Jadid, S., "Reliability constrained coordination of generation and transmission expansion planning in power systems using mixed integer programming," Generation, Transmission & Distribution, IET , vol.5, no.9, pp.948,960, September 2011.

[30] Rudkevich, A.M., "A nodal capacity market for co-optimization of generation and transmission expansion," Communication, Control, and Computing (Allerton), 2012 50th Annual Allerton Conference on, vol., no., pp.1080, 1088, 1-5 Oct. 2012.

[31] Jae Hyung Roh; Shahidehpour, M.; Yong Fu, "Market-based coordination of transmission and generation capacity planning," Power Systems, IEEE Transactions on, vol.22, no.4, pp.1406,1419, Nov. 2007.

[32] Khodaei, A.; Shahidehpour, M., "Microgrid-based co-optimization of generation and transmission planning in power systems," Power Systems, IEEE Transactions on, vol.28, no.2, pp.1582, 1590, May 2013.

[33] Hedman, K.W.; Ferris, M.C.; O'Neill, R.P.; Fisher, E.B.; Oren, S.S., "Co-optimization of generation unit commitment and transmission switching with N-1 reliability," Power Systems, IEEE Transactions on, vol.25, no.2, pp.1052,1063, May 2010.

[34] Guk-Hyun Moon; Jaehee Lee; Sung-Kwan Joo, "Integrated generation capacity and transmission network expansion planning with superconducting fault current limiter (SFCL)," Applied Superconductivity, IEEE Transactions on, vol.23, no.3, pp.5000510, 5000510, June 2013.

[35] Yong Fu; Shahidehpour, M.; Zuyi Li, "Security-constrained optimal coordination of generation and transmission maintenance outage scheduling," Power Systems, IEEE Transactions on, vol.22, no.3, pp.1302,1313, Aug. 2007.

[36] Midwest Independent System Operator, "Transmission expansion plan 2010," Carmel, IN, 2010.

[37] E. Ibanez, "A multiobjective optimization approach to the operation and investment of the national energy and transportation systems," Doctoral thesis, Iowa State University, Ames, Iowa, 2011.

[38] Electric Power Research Institute, EGEAS v9.02BW release note, [Online]. Available: http://www.epri.com/search/Pages/results.aspx?k=EGEAS+-+Electric+Generation+Expansion+Analysis+System,+Version+9.02BW.

[39] Energy Exemplar, PLEXOS Integrated Energy Model introduction, [Online]. Available: http://energyexemplar.com/software/plexos-desktop-edition/.

[40] J. Slegers, "N. America power system production cost model in NETPLAN", Masters' thesis, Iowa State University, Ames, Iowa, 2013.

[41] North America Electric Reliability Corporation, "2010 long-term reliability assessment," Oct. 2010.

[42] U.S. Energy Information Administration, "Annual energy outlook 2011," Report #: DOE/EIA-0383(2011), Dec. 2010.

[43] J. W. Tester, "The future of geothermal energy," Massachusetts Institute of Technology, Boston, MA, prepared under Idaho National Laboratory subcontract # 6300019, 2006.

[44] National Renewable Energy Lab, Geothermal technologies data & resources, [Online]. Available: http://www.nrel.gov/geothermal/data_resources.html.

[45] National Renewable Energy Lab, Offshore wind research, [Online]. Available: http://www.nrel.gov/wind/offshore_wind.html.

[46] National Renewable Energy Lab, Wind maps, [Online]. Available: http://www.nrel.gov/gis/wind.html.

[47] National Renewable Energy Lab, Wind maps, [Online]. Available: http://www.nrel.gov/gis/solar.html.

[48] R. Gill, "Electric transmission line routing using a decision landscape based methodology," Master thesis, Wichita State University, Wichita, Kansas, 2005.

[49] Graham, R. L.; Hell, Pavol (1985), "On the history of the minimum spanning tree problem", Annals of the History of Computing 7 (1): 43–57, doi: 10.1109/MAHC.1985.10011, MR 783327.

[50] Borůvka, Otakar (1926). "O jistém problému minimálním (About a certain minimal problem)". Práce mor. přírodověd. spol. v Brně III (in Czech, German summary) 3: 37–58.

[51] Infrastructure USA, "Visualizing the U.S. electric grid", [Online]. Available: http://www.infrastructureusa.org/interactive-map-visualizing-the-us-electric-grid/.

[52] Academic Dictionaries and Encyclopedias, "Transportation in the United States", [Online]. Available: http://en.academic.ru/dic.nsf/enwiki/19678.

[53] Independent Protection Co., "Lightning risk evaluation of my home", [Online]. Available: http://www.ipclp.com/html/aud_ho_risk.html#.

[54] National NAGPRA, "Indian reservations in the continental U.S.", [Online]. Available: http://www.nps.gov/NAGPRA/DOCUMENTS/ResMAP.HTM.

[55] How Stuff Works, "United States elevation map", [Online]. Available: http://maps.howstuffworks.com/united-states-elevation-map.htm.

[56] How Stuff Works, "United States land use map ", [Online]. Available: http://maps.howstuffworks.com/united-states-land-use-map.htm.

[57] K. P. Eswaran and R.E. Tarjan, Augmentation problems, SIAM J. Comput., 5(1976), pp.653-665.

[58] M. Pereira and S. Granville, “Analysis of the linearized power flow model in Benders decomposition,” SOL Lab, Dept. of Oper. Research, Stanford University, Technical Report SOL 85-04, 1985.

[59] Y. Li, H. Villegas, J. McCalley, and D. Aliprantis, "A national transmission overlay," in Proc. 2013 PSERC Industry Advising Board Meeting, Madison, WI, May 29-31, 2013.

[60] D. Osborn, “Advantages Power Electronics May Provide as Part of Conceptual HVDC and AC Transmission Overlays to Efficiently Integrate Large Amounts of Wind Energy to the Eastern Interconnection,” Proc. of the IEEE PES General Meeting, 2010.

[61] S. Binato, “Optimal expansion of transmission networks by Benders decomposition and cutting planes,” Ph.D. dissertation (in Portuguese), Federal University of Rio de Janeiro, 2000.

[62] M. P. Bahrman and B. K. Johnson, "The ABCs of HVDC transmission technologies," IEEE power&energy magazine, pp.32-44, Mar/Apr 2007.

[63] M. Shahidehpour and Y. Fu, “Applying benders decomposition to power systems,” IEEE Power Energy Mag., vol. 3, no. 2, pp. 20–21, Mar.–Apr. 2005.

[64] Lodha, A.; Gumaste, A.; Bafna, P.; Ghani, N., "Stochastic Optimization of Light-trail WDM Ring Networks using Bender's Decomposition," High Performance Switching and Routing, 2007. HPSR '07. Workshop on., vol., no., pp.1,7, May 30 2007-June 1 2007.

[65] Midcontinent Independent System Operator (MISO), Market Efficiency Planning Study Draft (MEPS) 2013 [Online]. Available: http://www.misoenergy.org/Library/Repository/Study/MTEP/2013%20Market%20Efficiency%20Planning%20Study%20Report%20Draft.pdf

[66] Jun Hua Zhao; Zhao-Yang Dong; Lindsay, P.; Kit-Po Wong, "Flexible Transmission Expansion Planning With Uncertainties in an Electricity Market," Power Systems, IEEE Transactions on , vol.24, no.1, pp.479,488, Feb. 2009.

[67] Electric Light and Power, "Underground vs. overhead: power line installation-cost comparison and mitigation", [Online]. Available: http://www.elp.com/articles/powergrid_international/print/volume-18/issue-2/features/underground-vs-overhead-power-line-installation-cost-comparison-.html.

[68] Diemond, C.C., Bowles, J.P., Burtnyk, V. et al. (1990) AC–DC economics and alternatives – 1987 panel session report, IEEE Transactions on Volume Power Delivery, 5(4), 1956–1979.

[69] G. Asplund, B. Jacobson, B. Berggren, and K. Linden (ABB Sweden), "Continental overlay HVDC grid," CIGRE Paper, B4-109, 2010.

[70] J. McCalley, EE552 course project statement, Iowa State University, Ames, Iowa, 2010.

[71] R. Dunlop, R. Gutman, and P. Marchenko, "Analytical development of loadability characteristics for EHV and UHV transmission lines," IEEE Transactions on Power Apparatus and Systems, vol. PAS-98, No. 2 March/April 1979.

[72] T. J. Gentile, D. J. Morrow and D. Elizondo, "Merits of 765kV and insights of its application," Electric Transmission America, project #: 09T024, Sept. 2009.

[73] Haifeng Liu; Tesfatsion, L.; Chowdhury, A.A., "Locational marginal pricing basics for restructured wholesale power markets," Power & Energy Society General Meeting, 2009. PES '09. IEEE , vol., no., pp.1,8, 26-30 July 2009.

[74] Michael Renner, Sean Sweeney, and Jill Kubit, "Green Jobs: Towards Sustainable Work in a Low-Carbon World, Commissioned by the United Nations Environment Program for its joint Green Jobs," Initiative with the International Labor Organization and the International Trade Union Confederation, forthcoming. Preliminary available: www.unep.org/labour_environment/features/greenjobs.asp.

[75] Roger Bezdek, "Renewable Energy and Energy Efficiency: Economic Drivers for the 21st Century," American Solar Energy Society, Boulder, CO, 2007.

[76] "Wind Turbine Development, Location of Manufacturing Activity, Renewable Energy Policy Project," September 2004, [Online]. Available: http://www.crest.org/articles/static/1/binaries/WindLocator.pdf.

[77] A joint analysis by Greenpeace and European Photovoltaic Industries Association (EPIA). [Online]. Available: http://alternativeenergy.procon.org/sourcefiles/greenpeacesolar.pdf.

[78] "All about Geothermal Energy: Employment, Geothermal Energy Association," September 2005, available: http://www.geoenergy.org/aboutGE/employment.asp.